INFORMATION TO USERS

This was produced from a copy of a document sent to us for microfilming. While the most advanced technological means to photograph and reproduce this document have been used, the quality is heavily dependent upon the quality of the material submitted.

The following explanation of techniques is provided to help you understand markings or notations which may appear on this reproduction.

1. The sign or "target" for pages apparently lacking from the document photographed is "Missing Page(s)". If it was possible to obtain the missing page(s) or section, they are spliced into the film along with adjacent pages. This may have necessitated cutting through an image and duplicating adjacent pages to assure you of complete continuity.

2. When an image on the film is obliterated with a round black mark it is an indication that the film inspector noticed either blurred copy because of movement during exposure, or duplicate copy. Unless we meant to delete copyrighted materials that should not have been filmed, you will find a good image of the page in the adjacent frame. If copyrighted materials were deleted you will find a target note listing the pages in the adjacent frame.

3. When a map, drawing or chart, etc., is part of the material being photographed the photographer has followed a definite method in "sectioning" the material. It is customary to begin filming at the upper left hand corner of a large sheet and to continue from left to right in equal sections with small overlaps. If necessary, sectioning is continued again—beginning below the first row and continuing on until complete.

4. For any illustrations that cannot be reproduced satisfactorily by xerography, photographic prints can be purchased at additional cost and tipped into your xerographic copy. Requests can be made to our Dissertations Customer Services Department.

5. Some pages in any document may have indistinct print. In all cases we have filmed the best available copy.

8122546

NANDA, ARUN K.

THE KINETICS OF THE REVERSE DEACON REACTION

Iowa State University   PH.D.   1981

University Microfilms International

300 N. Zeeb Road, Ann Arbor, MI 48106

The kinetics of the

reverse Deacon reaction

by

Arun K. Nanda

A Dissertation Submitted to the

Graduate Faculty in Partial Fulfillment of the

Requirements for the Degree of

DOCTOR OF PHILOSOPHY

Major: Chemical Engineering

Approved:

Signature was redacted for privacy.

In Charge of Major Work

Signature was redacted for privacy.

For the Major Department

Signature was redacted for privacy.

For the Graduate College

Iowa State University
Ames, Iowa

1981

TABLE OF CONTENTS

LIST OF FIGURES

LIST OF TABLES

viii

NOMENCLATURE

a	stoichiometric coefficient for chlorine
a_i	activity of component i
A	reaction component, chlorine
A_0	frequency factor in Arrhenius equation, liter/g mole/sec
b	stoichiometric coefficient for water
B	reaction component, water
c	stoichiometric coefficient for hydrogen chloride
C	reaction product, hydrogen chloride
C'	concentration used in RTD, cm
Ci or (i)	concentration of species i, $mole/cm^3$
C_p	molar specific heat, $cal/mole/^oC$
d	stoichiometric coefficient for oxygen
D	reaction product, oxygen
D_1	axial dispersion coefficient used in RTD, cm^2/sec
D_t	Diameter of reactor, cm
$\mathscr{D}$	molecular diffusion coefficient, cm^2/sec
E_a	activation energy, cal/g mole
f	fugacity, atm
F_i	molar flow rate of species i, moles/sec
ΔG^o	standard free energy of the reaction for the stoichometry as written, K-cal/mole
h	Planck's constant, 6.624×10^{-27} ergs (secs)
H	enthalpy, K-cal/mole

ΔH heat of reaction at temperature T for the stoichiometry as written, K-cal/mol

k_b Bolzman's constant, 1.3805×10^{-16} erg/°K

k_1 reaction rate constant, for the forward reaction, $(\frac{mole}{cm^3})^{1-\eta}$ sec

k_{-1} reaction rate constant for the reverse reaction, $(\frac{mole}{cm^3})^{1-\eta}$ sec

K_a equilibrium constant based on activity

K_e equilibrium constant $(= k_1/k_{-1})$ for the stoichiometry as written, dimensionless

L length of reaction, Cm

m slope in equation $y = mx + c$

M_i molecular weight of Component i

n_i moles of Component i

P_i partial pressure of Component i

r_i rate of reaction based on volume of fluid, moles of i formed per cm^3 per sec

R ideal gas law constant

     = 1.987 cal/g mole/°K

     = 82.06 cm^3-atm/g mol/°K

R^2 regression coefficient, dimensionless

ΔS entropy change for the reaction for the stoichiometry written, cal/mole

T temperature, °K or °C

u superficial velocity, cm/sec

v_i volumetric flow rate of component i, cm^3/sec

v total volumetric flow rate, cm^3/sec

V volume of reactor, cm^3

X_i	fraction of reactant component i converted into product
y_i	mole fraction of component i in gases
z	$= \ell/L$, fractional distance through the reactor, dimensionless
Z	compressibility factor

Greek Symbols

α	order of reaction with respect to chlorine
β	order of reaction with r spect to water
γ	· order of reaction with respect to hydrogen chloride
δ	order of reaction with respect to oxygen
δ_i	expansion per mole of reference component i
ϵ_i	expansion factor, $Y_{io}\delta_i$
η	order of reaction
θ	exit age time, sec
θ_i	molar flow ratio at inlet conditions, $(\theta_B = F_{Bo}/F_{Ao})$
θ'	dimensionless time used in RTD, $\theta' = \theta/\bar{\tau}$
μ_i	viscosity of component i, gm/cm/sec
π	total pressure of gaseous mixture, atm
ρ_i	density of component i, gm/cm^3
σ	standard deviation
σ^2	variance of response values of tracer curves, sec^2
τ	space-time, or residence time, sec
$\bar{\tau}$	mean residence time, sec

Subscripts

A, B	with respect to A, B ...
Avg	average values

c   critical conditions

e   at chemical equilibrium

f   at final conversion or final conditions

i, j   with respect to ith or jth component, respectively

o   initial or inlet conditions

t   total

Superscript

o   standard state

.   radical

$\#$ activated complex

INTRODUCTION

Energy is considered to be one of the most important and essential ingredients of the economy of an advanced society. People have inherent desire to improve their standard of living, which is directly proportional to the consumption of energy. Hence, the demand for more energy is growing. At this present rate of consumption, it has been predicted that a major energy deficit is inevitable towards the end of this century. To meet these tremendous energy needs, many resources will be pressed into service: coal, nuclear, geothermal, solar, wind, and fossil fuels. Among these coal and nuclear energy sources may be used primarily to generate electricity, whereas other fossil fuels will serve for heating and transportation needs. But, the world contains a limited amount of fossil fuels. They are being depleted at a faster rate to meet the present day energy needs. In the coming years, fossil fuel reserves will be too valuable as feedstocks for chemical production. It will be unwise then to burn fossil fuel for its energy contents. In addition to this problem of depletion of fossil fuel reserves, people in the modern world want to live in a cleaner environment, which fossil fuel cannot provide adequately. Today, many engineers and scientists believe that hydrogen is a potential "universal fuel" for the future, capable of supplying most of the needs currently filled by natural gas and other fossil fuels. Moreover, hydrogen will be relatively cheap, abundant, and clean (13, 17, 21, 32, 43, 62, 64, 86, 88).

In the recent years the concept of a "Hydrogen Economy" has been

introduced (32, 44, 62). The use of hydrogen plays an important role in our present economy and has the potential to play a major role in the future. The major problems involved in using hydrogen as a common fuel are storage and transportation. Storage is possible as a gas under pressure, or as a cryogenic liquid or as a metal hydride (44, 54). In previous studies, it has been concluded that hydrogen will be more economical than electricity under conditions of long distance distribution (66). Other researchers also have studied this aspect extensively (15, 32, 42, 62, 80).

In many ways hydrogen is virtually an ideal fuel. When burned in air, the only possible pollutant is a low concentration of nitrogen oxides derived from air itself. However, it has been reported that the exhaust from an internal combustion engine running on the hydrogen-air system contained 220 ppm of H_2O_2 (45). It can be used for supersonic airplanes (61), for ordinary boilers and for household appliances (44). Burned with pure oxygen, the only product is water (H_2O), and there is no pollutant at all; and therefore, is attractive for production of electricity from fuel cells (83). Other important applications of hydrogen are for the production of synthetic ammonia and for fertilizers, and for the production of steel by reduction of iron ore (60, 64, 65, 76).

In the past as well as in the present the main source of hydrogen has been natural gas and liquid hydrocarbons (84). But this source is not our primary interest because the reserves are diminishing rapidly. The other source of hydrogen is water, which is inexhaustible and abundant. Hydrogen can be produced by decomposing water, but a

considerable amount of primary energy is required for its decomposition. The decomposition of water can be effected by: (i) electrolysis, (ii) direct thermal decomposition, (iii) chemical reaction, and (iv) thermochemical cycles. The advantages and disadvantages of these processes with respect to production of hydrogen by thermochemical cycles are discussed in the following paragraphs as the interest of this work lies in this process.

Electrolysis

The production of hydrogen by electrolysis of water has been known since the 19th century. Significant improvements in efficiency and equipment design have been achieved in recent years. However, the process is quite expensive when the existing technology and present cost of electricity are used (82). It is well-known that the efficiency of conversion of electricity to hydrogen and oxygen is as high as 80% (86). But the conversion of heat to electricity is less than 40%; thus, making the overall efficiency of heat to hydrogen less than 32% (4). It cannot be ruled out that modern technology for generation of electricity and process of electrolysis may result in improved efficiencies to make this aspect of hydrogen production from water comparable on the basis of economics (10). Also, electrolysis of sea water for production of hydrogen has been studied as a feasible source and the problems involved are formation of insoluble deposits on and near the cathode, and the addition of dissolved free chlorine with its effect on ocean life (87).

Direct Thermal Cracking

Water may be decomposed directly by raising it to high temperatures. The theoretical equilibrium conversion of water to oxygen and hydrogen is very low. Chao and Cox (19) have reported that equilibrium yields increase with increasing temperature. Also, a lower operating pressure favors increased conversion. They have reported that direct thermal splitting of water may be impractical for a variety of reasons. A high temperature energy source is presently unavailable and a material problem has been encountered in obtaining separation. Present studies indicate that high temperature is possible with the use of solar concentrators, but in practice it is not suitable at reasonable cost (4).

Chemical Reaction

In the past, the reaction, $C + 2H_2O = CO_2 + 2H_2$, has been used to generate hydrogen. The element C, which is abundant in coal, is the primary raw material. This process is receiving renewed attention (81). This is an endothermic reaction, and necessary heat to drive this reaction can be acquired by use of nuclear reactors. Then burning of coal will be the primary source of pollution. With stricter pollution control and with the rising cost of fossil fuels, this open cycle process will have some disadvantages compared to closed-cycle thermochemical processes.

Thermochemical Closed-Cycle Processes

In the last decade, the thermochemical water decomposition by closed cycle processes has received increasing attention. In a thermochemical process, thermal energy is transferred into chemical energy. The cycle consists of a series of chemical reactions and these reactions are operated at different temperatures. The cycle results in production of hydrogen and oxygen from water with no net consumption of other chemical species. For this reason and for the following reasons, this process has become very attractive (4, 19):

- No major technological breakthroughs are needed to get a feasible chemical process.

- An infinite supply of raw material (water) is available.

- Heat required for the process can readily be obtained either from nuclear reactors or from solar concentrators.

A temperature in the range of 500-1000°C is required for the decomposition of water by means of thermochemical cycles. Solar collectors are understood to produce tempratures as high as 600-700°C. However, this temperature range can be raised substantially with capital investment, but this might make the process noncompetitive. The High Temperature Gas (cooled) Reactor (HTGR) may be the most appropriate and a possible economical source of energy for thermochemical cycles (5, 73, 75).

It is reasonable to expect that thermochemical cycles will become a practical means for production of hydrogen from water in view of current and future shortages of fossil fuels and also in view of current

development of nuclear and solar energy sources.

Several closed-cycle thermochemical processes have been reported in the literature (2, 11, 17, 34, 57). A good review of development of thermochemical cycles and a table containing 72 such cycles have been published by Bamberger and Richardson (4). Many thermochemical closed-cycles have been based on the chemistry of halide compounds. Calcium bromide at 730°C was used by De Beni in one of the cycles and he named his process as "Mark 1" (25, 26). Hardy used iron chlorides in his process (46), and also several variations of "Mark 1" have been presented (25). In their report, Abraham and Schreiner (1) have proposed a novel thermochemical cycle to produce hydrogen and oxygen from water. They used the process of oxidation of lithium nitrite by iodine at 300°K in aqueous solution. A good number of thermochemical processes have been built around the reaction of chlorine gas and water to form hydrogen chloride and oxygen. The opposite reaction is known as the Deacon reaction and was in use for chlorine manufacture. By increasing the temperature, the equilibrium can be shifted to hydrogen chloride and oxygen production. The reverse Deacon reaction proceeds with a 60% conversion of water at 730°C and 50% conversion at 620°C, at atmospheric pressure (19).

The chemical reactions involved in the closed-cycle process can be classified into three essential functions: (i) water binding, (ii) product recovery, and (iii) reagent generations. A single reaction step, namely the reverse Deacon reaction, i.e.

$$Cl_2 \text{ (g)} + H_2O \text{ (g)} \rightleftharpoons 2HCl \text{ (g)} + \frac{1}{2} O_2 \text{ (g)}$$
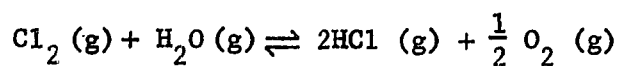
can perform two of the above three functions. Water binding is combined with the oxygen (product) recovery step in the reverse Deacon reaction. Therefore, it has been a very attractive first step for many water decomposition processes. In the following closed-cycle process, the importance of the reverse Deacon reaction is well-understood (18, 57):

$$Cl_2 + H_2O \rightarrow 2HCl + \frac{1}{2} O_2 \qquad 1000^{\circ}K$$

$$2FeCl_2 + 2HCl \rightarrow 2FeCl_3 + H_2$$

$$\underline{2FeCl_3 \rightarrow 2FeCl_2 + Cl_2}$$

Net reaction: $H_2O \rightarrow H_2 + \frac{1}{2} O_2$
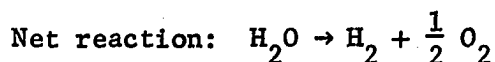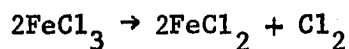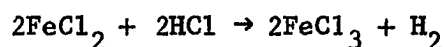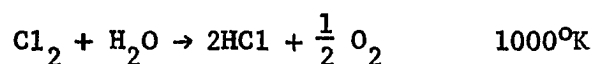
A large number of such thermochemical cycles are believed to be possible from a scientific standpoint, but it is not yet clear which cycles offer the best economic potential. Some of the experimentally valid cycles that are identified have been described by Bowmann (12). A partial list of these cycles is given in Appendix A.

The thermodynamics of thermochemical cycles have been described by Funk (33), Knoche (58), and Kerns (55). Several other authors have reported systematic and computerized techniques for seeking thermochemical cycles that would be thermodynamically sound (34, 35, 56, 59, 86). A comprehensive and critical bibliography on these and on other aspects of the hydrogen economy has been published by Cox (22). Although the thermodynamics of the reverse Deacon reaction have been studied extensively and are well-known, the kinetics of the reaction

have not been studied thoroughly. The purpose of this work is to
determine the kinetic parameters of the reaction. When such a rate
expression is known, it will be quite helpful for a comparative evalua-
tion of the closed-cycle thermochemical water-splitting processes.

LITERATURE REVIEW

The oxidation of hydrogen chloride with air was in practice as early as 1845. Deacon (23) in 1865 made this operation a continuous one by rearranging the reactions, and his process has been of commercial interest for manufacture of chlorine (62, 77). The development of the electrolytic caustic-chlorine cell eliminated the Deacon process as a source of commercial chlorine. But the reverse process has attracted renewed attention in recent years because its potential for use in thermochemical cycles for production of hydrogen from water.

Falckenstein (31) concluded that the reaction, $4HCl + O_2 \rightleftharpoons 2Cl_2 + 2H_2O$, is equally balanced at temperatures of about 600°C. At temperatures below 600°C, the reaction proceeding to the right predominates and the equilibrium becomes more favorable to the formation of chlorine by oxidation of hydrogen chloride as in the Deacon process. On the other hand, at temperatures above 600°C, the equilibrium favors the formation of hydrogen chloride by the reaction of chlorine and water vapor. Falckenstein also discussed the equilibrium constants for both the Deacon and reverse Deacon processes. Johnstone (52) published the free energy data for the Deacon reaction. Also, free energy and heat of reaction data for $\frac{1}{2} H_2 + \frac{1}{2} Cl_2 = HCl$, are available (39). Arnold and Kobe (3) in their pioneer work suggested the following equation for the Deacon process to calculate the equilibrium constant:

$$\ln K_e = \frac{5881.7}{T} - 0.93035 \ln T + (1.3704 \times 10^{-4})T$$
$$- (1.7581 \times 10^{-8})T^2 - 4.1744 \qquad (1)$$

The equilibrium constants calculated from the spectroscopic data, as done by Gordon and Barnes (41), compare favorably with the accepted experimental value. Kobe also studied the effects of temperature, pressure, impurities, and ratio of reactants on equilibrium. In a recent study van Dijk and Schreiner (85) have discussed the process function and economics of the Kel-Chlor process, in which waste hydrochloric acid is used for manufacture of chlorine. The effects of catalysts in the process of oxidative recovery of chlorine from hydrochloric acid have been studied by Engel, et al. (29). They have suggested improvements in the Deacon process for manufacture of chlorine.

Funk, et al. (36) in their research work described an evaluation procedure to determine the thermodynamic properties inside the process for multistep thermochemical water decomposition processes. This information can be used to study the effect of operating temperature, approach to equilibrium in the chemical reaction, and thermal regeneration on thermochemical cycles. Pangborn and Sharer (69) have concluded that accurate thermodynamic data are required for each step for complete evaluation of a thermochemical cycle along with acceptable experimental chemical conversion and kinetic data.

As a part of an overall project of chlorination of methane using air and HCl, Parthasarathy (70) determined the rate for the Deacon process as a function of conversion. Jones (53) wrote his Ph.D. dissertation on the kinetics of oxidation of hydrogen chloride. He used a batch differential reactor for his investigation. He concluded that chromia-alumina catalysts gave good results, a high reaction rate was obtained with the catalyst with the higher percentage of

chromic acid. He proposed an empirical expression and the rate
constants were evaluated from his experimental data. Three tempera-
tures used were: 598, 613 and 628°K. He also studied the reverse
Deacon reaction at 628 and 643°K, but his experiments were based on
the heterogeneous catalytic reaction.

There have been many patents issued regarding the use of
catalysts and operating conditions for the Deacon process (24).
Hirschkind (49) used a reducing agent, namely carbon, with water and
chlorine for manufacture of oxygen to make the process commercially
possible. He found that under the best conditions, the exit gas
leaving the furnace at 900°C contained 73.5% of HCl, 19% of CO_2, and
3% of CO. Peters claimed a process for quantitative conversion of
chlorine into hydrochloric acid by reacting it with coke and steam
at temperatures between the boiling point of water and red heat (72).
A U.S. patent was granted to Paulus (71) who claimed a simultaneous
production of hydrochloric acid and carbon monoxide according to the
following reaction:

$$C + Cl_2 + H_2O = 2HCl + CO$$
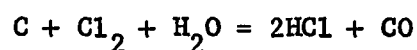
Gibbs showed that the reaction between carbon, chlorine, and steam
could be carried out producing hydrochloric acid and carbon dioxide
(40). He suggested a temperature range from 0°C to 130°C. Barstow
and Heath (6) in their invention discussed the synthetic formation of
hydrochloric acid by reaction of chlorine and water vapor at an
elevated temperature. They have a patent for equi-molal proportions of
chlorine and steam reacted at 1000-1600°C in the substantial absence of

reducing substances. Apparatus and various details of their operation are described in their publications. Reference (20) also discusses running the experimental reaction without a reducing agent. Ohkawa (68) has a patent to use ultraviolet light to make the dissolved chlorine react with water to form hydrochloric acid. Patents issued for reaction of H_2O and Cl_2 in the presence of a reducing agent are listed in reference (74).

A catalyst containing 20% of MgO, 25% of $MgCl_2$, and 25% of CaO was used by Shelud'ko (78) to obtain a 97% yield of HCl for the reverse Deacon reaction at 900°C. Survey of past research work shows that the reverse Deacon reaction is a possible way to react water with chlorine to produce oxygen and hydrogen chloride. Yeh (89) worked on preliminary kinetics of high-temperature reaction of chlorine and water. He used a single pass and a five pass reactor at atmospheric pressure and two temperatures: 900 and 950°K. He found measured conversions were always less than 50% of the equilibrium conversion; and therefore, neglected the effect of the reverse reaction. He studied 12 rate expressions by integral approach and recommended the following two for the forward reaction of the reverse Deacon reaction:

(1) $- r_{Cl_2} = k\, C_{Cl_2}^2 C_{H_2O}$

(2) $- r_{Cl_2} = k\, C_{Cl_2}$

He also suggested to study many more rate expressions along with these two rate expressions:

THEORY

In a tubular flow reactor the feed enters one end of the cylindrical tube and the product leaves at the other end as shown in Figure 1. A mole balance on species j, at any instant in time t, will yield the following equation:

$$\begin{bmatrix} \text{rate of flow} \\ \text{of j into} \\ \text{the system} \\[4pt] \text{(moles/time)} \end{bmatrix} + \begin{bmatrix} \text{rate of generation} \\ \text{of j by chemical} \\ \text{reaction within} \\ \text{the time} \\[4pt] \text{(moles/time)} \end{bmatrix} + \begin{bmatrix} \text{rate of flow} \\ \text{of j out of} \\ \text{the system} \\[4pt] \text{(moles/time)} \end{bmatrix}$$

$$= \begin{bmatrix} \text{rate of accumulation of} \\ \text{species j within the} \\ \text{system} \\[4pt] \text{(moles/time)} \end{bmatrix} \tag{2}$$

The reactor normally operates at steady state except at the start-up and the shut down operations. Therefore, the right-hand side of the above equation is essentially zero at steady state conditions. In symbols Equation (2) can be written as:

$$F_{jo} + \int_V r_j dV - F_j = 0 \tag{3}$$

The properties of the feed and product for the reactor are constant with respect to time, but the properties of the flowing stream may vary from point-to-point. The assumptions made are:

(1) no mixing in the axial direction (i.e., in the direction of flow).

(2) complete mixing in the radial direction.
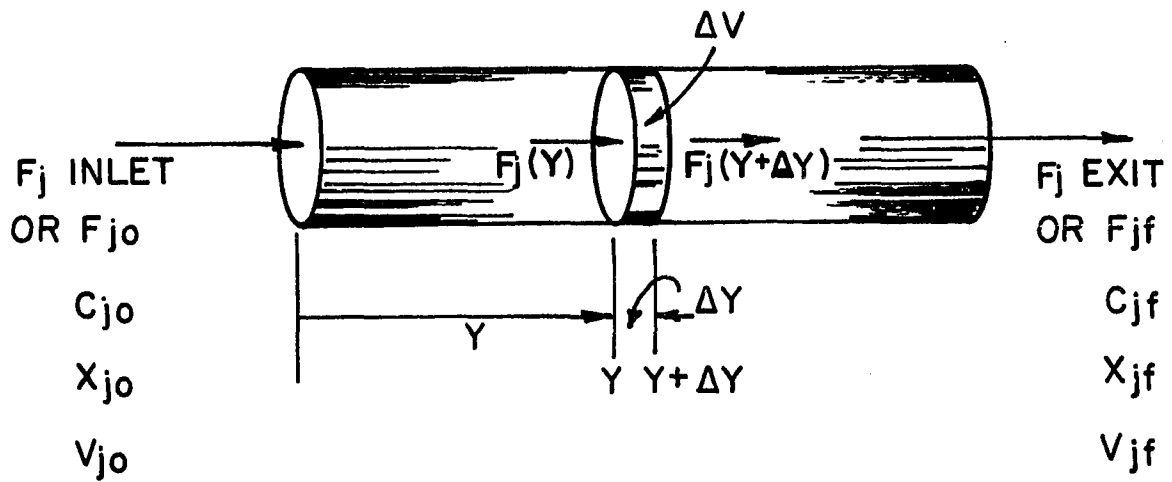
$$C_j \; : \; \text{CONCENTRATION OF } j \text{ (moles/volume)}$$

$$F_j \; : \; \text{MOLAL FLOW RATE OF } j \text{ (moles/time)}$$

$$X_j \; : \; \text{FRACTION OF } j \text{ CONVERTED INTO PRODUCT}$$

$$V_j \; : \; \text{VOLUMETRIC FLOW RATE OF } j \text{ (VOLUME/TIME)}$$

Figure 1. Tubular flow reactor

(3) a uniform velocity profile across the radius.

The absence of longitudinal mixing makes this reactor a special type of tubular flow reactor. The assumptions meet the criteria of the plug flow reactor. The validity of these assumptions will depend on the geometry of the reactor and the flow conditions. In the next section we have discussed the deviations from the ideal conditions and in subsequent sections it has been established on analysis of residence time distribution (RTD) that there is no significant longitudinal mixing in the existing reactor.

Design Equation of Plug Flow Reactor

The reactor in Figure 1 is conceptually divided into a number of subvolumes ΔV, to develop the design equation. The rate of reaction in each of these subvolumes may be considered spatially uniform. Let us consider a subvolume ΔV, located at a distance y from the entrance of the reactor. Let $F_j(y)$ be the molar flow rate of species j into the volume ΔV at y, and $F_j(y + \Delta y)$ be the molar rate of j out of the volume ΔV at point $y + \Delta y$. The mole balance equation for steady state operation can be written as:

$$F_j(y) - F_j(y + \Delta y) + r_j \Delta V = 0 \qquad (4)$$

The subvolume ΔV, can be written as a product of cross-sectional area A of the reactor and the element reactor length: Then,

$$F_j(y) - F_j(y + \Delta y) + r_j \Delta y A = 0 \qquad (5)$$

Dividing through Equation (5) by Δy and rearranging the terms, and taking the limit as $\Delta y \rightarrow 0$, the differential equation obtained is:

$$- \frac{dF_i}{dy} = - r_j A \tag{6}$$

or,

$$\frac{dF_i}{dV} = r_j \tag{7}$$

The Equations (6) and (7) are generalized equations and are applicable to reactors of variable and constant cross-sectional areas.

The reverse Deacon reaction can be written in either of the following two terms:

$$Cl_2(g) + H_2O\ (g) \underset{k_2}{\overset{k_1}{\rightleftharpoons}} 2HCl\ (g) + \frac{1}{2} O_2\ (g) \qquad \text{Reaction I}$$

$$2Cl_2\ (g) + 2H_2O\ (g) \underset{k_2'}{\overset{k_1'}{\rightleftharpoons}} 4HCl\ (g) + O_2\ (g) \qquad \text{Reaction II}$$
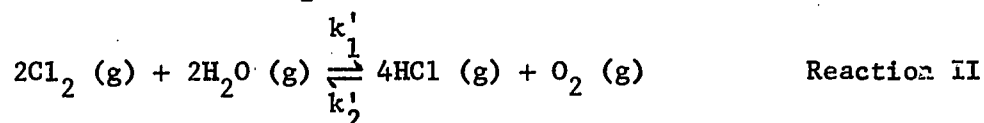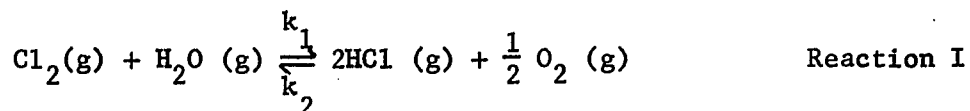
Let A denote chlorine (Cl_2), B denote water vapor (H_2O), C denote hydrogen chloride (HCl), and D denote oxygen (O_2) in the subsequent equation developments.

Chlorine as the limiting species

Taking A as our basis, and thus dividing both the reactions through by their respective stoichiometric coefficients of A, we can rewrite Reaction I and Reaction II, not considering the reverse reaction, as:

$$A + B \rightarrow 2C + \frac{1}{2} D \tag{8}$$

or in a more general way,

$$A + \frac{b}{a} B \rightarrow \frac{c}{a} C + \frac{d}{a} D \qquad (9)$$

where, $\quad b/a = 1$, $c/a = 2$, and $d/a = \frac{1}{2}$. $\qquad (10)$

For a flow system, the conversion of species A is defined as the moles of A reacted per mole of A fed to the system. Normally, the conversion increases with the time the reactants spend in the reactor. This time, for a continuous flow system, usually increases with increasing reactor volume and consequently, the conversion X_A is a function of the reactor volume V. If F_{Ao} is the molar flow rate of A fed to the system, which is operated at steady state, the molar rate at which A is reacting within the entire system will be $F_{Ao}X_A$. The molar flow rate to the system minus the rate of reaction of A within the system will be equal to the molar flow rate of A leaving the system F_A. With symbols,

$$F_A = F_{Ao} - F_{Ao}X_A = F_{Ao}(1 - X_A) \qquad (11)$$

Similar expressions for species B, C, and D can be derived. Taking A as our basis, a stoichiometric table (Table 1) for the flow system with reference to the reaction of Equation (9) can be set up. It is to be noted that the values of F_{Co} and F_{Do} are zero, since they are not present in the feed stream.

The equation of state we shall use is:

$$\pi v = ZF_t RT \qquad (12)$$

Table 1. Stoichiometric table with respect to species A for the reaction, $A + \frac{b}{a} B \rightarrow \frac{c}{a} C + \frac{d}{a} D$

Species	Feed rate to reactor (moles/time)	Change within reactor (moles/time)	Effluent rate from reactor (moles/time)
A	F_{Ao}	$- F_{Ao} X_A$	$F_A = F_{Ao} - F_{Ao} X_A$
B	F_{Bo}	$- \frac{b}{a} F_{Ao} X_A$	$F_B = F_{Bo} - \frac{b}{a} F_{Ao} X_A$
C	F_{Co}	$+ \frac{c}{a} F_{Ao} X_A$	$F_C = F_{Co} + \frac{c}{a} F_{Ao} X_A$
D	F_{Do}	$+ \frac{d}{a} F_{Ao} X_A$	$F_D = F_{Do} + \frac{d}{a} F_{Ao} X_A$
I	F_{Io}	—	$F_I = F_{Io}$
Total[a]	F_{to}	—	$F_t = F_{to} + \delta_A F_{Ao} X_A$ [b]

[a] $F_{to} = F_{Ao} + F_{Bo} + F_{Co} + F_{Do} + F_{Io}.$

[b] $\delta_A = \frac{d}{a} + \frac{c}{a} - \frac{b}{a} - 1.$

where, T = temperature, ^{O}K

π = total pressure, atm.

Z = compressibility factor

R = gas constant, (atm-liter)/(mole-^{O}K)

v = volumetric feed rate, (liter/time)

F_t = total number of moles fed to the system at time t, (moles/time).

Equation (12) is valid at any point in the system at any time t. At time t = 0, this equation can be rewritten as:

$$\pi_o v_o = Z_o F_{to} RT_o \tag{13}$$

Dividing Equation (12) by Equation (13), and rearranging the terms, we obtain,

$$v = v_o (\frac{\pi_o}{\pi}) (\frac{T}{T_o}) (\frac{Z}{Z_o}) (\frac{F_t}{F_{to}}) \tag{14}$$

Let the change in moles due to reaction in Equation (9) be δ_A, where,

$$\delta_A = d/a + c/a - b/a - 1 \; (= \frac{1}{2} \text{ , in the present case}) \tag{15}$$

From Table 1, we can write

$$F_t = F_{to} + F_{Ao} \delta_A X_A \tag{16}$$

Dividing Equation (16) by F_{to} gives

$$\frac{F_t}{F_{to}} = 1 + F_{Ao}/F_{to} \; \delta_A X_A \tag{17}$$

If $F_{Ao}/F_{to} = y_{Ao}$, the mole fraction of A at feed conditions, then Equation (17) can be rewritten as:

$$F_t = F_{to}(1 + \epsilon_A X_A) \tag{18}$$

where, $\quad \epsilon_A = \delta_A y_{Ao} \tag{19}$

In most gas phase systems the temperature and pressure are such that the compressibility factor will not change significantly during the course of reaction; hence, for our purpose, we can say $Z = Z_o$. In addition, if we could use an isothermal condition (i.e., $T = T_o$), and operate the system at atmospheric pressure ($\pi = \pi_o$), then Equation (14) reduces to

$$v = v_o F_t / F_{to} \tag{20}$$

Inserting the value of F_t as defined in Equation (18), we get,

$$v = v_o(1 + \epsilon_A X_A) \tag{21}$$

Equation (21) is the gas volumetric flow rate in a flow system at any time.

Let the molar flow ratios of the reactants be defined as:

$$\theta_B = F_{Bo}/F_{Ao} \tag{22}$$

$$\theta_C = F_{Co}/F_{Ao} \quad (= 0, \text{ as defined earlier}) \tag{23}$$

$$\theta_D = F_{Do}/F_{Ao} \quad (= 0, \text{ as defined earlier}) \tag{24}$$

We can then define the concentrations of species A, B, C, and D as a function of conversion X_A, in the following manner:

$$C_A = F_A/v = \frac{F_{Ao}(1 - X_A)}{v_o(1 + \epsilon_A X_A)} = \frac{C_{Ao}(1 - X_A)}{(1 + \epsilon_A X_A)} \tag{25}$$

$$C_B = \frac{F_B}{v} = \frac{F_{Ao}(\theta_B - X_A)}{v_o(1 + \epsilon_A X_A)} = \frac{C_{Ao}(\theta_B - X_A)}{(1 + \epsilon_A X_A)} \tag{26}$$

$$C_C = \frac{F_C}{v} = \frac{F_{Ao}(\theta_C + 2X_A)}{v_o(1 + \epsilon_A A)} = \frac{2C_{Ao}X_A}{(1 + \epsilon_A X_A)} \tag{27}$$

$$C_D = \frac{F_D}{v} = \frac{F_{Ao}(\theta_D + 0.5X_A)}{v_o(1 + \epsilon_A X_A)} = \frac{0.5C_{Ao}X_A}{(1 + \epsilon_A X_A)} \tag{28}$$

Substituting the value of F_A from Equation (11) into the Equation (7), we can rewrite the design equation for species A as:

$$\frac{d}{dV}[F_{Ao}(1 - X_A)] = r_A \tag{29}$$

which is simplified to

$$- r_A = F_{Ao}\frac{dX_A}{dV} \tag{30}$$

Substituting $\tau = V/v_o$, and $F_{Ao} = C_{Ao}v_o$ in the above equation, we obtain,

$$- r_A = C_{Ao}\frac{dX_A}{d\tau} \tag{31}$$

Equation (31) is known as the differential form of the design equation for the plug flow reactor, and is the relationship between conversion and the size of the reactor. Equation (30) can be written in the integral form by rearranging it and integrating both sides:

$$V = F_{Ao}\int_0^{X_{Af}}\frac{dX_A}{- r_A} \tag{32}$$

Further rearrangement yields another convenient form of the integral expression:

$$\tau = \frac{V}{v_o} = \frac{F_{Ao}}{v_o} \int_0^{X_{Af}} \frac{dX_A}{-r_A} = C_{Ao} \int_0^{X_{Af}} \frac{dX_A}{-r_A} \tag{33}$$

Steam as the limiting species

A similar procedure can be followed when steam is considered as the limiting species instead of chlorine. A similar stoichiometric table for the reaction,

$$(a/b)A + B \rightarrow (c/b)C + (d/b)D \tag{34}$$

where $\quad a = 1, \; b = 1, \; c = 2, \; \text{and} \; d = \frac{1}{2}$ \hfill (35)

and $\quad \delta_B = d/b + c/b - a/b - 1 = \frac{1}{2}$ (same as δ_A) \hfill (36)

is shown in Table 2. Also, the values of F_{Co} and F_{Do} in this table are zero, since they are not present in the feed stream.

The volumetric flow rate can be written as:

$$v = v_o(1 + \frac{F_{Bo}}{F_{to}} \delta_B X_B) \tag{37}$$

or $\quad v = v_o(1 + \varepsilon_B X_B)$ \hfill (38)

where $\quad \varepsilon_B = \delta_B y_{Bo} = \delta_B F_{Bo}/F_{to}$ \hfill (39)

The concentration of species A, B, C, and D could be defined in terms of conversion X_B as follows:

$$C_A = \frac{F_A}{v} = \frac{F_{Bo}(\theta_A - X_B)}{v_o(1 + \varepsilon_B X_B)} = \frac{C_{Bo}(\theta_A - X_B)}{(1 + \varepsilon_B X_B)} \tag{40}$$

where $\quad \theta_A = \frac{F_{Ao}}{F_{Bo}}$ \hfill (41)

Table 2. Stoichiometric table with respect to species B for the
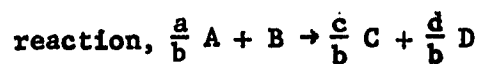
reaction, $\frac{a}{b} A + B \rightarrow \frac{c}{b} C + \frac{d}{b} D$

Species	Feed rate to reactor (moles/time)	Change within reactor (moles/time)	Effluent rate from reactor (moles/time)
A	F_{Ao}	$-\frac{a}{b} F_{Bo} X_B$	$F_A = F_{Ao} - \frac{a}{b} F_{Bo} X_B$
B	F_{Bo}	$- F_{Bo} X_B$	$F_B = F_{Bo} - F_{Bo} X_B$
C	F_{Co}	$+\frac{c}{b} F_{Bo} X_B$	$F_C = F_{Co} + \frac{c}{b} F_{Bo} X_B$
D	F_{Do}	$+\frac{d}{b} F_{Bo} X_B$	$F_D = F_{Do} + \frac{d}{b} F_{Bo} X_B$
I	F_{Io}	—	$F_I = F_{Io}$
Total[a]	F_{to}	—	$F_t = F_{to} + \delta_B F_{Bo} X_B$ [b]

[a] $F_{to} = F_{Ao} + F_{Bo} + F_{Co} + F_{Do} + F_{Io}$.

[b] $\delta_B = \frac{d}{b} + \frac{c}{b} - \frac{a}{b} - 1$.

$$C_B = \frac{F_B}{v} = \frac{F_{Bo}(1 - X_B)}{v_o(1 + \epsilon_B X_B)} = \frac{C_{Bo}(1 - X_B)}{(1 + \epsilon_B X_B)} \tag{42}$$

$$C_C = \frac{F_C}{v} = \frac{F_{Co}(\theta_C + 2X_B)}{v_o(1 + \epsilon_B X_B)} = \frac{2C_{Bo}X_B}{(1 + \epsilon_B X_B)} \tag{43}$$

$$C_D = \frac{F_D}{v} = \frac{F_{Do}(\theta_D + 0.5X_B)}{v_o(1 + \epsilon_B X_B)} = \frac{0.5C_{Bo}X_B}{(1 + \epsilon_B X_B)} \tag{44}$$

Hence, Equation (7) for species B is of the form:

$$\frac{d}{dV} F_{Bo}(1 - X_B) = r_B \tag{45}$$

which simplifies to

$$- r_B = F_{Bo} \frac{dX_B}{dV} \tag{46}$$

Substituting $\tau = V/v_o$, and $F_{Bo} = C_{Bo}v_o$ in the above equation, we obtain,

$$- r_A = C_{Bo} \frac{dX_B}{d\tau} \tag{47}$$

which is the differential form of the design equation for the plug flow reactor when species B is considered as the limiting species. The integral form is similarly developed, and is shown below:

$$\tau = C_{Bo} \int_0^{X_{Bf}} \frac{dX_B}{- r_B} \tag{48}$$

In these equations $- r_B$ is the rate expression for the forward reaction when steam is the limiting species.

Analysis of Rate Equations

The most common experimental procedure for establishing rate equations is to measure the composition of the reaction mixture at various stages during the course of the reaction. Methods used are: the differential, integral, initial rate, and half-life methods. In this experimental work, the reactor was operated at steady state, therefore, we are left with one method, i.e., integral method. For this approach, it is necessary to integrate the rate expression to give concentration as a function of time. Another approach, called differential method, for interpreting integral reactor data is also in use. In this case the rate has to be evaluated first by operating the reactor at various space-times but at the same molar flow ratio. The procedure is repeated by varying molar flow rates so as to obtain a wide range of data.

Integral method for treating the integral reactor data

When the reaction rate law is known or can be guessed, the integral method of analysis may be used after performing experiments to obtain the specific reaction rate. This procedure is useful when the reaction order and the specific rate at one temperature are already known from previous experiments. The specific reaction rate at some other temperature can then be obtained easily.

The rate equation is the number of moles reacting per unit time per unit volume. The rate equation is solely a function of the properties of the reacting materials (e.g., specific concentrations, pressure and temperature) at a point in the system and is independent of the system.

Since the pressure and temperature are kept constant, the chemical
reaction rate becomes a function of concentrations only; and for the
forward reaction of the reverse Deacon reaction can be written as:

$$- r_A = k_1 c_A^\alpha c_B^\beta \quad \text{for the reaction I} \tag{49}$$

In this equation α and β are the order of reaction with respect to
chlorine and water, respectively. Substitution of Equation (25) and
Equation (26) results in:

$$- r_A = k_1 \left[\frac{C_{Ao}(1 - X_A)}{(1 + \epsilon_A X_A)}\right]^\alpha \left[\frac{C_{Ao}(\theta_B - X_A)}{(1 + \epsilon_A X_A)}\right]^\beta \tag{50}$$

rearranging the terms,

$$- r_A = k_1 \frac{c_{Ao}^{\alpha+\beta}(1 - X_A)^\alpha(\theta_B - X_A)^\beta}{(1 + \epsilon_A X_A)^{\alpha+\beta}} \tag{51}$$

Replacing the term $- r_A$ in Equation (33) and rewriting, we get:

$$\tau = \frac{1}{k_1} \int_o^{X_{Af}} \frac{(1 + \epsilon_A X_A)^{\alpha+\beta} dX_A}{c_{Ao}^{\alpha+\beta-1}(1 - X_A)^\alpha(\theta_B - X_A)^\beta} \tag{52}$$

If we define

$$I = \int_o^{X_{Af}} \frac{(1 + \epsilon_A X_A)^{\alpha+\beta}}{c_{Ao}^{\alpha+\beta-1}(1 - X_A)^\alpha(\theta_B - X_A)^\beta} dX_A \tag{53}$$

then $\quad k_1 \tau = I \tag{54}$

A plot of τ versus I will give a straight line of slope k_1, if the
correct rate expression (i.e., the correct order of reaction) is
chosen. Regression analysis (least-square fit) will result in a
correlation coefficient, which can be used as a measure of correlation

between τ and I. A number of values of α and β may be guessed, and the resulting integral expression be evaluated by numerical methods.

The forward rate expression when steam is the limiting species can be written as:

$$- r_B = k_1 C_A^{\alpha} C_B^{\beta} \tag{55}$$

Inserting the values of C_A and C_B from Equations (40) and (41), respectively in the above equation, and using the result in the design equation (Equation 48), we get,

$$\tau = \frac{1}{k_1} \int_0^{X_{Bf}} \frac{(1 + \epsilon_B X_B)^{\alpha+\beta}}{C_{Bo}^{\alpha+\beta-1}(\theta_A - X_B)^{\alpha}(1 - X_B)^{\beta}} \, dX_B \tag{56}$$

It could be shown that

$$\theta_B = F_{Bo}/F_{Ao} = C_{Bo}/C_{Ao} = 1/\theta_A \tag{57}$$

$$X_B = X_A/\theta_B, \quad dX_B = dX_A/\theta_B \tag{58}$$

and, $\quad \epsilon_A/\epsilon_B = F_{Ao}/F_{Bo} = \theta_A \tag{59}$

Using Equations (57), (58), and (59) in Equation (56), we get,

$$\tau = \frac{1}{k_1} \int_0^{X_{Bf}} \frac{(1 + \epsilon_A X_A)^{\alpha+\beta}}{(1 - X_A)^{\alpha}(\theta_B - X_A)^{\beta}} \, dX_A \tag{60}$$

Equation (60) is the same expression as Equation (52); which was derived earlier considering chlorine as the limiting species. Hence, it is not necessary to evaluate the integrals of Equation (60) separately.

Differential method for treating the integral reactor data

For the reverse Deacon reaction, the reaction rate depends on
more than one species (89). We can use the single variation of
species technique (38). In this approach, the concentration of one
reactant is varied, while the concentration of the other is held constant
by use of inert gases. At each molar flow ratio (i.e., when θ_B is
held constant), the experiments are to be repeated for various space-
times. The slope $dX_A/d\tau$, is obtained from the plot of conversion
against space-time. Then the rate is calculated for a given chlorine
concentration by use of the differential form of the design equation
(i.e., Equation (31)). The concentration of products can be evaluated
from Equations (22), (25), (26), (27), and (28). When the rate is
plotted against concentrations on a log-lot plot, the slope will be
the order of reaction for this species. After determining the reaction
order for the first species, the concentration of the second species is
varied while that of the first one is held constant. The procedure is
repeated for the second species to determine its order. In order to
determine the effects of product concentrations, it is necessary to
run experiments at equi-molar reactant flow rates (i.e., $\theta_B = 1$).
The operating range of the temperature should be such that the re-
verse reaction may be considered minimum.

The results of the concentration dependency of individual species
on rate are then synthesized to form the rate expression (38). The
rate law so obtained is only approximate, with unknown parameters.
This is to be verified by use of regression analysis, which will
result in a correlation coefficient and values of the parameters. The

known rate expression is then subjected to verification by integral
approach at the same temperature. A comparison can be made when
the specific reaction rate is obtained by these methods. If the
validity of the resulting expression is acceptable, the rate law
then can be extended to other temperatures to determine the value of
the rate constants at those temperatures.

Calculation of Equilibrium Constant and Equilibrium Conversion

The activity of a component i is defined as

$$a_i = \frac{\bar{f}_i}{f_i^o} = \frac{y_i f_i}{f_i^o} = \frac{y_i \nu_i P}{f_i^o} \tag{61}$$

where, a_i = activity of a component i in a mixture

$\bar{f}_i$ = partial fugacity of component i

f_i^o = fugacity of component i in its standard state

y_i = mole fraction of component i

f_i = fugacity of pure component i at the pressure and
temperature of the reacting system

$\nu_i = (f/P)_i$ = fugacity coefficient for component i evaluated
at temperature and pressure of the reacting system.

Let the standard state of all components be chosen as pure gases at
1 atmosphere. The assumptions of ideal gas behavior for all pure
components lead to the results:

$$f_i^o = 1 \text{ atm, and } \nu_i = 1$$

When the reaction is operated at 1 atmosphere, the activity of

component i simplifies to

$$a_i = y_i = n_i/n_t \tag{62}$$

where, n_i = number of moles of species i at equilibrium, and

   n_t = total number of moles of gaseous mixture at equilibrium.

The equilibrium constant K_a, based on activity can be expressed

as ratio of products to reactants; and for the reverse Deacon reac-

tion, the equilibrium constant can be written as:

$$K_a = \frac{(a_C)^2 (a_D)^{1/2}}{(a_A)(a_B)} \tag{63}$$

Inserting the values of a_i's as derived earlier in Equation (62), we

obtain:

$$K_a = \frac{(n_C/n_t)^2 (n_D/n_t)^{1/2}}{(n_A/n_t)(n_B/n_t)} \tag{64}$$

Dividing through the numerator and denominator of Equation (64) by V,

and rearranging the terms, the following equation will be obtained:

$$K_e = K_a = \frac{C_C^2 C_D^{1/2} V^{1/2}}{C_A C_B n_t^{1/2}} \tag{65}$$

where $C_i = n_i/V$ \hfill (66)

Using ideal gas law, PV = nRT, or (P/RT) = (n/V), Equation (65) can

be reduced to

$$K_e = \frac{C_C^2 C_D^{1/2}}{C_A C_B} \left(\frac{RT}{n_t}\right)^{1/2} \tag{67}$$

Inserting the values of C_A, C_B, C_C, and C_D as defined in Equations (25)

through (28), we can rewrite the equilibrium constant expression, which

upon simplification will give:

$$K_e = (\frac{RT}{P})^{1/2}(2\sqrt{2})\frac{C_{Ao}^{1/2}X_e^{5/2}}{(1 + \frac{1}{2}y_{Ao}X_e)^{1/2}(1 - X_e)(\theta_B - X_e)} \qquad (68)$$

C_{Ao} in the above equation can be eliminated by $y_{Ao}P/RT$, and hence, the expression for the equilibrium constant becomes,

$$K_e = \frac{(2\sqrt{2})(y_{Ao})^{1/2}(X_e)^{5/2}}{(1 + \frac{1}{2}y_{Ao}X_e)^{1/2}(1 - X_e)(\theta_B - X_e)} \qquad (69)$$

Equation (69) is the expression for the equilibrium constant in terms of equilibrium conversion.

Equation (1) was written for the Deacon reaction, and this expression can be modified for the reverse Deacon reaction. The equilibrium constant as a function of temperature is written as:

$$\ln K_e = \frac{1}{2}[- \frac{5881.7}{T} + 0.93035 \ln T - (1.3704)(10^{-4})T$$

$$+ (1.7581)(10^{-8})T^2 + 4.1744] \qquad (70)$$

The numerical value of the equilibrium constant K_e, from Equation (70) can be inserted in Equation (69) and the resulting equation can be solved for equilibrium conversion X_e. A numerical technique, namely Newton-Raphson's technique, could be used to find the value of equilibrium conversion (16).

Reverse Reaction

If the measured conversions are less than 50% of the equilibrium conversion, the reverse reaction can be neglected. It is assumed that

the reverse reaction does not have any significant contribution at this condition. However, it is not so when the measured conversion is more than 50% of the equilibrium conversion. The method to evaluate the equilibrium conversion was described above, and the experimental observations can be compared with this value to determine the impact of the reverse reaction.

When the reaction reaches equilibrium, the rate of the forward reaction should equal the rate of the reverse reaction. The equilibrium constant K_e, can be written in terms of forward and backward reaction rate constants as

$$K_e = k_1/k_{-1} \tag{71}$$

In the overall reaction, which is the combination of the forward and backward reaction, one of the rate constants can be eliminated by use of equilibrium constant. The resulting equation is then subjected to verification for linear relationship between τ and the integral I. The method of treating the overall reaction rate expression will be similar to the integral analysis as discussed earlier.

Stimulus Response Technique

In the previous sections we developed analytical expressions to calculate space-time for a plug flow reactor from the given conversion data. In order to get this information, we assume that the reactor in question is an ideal plug flow reactor. But, in real situations the deviations from an ideal reactor can be considerable. Channeling

of fluid or creation of stagnant regions in the vessel normally cause

such deviations. According to Denbigh (27), transverse temperature

gradient, transverse and longitudinal diffusion, and transverse

velocity gradient are major factors to cause deviations. Nonideal

flow factors cannot be ignored, because they may lead to gross errors

in design of scale up operations.

It is, indeed, required to know what is happening in the reactor

vessel when fluids are allowed to react in it. If we know the velocity

distribution map of the fluid, then we can predict the behavior of the

vessel as a reactor. But is is difficult to measure velocities and

concentrations of the species within the reactor. However, it is

possible to get data on the feed and effluent streams. The extent of

nonideal flow can be characterized by means of the exit age distribu-

tion function (37, 63). The experiments involved for determining the

effluent age distribution use stimulus response technique. The system

is disturbed and the response to this stimulus is studied in such

experiments. Many kinds of input signals are used in practice (37).

In our experiments, we treated a pulse signal to study the behavior of

the vessel. In addition to this, we assume that there is no reaction

and no density change in the flow process, and the flow is considered

to be at its steady state.

Development of equations

Nonideal flow within the reactor is described by many types of flow

models. An analogy can be drawn between mixing in an actual flow and

a diffusional process. This type of model is called a dispersion model,

which is important to us in the existing system as we hope to use a plug flow model in our experiment. In a plug flow reactor, back mixing and intermixing may superimpose the flow field. It is also required that there be no gross bypassing or short circuiting of the fluid in the vessel. But fluctuations may be caused by different flow velocities and by molecular and turbulent diffusion. Shuffling of material and eddies are involved in a mixing process, and they are repeated quite frequently during the flow of fluid through the vessel. It is assumed that this disturbance is statistical in nature and is very similar to molecular diffusion (37). The one-dimensional (in the direction of flow) equation for molecular diffusion can be written as (76):

$$\frac{\partial c'}{\partial \theta} = \mathcal{D} \frac{\partial^2 c'}{\partial x^2} - u \frac{\partial c'}{\partial x} \tag{72}$$

In a similar fashion, we may consider all contributions to back mixing of fluid in the x-direction and the resulting equation is (37):

$$\frac{\partial c'}{\partial \theta} = D_1 \frac{\partial^2 c'}{\partial x^2} - u \frac{\partial c'}{\partial x} \tag{73}$$

Here, the parameter D_1 (not $\mathcal{D}$) is known as the axial or longitudinal dispersion coefficient. This parameter uniquely characterizes the degree of back mixing. The radial and lateral mixing effects are not considered in Equation (73), as they are believed not to make a significant contribution. To make Equation (73) dimensionless, the following expressions are introduced:

dimensionless length, $z = x/L$

dimensionless concentration, $C = C'/C'_o$

dimensionless time, $\theta' = \theta/\bar{\tau}$

where, $\bar{\tau}$ = mean residence time

u = linear velocity of fluid

L = length of the reactor vessel

and the dimensionless equation is

$$\frac{\partial C}{\partial \theta'} = (\frac{D_1}{uL}) \frac{\partial^2 C}{\partial z^2} - \frac{\partial C}{\partial z} \qquad (74)$$

The dimensionless group (D_1/uL), is called the vessel dispersion number, and it measures the extent of axial dispersion in the vessel. The limits of this parameter are:

$D_1/uL \to 0$, negligible dispersion, hence plug flow

$D_1/uL \to \infty$, large dispersion, hence mixed flow.

Determination of dispersion number

In order to determine the value of dispersion number (D_1/uL), quantitatively, the following terms are defined:

$E(\theta)d\theta$ = fraction of fluid leaving vessel that has residence time (exit age) of $(\theta, \theta + d\theta)$.

Since all the fluid has some residence time in the vessel, the RTD is properly normalized, i.e.,

$$\int_0^\infty E(\theta)d\theta = 1 \qquad (76)$$

For the pulse tracer, $E(\theta)$ is defined as

$$E(\theta) = \frac{C(\theta)}{\int_0^\infty C(\theta)d\theta} \qquad (77)$$

$E(\theta)$ is found from the measured outlet concentrations in arbitrary units, because the outlet concentrations are themselves in arbitrary units. The exact amount of tracer injected need not be known. Then, the mean residence time can be calculated from

$$\overline{\tau} = \frac{\int_0^\infty \theta C(\theta)d\theta}{\int_0^\infty C(\theta)d\theta} \qquad (78)$$

or from discrete time values,

$$\overline{\tau} = \frac{\sum_{i=0}^\infty \theta_i C_i(\theta)\Delta\theta_i}{\sum_{i=0}^\infty C_i(\theta)\Delta\theta_i} \qquad (79)$$

where, $\overline{\tau}$ is the mean value of the centroid of the distribution and is important for location of distribution. The measure of the spread of the distribution is called the variance and is defined for a continuous form as,

$$\sigma^2 = \frac{\int_0^\infty \theta^2 C(\theta)d\theta}{\int_0^\infty C(\theta)d\theta} - \overline{\tau}^2 \qquad (80)$$

or in the discrete form as,

$$\sigma^2 = \frac{\sum\limits_{i=0}^{\infty} C_i(\theta)\theta_i^2 \Delta\theta_i}{\sum\limits_{i=0}^{\infty} C_i(\theta)\Delta\theta_i} - \bar{\tau}^2 \tag{81}$$

It is often convenient to use a dimensionless form of time, $\theta' = \theta/\bar{\tau}$; and a corresponding version of RTD, $E(\theta')$, which is defined by

$$E(\theta') = \bar{\tau}E(\theta) \tag{82}$$

Then the variance can be written as:

$$\sigma^2 = \int_0^{\infty} \theta^2 E(\theta)d\theta - \bar{\tau}^2 \tag{83}$$

or, in dimensionless form:

$$\sigma_\theta^2 = \frac{\sigma^2}{\bar{\tau}^2} = \int_0^{\infty} \theta'^2 E(\theta')d\theta' - 1 \tag{84}$$

For small extent of dispersion (i.e., when D_1/uL is small), the spreading tracer curve does not significantly change in shape as it passes through the measuring point. In such a case, the solution to Equation (74) has been given by Levenspiel (63):

$$C(\theta') = \frac{1}{2\sqrt{\frac{\pi D_1}{uL}}} \exp\left[-\frac{(1-\theta')^2}{4(D_1/uL)}\right] \tag{85}$$

This equation is the family of Gaussian or normal curves with mean = 1, and variance

$$\sigma_\theta^2 = \frac{\sigma^2}{\bar{\tau}^2} = 2(D_1/uL) \tag{86}$$

From Equation (86), it is then possible to obtain the numerical value of the dispersion number. It has been reported that the maximum error in such an estimate of D_1/uL is (63):

5% when D_1/uL is less than 0.01, and

0.5% when D_1/uL is less than 0.001.

EXPERIMENTAL

The experimental work can be divided into two parts: the first part deals with the experimental work conducted in search of the rate expression and the order of the reaction; whereas the second part is the work conducted to evaluate the behavior of the reactor vessel at the experimental conditions used in part one. The first part is further subdivided into two sections: (1) the experimental technique was employed in such a way that data can be used for analysis by the integral approach, as well as for the factorial experimental design analysis; (2) the second section was designed to collect data for analysis by the differential approach. The experimental methods for the two subsections are the same, except for the fact that an inert gas was used along with the reactants in the second section.

Experimental Design

It is known from the literature that the reverse Deacon reaction is an endothermic high temperature gas phase reaction. The effects of flow rates of chlorine and steam are not well-documented in the literature. In order to study the effects of temperature, flow rate of chlorine, and flow rate of steam on conversion, it is important to plan the experiment sequence to ensure that the data analysis will lead immediately to valid statistical inferences. The purpose of statistically designing an experiment is to collect the maximum amount of relevant information with a minimum expenditure of time and resources.

The type of design, which has come to be called a factorial design,

has found great popularity in industrial investigation. A factorial experiment allows us to study the interactions of various factors which influence the yield (8). In studying the reverse Deacon reaction, it is essential to study the effects of reaction temperature, flow rate of chlorine, and flow rate of steam, and the effects of interactions between them on conversions. This yields a 3-factor experiment and in this factorial design, 3 levels of each factor were decided on and are shown in Table 3. For each experimental run, it was also decided to have 3 replicates. Thus, this 3^3 factorial design having 3 replicates in each case with a total of 81 experimental runs would make it possible to predict the best combination of levels of factors and also would help us to search for the rate expression.

Experimental Procedure for Integral Analysis

A schematic block diagram of the process as assembled for this experimental work is shown in Figure 2. The high purity chlorine gas cylinder was purchased from Matheson Gas Company. It was fitted with a Matheson's model B-15 regulator having two gauges, which controls the gas pressure to the desired level. A Brooks full view model 1110, rotameter size-2 with steel and fittings was used to measure the chlorine flow rate. The rotameter with a tube No. R-2-15-AA and a glass float was specially designed to handle chlorine. Its range was from 10.4 to 154 cc/min of chlorine at STP. The rotameter was calibrated and operated at 10 psig and room temperature. Water from a syringe of 50 ml capacity was pumped by means of a syringe pump.

Table 3. Conditions for experimental factorial design

Factors	Levels		
	Low (1)	Medium (2)	High (3)
Temperature (^{O}K)	777.0	879.0	983.0
Chlorine flow rate at 294.0^{O}K and 1 atm. (cc/min)	51.02	76.92	100.00
Water vapor flow rate at 294.0^{O}K and 1 atm. (cc/min)	25.60	51.20	102.40
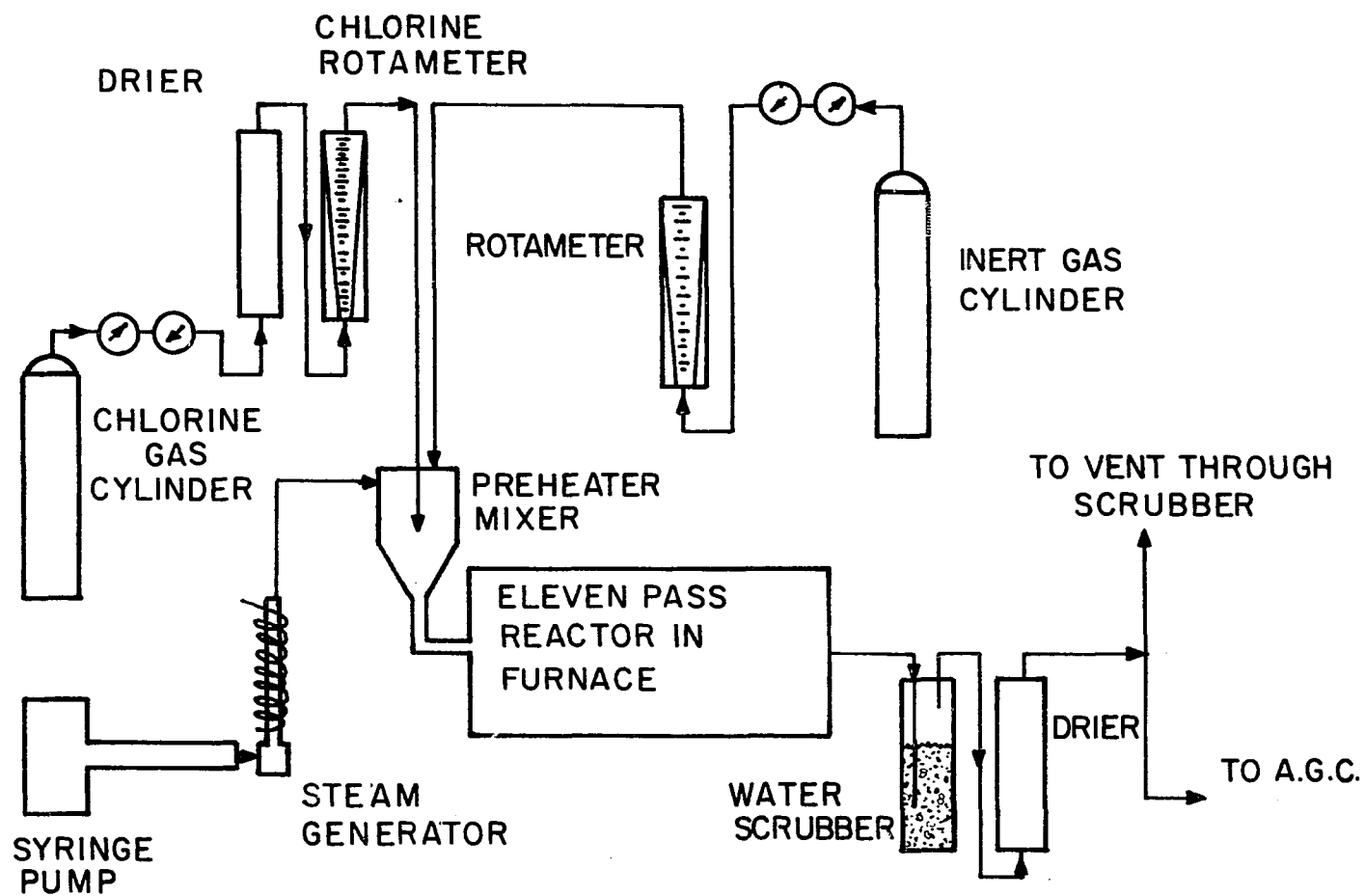
Figure 2.   Schematic block diagram of experimental equipment

The range of this syringe pump was from 0.00764 to 38.2 ml/min liquid water at STP. It was calibrated before installation in the system. The pump operated on a fixed gear system, hence it was not possible to get any intermediate flow rate of water between 0.0191 and 0.0382 ml/min, or 0.0382 and 0.0764 ml/min, and so forth. However, by use of a syringe of different size, an intermediate flow rate could be obtained. Water from the syringe pump was received by the steam generator, which was constructed of stainless steel. The heat input to the steam generator was supplied with heating tape controlled by a power-stat and a temperature of about 150°C was maintained throughout the generator so as to ensure that the steam would not condense on its way to the preheater mixer. Steam from the steam generator and chlorine gas from the rotameter and gas drier were allowed to mix in a preheater mixer, where a temperature of about 175-200°C was maintained throughout by means of a power-stat and heavy insulation of electrical heating tapes. Pope's 4 mm I.D. flow-tite corrugated flexible teflon tubes were used for connecting the chlorine lines. Glass tubing in the set up was normally joined by ball and socket joints. The chlorine gas inlet to the preheater mixer was extended towards the conical edge to prevent back flow of chlorine through steam lines. The reactor used was an eleven pass reactor having an I.D. of 4 mm and length of 511 cm. The total volume was calculated to be 64.25 ml. The reactor and the preheater mixer were made up of Vycor glass; their arrangements and sizes are shown in Figure 3 along with the syringe pump. The lines between the preheater mixer and the reactor were wrapped with insulating material.

The reactor furnace had four heating zones; two of these were
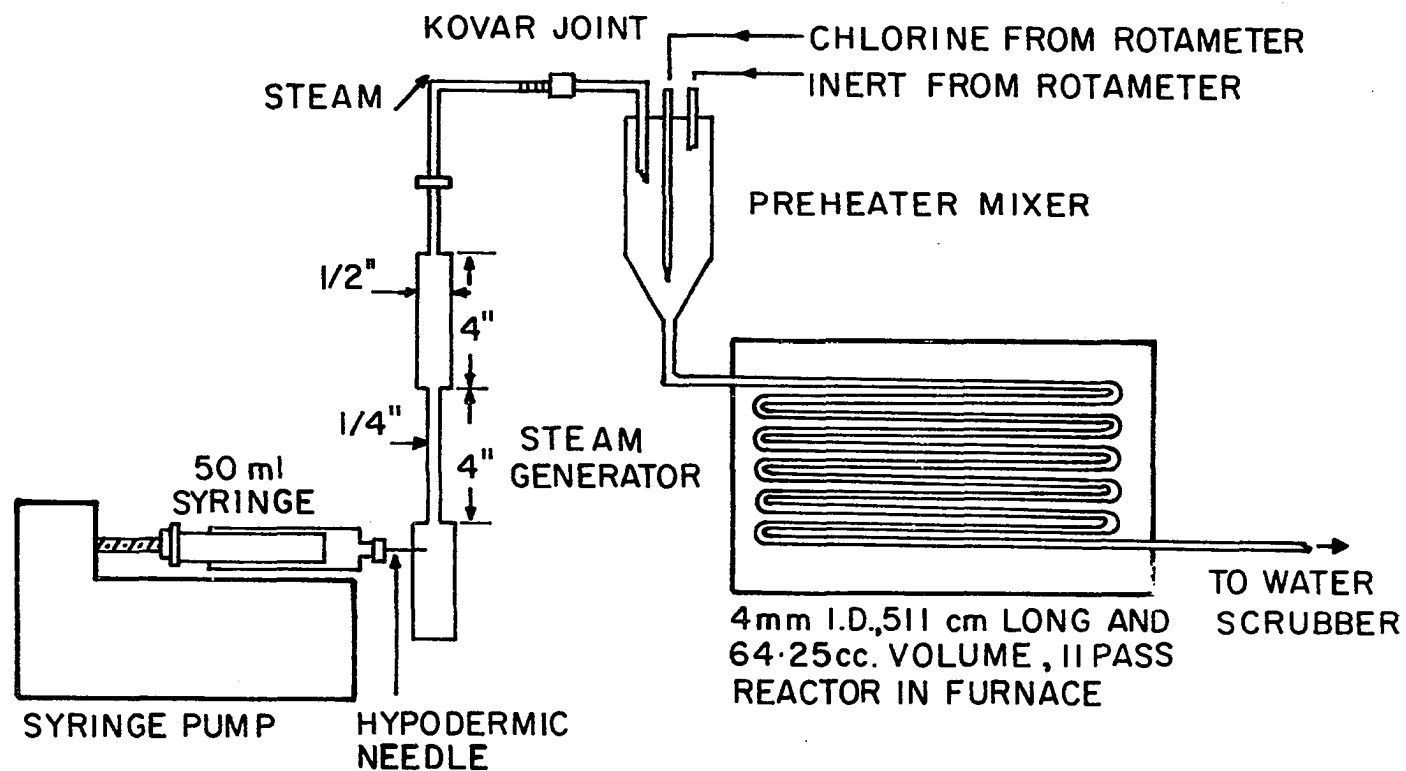
Figure 3. Syringe pump, steam generator, preheater mixer and eleven pass reactor assembly

controlled by a Honeywell Brown Protect-O-Van on-off controller; and the remaining two were controlled manually. The alumel-cromel thermocouples were used to measure temperature at different points in the reactor. A Leeds and Northrup millivolt potentiometer was used for calibration of scales, which read the furnace temperature. The reactor, which was inside the furnace, had five thermocouples to read temperature; and the steady average reading was taken as the reaction temperature.

The effluent gas from the outer end of the reactor was quenched with cold water in a scrubber. This makes it possible to stop any further conversion in either the forward or reverse direction as the temperature will be well below the reaction temperature. Also, one of the products, i.e., hydrogen chloride, will be absorbed by water. The remaining effluent stream consisted of unreacted chlorine and oxygen produced during the course of the reaction. The mixture of oxygen and chlorine gas was passed through a drier to absorb the mist in the stream. The dry gas was sent to the vent through a NaOH scrubber. Samples of dry gas were drawn periodically (every five minutes) during the steady state period. These samples were purged through an analytical gas chromatograph (Carle Model 111).

The chromatograph was operated at a column temperature of $45^{\circ}C$ and a purge flow rate of 30 ml per minute. To detect the concentrations of chlorine and oxygen thermisters were used. The columns used in the chromatograph were made up of tantalum with dimensions 1' x 1/8" and 1' x 1/8". Parapole T coated with 15% K-352 halocarbon oil with a mesh 80-100 were used as packing material in the columns. The oxygen peak eluted first and chlorine was back flushed, thus making a total retention

time of about five minutes. A tantalum sampling valve of 0.25 ml

capacity was installed for accurate injections of samples to the

columns. As carrier gas pure and dry helium gas was used at specified

flow rates (i.e., 30 ml/min).

Gas calibrations were based on injections of pure gas at the

same conditions; and it was assumed that the concentration dependence

was linear. This assumption is often used in the case of thermal con-

ductivity detectors. The calibration of the chromatograph was checked

every seven days during the course of the experimental work, and the

deviations noted were adjusted in the calculation of concentrations.

As the retention time was about five minutes, of sample a dry effluent

gas was injected every five minutes during the steady state period

and the process was repeated 4 to 5 times during a run. Weights of

graph paper under eluted peaks were recorded and were compared with

that of pure components for evaluation of composition in the ef-

fluent. The average of these 4 or 5 readings was used for calculation

of species concentration.

The experimental conditions used for this collection of conversion

data are shown in Table 3.

Experimental Procedure for Differential Analysis

The experimental equipment was the same as above for this work.

To obtain data for analysis by the differential method, the experi-

ments were conducted with an inert gas in the feed stream. Helium

was used as the inert gas to maintain the desired partial pressure

of the reactants. It passed through a calibrated rotameter at a desired flow rate to the preheater mixer as shown in Figure 2. It was thus mixed with the reactants before entering the reactor. In this experimental work, a wide range of flow rates of chlorine and helium were used. This was accomplished by replacing the rotameter tubes with No. R-2-15-B and No. R-2-15-AAA (along with steel and quartz floats as required). The rotameters were calibrated with the respective gases prior to use in the system, and the calibrations were checked every 15 days.

In this case, the samples drawn from the effluent stream were a mixture of helium, oxygen and chlorine. Since the carrier gas in the chromatograph was helium, helium in the effluent stream did not cause a difference in the thermal conductivity, and therefore, no helium peak was recorded by the recorder. The operating conditions for the gas chromatograph were the same as in the integral analysis. The composition of the effluent stream was calculated in the same manner as described earlier.

In the present experimental work, the partial pressure of chlorine was held constant at 0.8 atm., while that of water vapor was varied from 0.01 to 0.2 atm. At each molar flow ratio (θ_B) the experiments were repeated for different space-times. The procedure was reversed by holding the partial pressure of water vapor constant at 0.8 atm, and varying that of chlorine from 0.01 to 0.2 atm. Eight experimental runs were designed at different volumetric flow rates, but at equi-molar flow. In this case the partial pressure of each reactant was held constant at 0.5 atm, and no inert gas was used. The reaction

temperature for the experimental work (collection of data for differential analysis) was held constant at 879°K.

Stimulus Response Experiment

For studying the reactor behavior in the stimulus response experiment, the experimental set up was modified as shown in Figure 4. It was not possible to operate with chlorine in the reactor at the desired flow conditions. Instead, helium was allowed to pass through the reactor constantly. The flow rate of helium was measured by means of a calibrated rotameter or by means of a Wet Test Meter made by Precision Scientific Company. Air was injected into the flow of helium as a pulse input. About 50 to 250 ml of air was used for each experimental run. The off gas from the reactor was allowed to pass through the chromatograph. The columns of the chromatograph were bypassed and the effluent gas from the reactor was introduced directly to the thermal conductivity cell at one entrance. Helium was also used as carrier gas in this case and was introduced at the other entrance of the thermal conductivity cell. The thermal conductivity cell recorded the concentration difference between the carrier gas and the off gas constantly. When a pulse was introduced with the flow of helium at one entrance, a change in concentration occurred, and this change in concentration was recorded as sharp peaks by the recorder. The areas under the curve were calculated using Simpson's rule. Variance, mean time, and dispersion number were calculated for these peaks as described in the theory section.
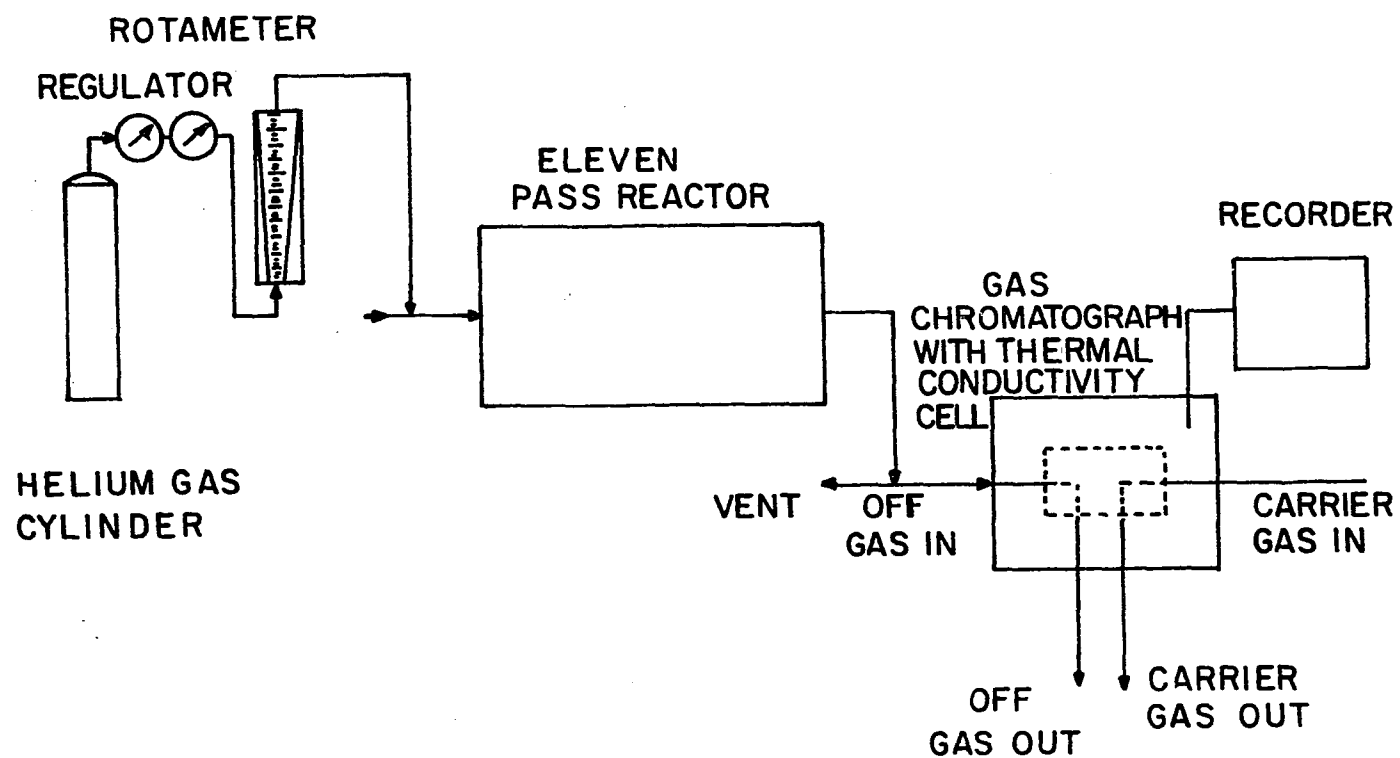
Figure 4.   Stimulus response experiment

EXPERIMENTAL RESULTS AND DISCUSSION

In order to use the plug flow assumptions for analysis of rate
data, it is necessary to know the behavior of the reaction vessel.
Therefore, the stimulus response experimental results are discussed
first after stating the general conditions for the experimental work
under which the measurements were made. Data were collected in two
phases: (1) for analysis using the integral technique at three
temperatures (504, 606, and 710°C). These results were also used for
the statistical analysis of the 3^3 factorial design. (2) For analysis
using the differential technique at 606°C. An approximate rate
expression was developed by this method and was verified by using data
obtained at 606°C by the integral analysis. Then the results were ex-
tended to other temperatures for evaluation of specific reaction
rates.

The principal experimental work was run at one atmosphere pressure
and at three different temperatures. The average furnace temperature
measured within the reactor by the thermocouples was considered as the
reaction temperature. Every time the furnace was turned on, it took
about 6 to 8 hours to get a steady temperature profile. A variation of
± 0.75 to ± 1.0 percent from the average value was observed, which is
considered to be within range. To get steady flow conditions, we had
to wait for 45 to 60 minutes for each experimental run. When the
variation in the peak heights as recorded by the recorder was found
to be fairly constant or the variation was found to be minimum, then
it was believed that the off-gas concentration was at its steady state.

However, the weights of the concentration peaks were found to vary by 3 to 4 percent from the average value. The measured conversions were calculated from the value of these peaks obtained at steady state conditions.

In Table 4, the experimental conditions and the measured conversions are listed against their experiment numbers. It is to be noted that an experiment (say 3B) is a replicate of another experiment (such as 3C) having the same prefix; but is independent of other experiments (such as 5C) having a different prefix number. Replication, as stated here, is merely a complete repetition of the basic experiment, and was run to get an estimate of the magnitude of the experimental error. In Table 5, the flow rate of chlorine and flow rate of water vapor at the reaction temperature are shown along with the equilibrium conversions and the mean value of the experimental conversions with standard deviations for each independent run. The equilibrium conversions were calculated solving Equation (69) numerically. The Reynold's number, $(D_t u \rho / \mu)$, for each independent experiment was also calculated after determining the average value of densities and viscosities of the reactants. They are reported in the last column of Table 5. A sample calculation procedure to evaluate experimental and equilibrium conversions, volumetric flow rate of the reactants at the reaction temperature, and Reynold's number are shown in Appendix B.

Table 4. Experimental conversions

Expt. #	Reaction temperature (°C)	Water vapor[a] flow rate (cc/min)	Chlorine[a] flow rate (cc/min)	Experimental conversion (%)
1A	504.0	25.60	51.02	6.67
1B	504.0	25.60	51.02	6.48
1C	504.0	25.60	51.02	5.37
2A	504.0	25.60	76.92	5.43
2B	504.0	25.60	76.92	5.47
2C	504.0	25.60	76.92	5.52
3A	504.0	25.60	100.00	4.92
3B	504.0	25.60	100.00	4.94
4A	504.0	51.20	51.02	8.23
4B	504.0	51.20	51.02	8.10
4C	504.0	51.20	51.02	7.71
5A	504.0	51.20	76.92	6.01
5B	504.0	51.20	76.92	5.98
5C	504.0	51.20	76.92	6.79
6A	504.0	51.20	100.00	4.84
6B	504.0	51.20	100.00	6.22
6C	504.0	51.20	100.00	4.95
7A	504.0	102.40	51.02	10.48
7B	504.0	102.40	51.02	10.43
7C	504.0	102.40	51.02	9.36
8A	504.0	102.40	76.92	7.84
8B	504.0	102.40	76.92	7.85
8C	504.0	102.40	76.92	7.62
9A	504.0	102.40	100.00	4.89
9B	504.0	102.40	100.00	5.07
9C	504.0	102.40	100.00	5.64
10A	606.0	25.60	51.02	20.24
10B	606.0	25.60	51.02	19.79
10C	606.0	25.60	51.02	19.36
11A	606.0	25.60	76.92	17.01
11B	606.0	25.60	76.92	16.82
11C	606.0	25.60	76.92	15.34
12A	606.0	25.60	100.00	12.28
12B	606.0	25.60	100.00	12.52
12C	606.0	25.60	100.00	13.26
13A	606.0	51.20	51.02	22.81
13B	606.0	51.20	51.02	22.43
13C	606.0	51.20	51.02	21.58

[a] At 294°K and 1 atm.

Table 4. Continued

Expt. #	Reaction temperature (°C)	Water vapor[a] flow rate (cc/min)	Chlorine[a] flow rate (cc/min)	Experimental conversion (%)
14A	606.0	51.20	76.92	18.74
14B	606.0	51.20	76.92	19.93
14C	606.0	51.20	76.92	19.53
15A	606.0	51.20	100.00	16.38
15B	606.0	51.20	100.00	16.43
15C	606.0	51.20	100.00	15.94
16A	606.0	102.40	51.02	24.10
16B	606.0	102.40	51.02	24.81
16C	606.0	102.40	51.02	19.41
17A	606.0	102.40	76.92	18.25
17B	606.0	102.40	76.92	19.72
17C	606.0	102.40	76.92	20.43
18A	606.0	102.40	100.00	18.25
18B	606.0	102.40	100.00	17.35
18C	606.0	102.40	100.00	18.41
19A	710.0	25.60	51.02	31.54
19B	710.0	25.60	51.02	31.90
19C	710.0	25.60	51.02	34.64
20A	710.0	25.60	76.92	28.05
20B	710.0	25.60	76.92	23.74
20C	710.0	25.60	76.92	25.04
21A	710.0	25.60	100.00	21.60
21B	710.0	25.60	100.00	19.05
21C	710.0	25.60	100.00	22.85
22A	710.0	51.20	51.02	41.08
22B	710.0	51.20	51.02	40.52
22C	710.0	51.20	51.02	40.59
23A	710.0	51.20	76.92	34.34
23B	710.0	51.20	76.92	33.74
23C	710.0	51.20	76.92	33.74
24A	710.0	51.20	100.00	31.45
24B	710.0	51.20	100.00	28.08
24C	710.0	51.20	100.00	30.78
25A	710.0	102.40	51.02	46.88
25B	710.0	102.40	51.02	47.83
25C	710.0	102.40	51.02	44.79
26A	710.0	102.40	76.92	39.42
26B	710.0	102.40	76.92	41.77
26C	710.0	102.40	76.92	36.59
27A	710.0	102.40	100.00	32.27
27B	710.0	102.40	100.00	37.66
27C	710.0	102.40	100.00	37.72

Table 5. Experimental and equilibrium conversions, and Reynold's number with experimental conditions[a]

Expt. #	Reaction temperature (°K)	Water vapor[b] flow rate (cc/min)	Chlorine[b] flow rate (cc/min)	Experimental conversion ± deviation (%)	Equilibrium conversion, X_e (%)	Experimental conversion as of % X_e (%)	Reynold's number $(D_t u \rho / \mu)$
1	777	67.66	134.84	6.17 ± 0.70	40.75	15.14	29.04
2	777	67.66	203.29	5.47 ± 0.05	29.46	18.57	41.22
3	777	67.66	264.29	4.62 ± 0.53	23.51	19.65	51.62
4	777	135.32	134.84	8.01 ± 0.27	62.78	12.92	33.59
5	777	135.32	203.29	6.26 ± 0.46	49.59	12.77	46.19
6	777	135.32	264.29	5.34 ± 0.77	41.36	12.91	57.38
7	777	270.63	134.84	10.09 ± 0.63	81.37	12.40	42.65
8	777	270.63	203.29	7.77 ± 0.13	71.21	10.91	55.17
9	777	270.63	264.29	5.20 ± 0.39	63.41	7.30	66.57
10	879	76.54	152.54	19.80 ± 0.44	43.24	45.79	25.71
11	879	76.54	229.98	16.39 ± 0.91	30.66	53.46	32.78
12	879	76.54	298.98	12.69 ± 0.51	24.21	52.42	46.58
13	879	153.08	152.54	22.27 ± 0.63	68.02	32.74	29.93
14	879	153.08	229.98	19.37 ± 0.56	53.28	36.36	41.01
15	879	153.08	298.98	16.25 ± 0.25	43.93	36.99	50.76
16	879	306.16	152.54	22.77 ± 2.93	86.31	26.38	38.46
17	879	306.16	229.98	19.47 ± 1.11	76.82	25.34	49.23
18	879	306.16	298.98	18.00 ± 0.57	71.96	25.01	59.22
19	983	85.60	170.59	32.69 ± 1.70	44.93	72.76	23.60
20	983	85.60	257.19	25.61 ± 2.21	31.40	81.56	33.72
21	983	85.60	334.35	21.17 ± 1.94	24.63	85.95	42.68
22	983	171.19	170.59	40.73 ± 0.31	72.03	56.55	27.11
23	983	171.19	257.19	33.94 ± 0.35	55.96	60.65	37.56

[a]Sample calculation procedure is shown in Appendix B.

[b]At reaction temperature and 1 atm.

Table 5. Continued

Expt. #	Reaction temperature ($^\circ K$)	Water vapor[b] flow rate (cc/min)	Chlorine[b] flow rate (cc/min)	Experimental conversion $\pm$ deviation (%)	Equilibrium conversion, X_e (%)	Experimental conversion as of % X_e (%)	Reynold's number ($D_t u \rho/\mu$)
24	983	171.19	334.35	30.10 ± 1.78	45.69	65.88	46.85
25	983	342.38	170.59	46.50 ± 1.56	89.66	51.86	33.68
26	983	342.38	257.19	39.26 ± 2.59	81.00	48.85	44.49
27	983	342.38	334.35	35.88 ± 3.13	72.75	49.32	53.67

Residence Time Distribution

In the stimulus-response experiments, the flow conditions were disturbed by a pulse input. Sharp peaks were obtained as response to these inputs and were recorded by the recorder attached to the chromatograph. Analysis of these peaks leads to the residence time distribution (RTD). The response peaks so obtained are very much comparable to that of an ideal plug flow reactor. The areas under the response curve were calculated by use of Simpson's rule. Variance, and the dispersion number for these peaks were calculated using Equations (81) and (86), respectively. The results obtained are tabulated in Table 6, and a sample calculation procedure along with response peaks has been shown in Appendix C.

The flow rate of helium gas through the reactor was varied from 200 to 20,000 cc per minute. This flow range is quite comparable to the flow conditions of the main experimental work. The variance of these peaks steadily decreased with the increase of flow rate of helium; this was also evidenced by sharper response peaks. Normally, in an ideal plug flow reactor, sharp peaks are obtained as response to pulse inputs. This simple analysis of RTD could lead to prediction of the vessel behavior as a reactor. There are other more complex methods available to describe the reactor (63); but the maximum error involved in estimating the dispersion number (D_1/uL), by this simple treatment is not more than 5% for small dispersion numbers.

The reverse Deacon reaction is endothermic, but the conditions can be assumed to be isothermal without much error. Therefore, the

Table 6. Variance and dispersion number[a]

Flow rate[b] of helium (cc/min)	Variance σ^2 (sec^2)	Dispersion number D_1/uL
200	0.17273	0.00217
400	0.14040	0.0024
700	0.17316	0.00095
750	0.16978	0.00086
1,000	0.1527	0.00091
1,250	0.14726	0.00077
2,000	0.14836	0.00064
20,000	0.09	0.000377

[a]Sample calculation procedure is shown in Appendix C.

[b]At 294°K and 1 atm.

transverse temperature gradient would not be the cause for deviation from plug flow. Another cause of deviation, the velocity gradient, is less significant than the influences of transverse temperature gradient in actual practice. The flow pattern on the basis of Reynold's number was found to be laminar. But the information from Table 6 suggests that the dispersion numbers at these flow conditions are small; thus, the deviations caused by velocity gradient may be considered negligible. From these discussions, it could be concluded that dispersion is not significant for the existing reactor, and therefore, plug flow conditions in the reactor can be assumed without significant error.

Experimental Design

The experimental design was a 3^3 factorial design. A general linear model procedure was followed to obtain the results. The model assumed was:

$$y_{ijkl} = \mu_{ijk} + T_i + W_i + C_k + (T \times W)_{ij} + (T \times C)_{ik}$$

$$+ (W \times C)_{jk} + (T \times W \times C)_{ijk} + e_{ijkl} \qquad (87)$$

where, y_{ijkl} = expected conversion of chlorine

   μ_{ijk} = mean value of conversion of chlorine

   T_i, W_j, C_k = effects of temperature, water flow rate, and chlorine flow rate, respectively, on conversion.

$(T \times W)_{ij}$, $(W \times C)_{jk}$, $(T \times C)_{ik}$, $(T \times W \times C)_{ijk}$ are effect of corresponding interaction terms on conversion with e_{ijkl} being the residual error.

The statistical analysis results are shown in Table 7. A correlation coefficient of 0.99 was obtained, which suggested that this model well-described the experimental factors. Analysis reveals that, within 95% confidence interval, interaction of water flow rate and chlorine flow rate has little effect on conversion, whereas, the effects of chlorine flow rate, water flow rate, temperature, interaction of temperature and chlorine flow rate, and interaction of temperature and water flow rate are significant in the same confidence interval.

The optimum condition to get a high conversion was found to be a combination of low level of chlorine flow rate (51.02 cc/minute); a high level of temperature (983°K); and a high level of water vapor flow rate (102.4 cc/minute). Temperature was found to have the most profound effect on conversion, followed, in order, by water flow rate and chlorine flow rate.

The measured conversions varied from 4.84 to 47.83% (i.e., the fractional conversion of chlorine). It is evident from Table 5 that the measured conversion is strongly favored by the reaction temperature. This is supplemented by a plot of water vapor flow rate versus conversion of chlorine in Figure 5. At all temperatures conversion was found to decrease with increasing chlorine flow rate, and with decreasing water vapor flow rate. This figure agrees with the statistical inference that experimental conditions of high temperature, low chlorine flow rate and high water flow rate result in higher conversion.

Table 7. Summary of statistical analysis results[a]

Source[b]	DF	SS	F	Pr > F
Temperature	2	10216.26	2845.71	0.0001
Water flow rate	2	619.09	172.45	0.0001
Chlorine flow rate	2	602.74	167.89	0.0001
Temperature water flow rate	4	377.13	52.52	0.0001
Temperature chlorine flow rate	4	151.22	21.06	0.0001
Water flow rate chlorine flow rate	4	1.17	0.16	0.9565

[a]A General Linear Model procedure with conversion as dependent variable was used.

[b]DF = Degree of freedom,

SS = Sum of the squares, and

$$F = \frac{s_1^2/\sigma_1^2}{s_2^2/\sigma_2^2}.$$
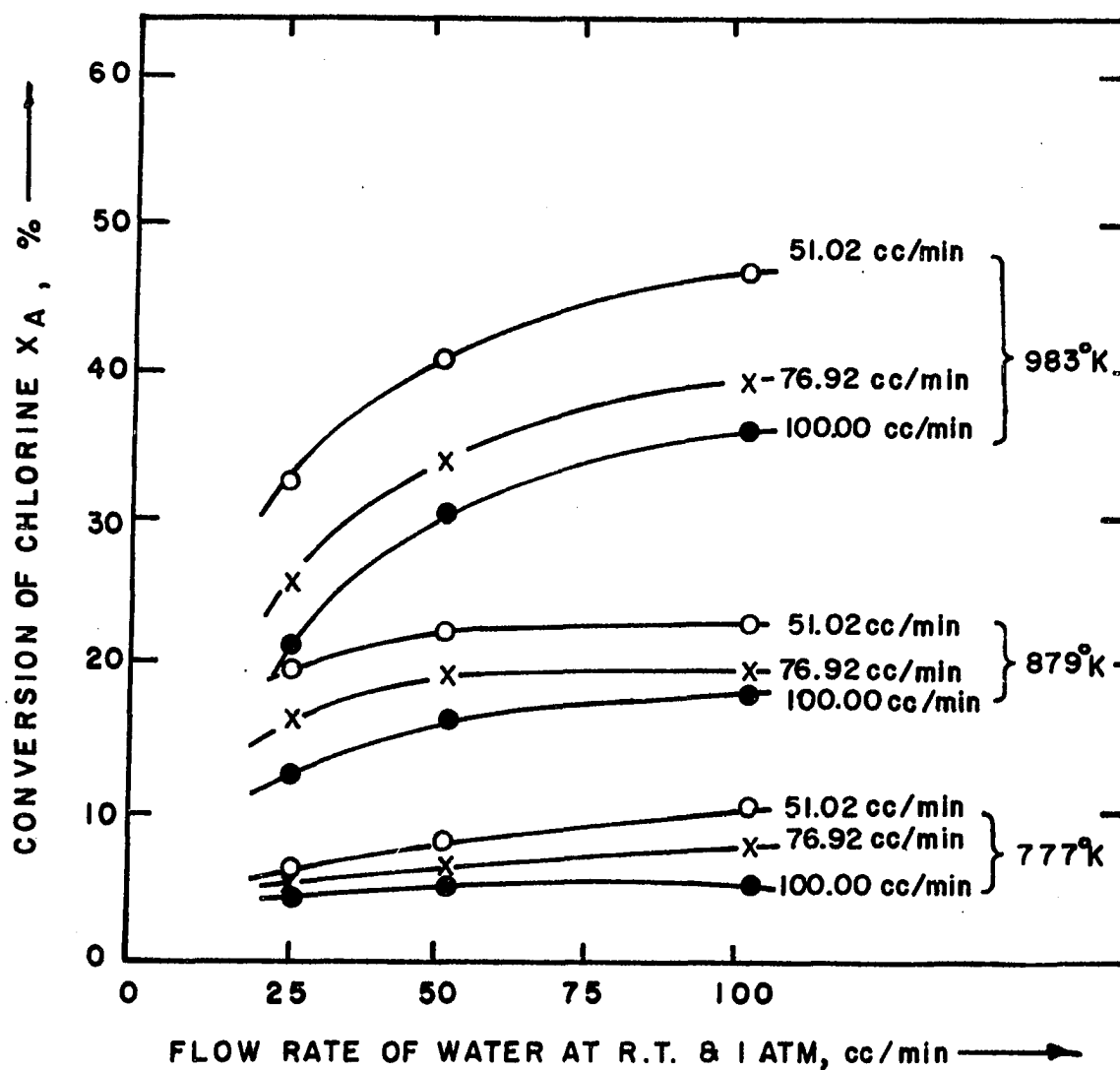
Figure 5. Conversion of chlorine as a function of water flow rate

Integral Analysis of Reactor Data

The calculated equilibrium conversion ranged from 23.51 to 89.6 percent at reaction conditions. On comparison of experimental conversion with these values (see Table 5), most results obtained at 777 and 879°K are less than 50% of the equilibrium values. But, this is not true for the results obtained at 983°K. It seems likely that the conversions at 777°K and 879°K are not affected by the reverse reaction, whereas, the results obtained at 983°K may have been influenced by the reverse reaction. The impact of this is discussed later. For the integral analysis, only the forward reaction was considered and only the lower temperature data were used.

The volume of the reactor V, and the volumetric flow rate of the reactants are known from the experimental conditions. The space-time, $(\tau = V/v_o)$, was calculated for each experimental run. The reactant flow rates (volumetric and molar), mole fraction in the feed stream, initial concentration of the reactants, and the molar feed ratios at feed conditions with space-time are shown in Table 8. Example calculations are done in Appendix B. The product concentrations were calculated using Equations (25) through (28), and are reported in Table 9.

Various combinations of order of reaction with respect to chlorine ($\alpha = 0.0, 0.5, 1.0, 1.5, 2.0$), and with respect to water ($\beta = 0.0, 0.5, 1.0, 1.5, 2.0$) were used in the integral form of the design equation. Equation (53) was integrated numerically using Simpson's rule. Regression analysis was used to test the correlation between space-time τ, and integral I. Among 25 possible models, the following

Table 8. Reactant flow rates, mole fraction and concentrations with space-time[a]

Expt. #	v_o (cc/min)	y_{Ao}	y_{Bo}	F_{Ao} (gmole/min) 10^3	F_{Bo} (gmole/min) 10^3	C_{Ao} (gmole/l) 10^3	C_{Bo} (gmole/l) 10^3	θ_B	Space-time τ (sec)
1	202.5	0.666	0.334	2.115	1.061	10.444	5.240	0.502	19.03
2	270.9	0.750	0.250	3.188	1.061	11.767	3.916	0.333	14.23
3	331.9	0.796	0.204	4.145	1.061	12.487	3.197	0.256	11.61
4	270.2	0.499	0.501	2.115	2.122	7.828	7.856	1.003	14.27
5	338.6	0.700	0.400	3.188	2.122	9.416	6.268	0.666	11.38
6	399.6	0.661	0.339	4.145	2.122	10.373	5.311	0.512	9.65
7	405.5	0.333	0.667	2.115	4.244	5.216	10.468	2.007	9.51
8	473.9	0.429	0.571	3.188	4.244	6.728	8.956	1.331	8.13
9	534.9	0.494	0.506	4.145	4.244	7.749	7.935	1.024	7.21
10	229.1	0.666	0.334	2.115	1.061	9.232	4.632	0.502	16.83
11	306.5	0.750	0.250	3.188	1.061	10.402	3.462	0.333	12.57
12	375.5	0.796	0.204	4.145	1.061	11.038	2.826	0.256	10.26
13	305.6	0.499	0.501	2.115	2.122	6.920	6.944	1.003	12.61
14	383.1	0 600	0.400	3.188	2.122	8.323	5.540	0.666	10.06
15	450.7	0.661	0.339	4.145	2.122	9.196	4.695	0.512	8.55
16	458.7	0.333	0.667	2.115	4.244	4.610	9.253	2.007	8.40
17	536.1	0.429	0.571	3.188	4.244	5.947	7.917	1.331	7.19
18	605.1	0.494	0.506	4.145	4.244	6.850	7.014	1.024	6.37
19	256.2	0.666	0.334	2.115	1.061	8.255	4.142	0.502	15.05
20	342.8	0.750	0.250	3.188	1.061	9.301	3.096	0.333	11.24
21	420.0	0.796	0.204	4.145	1.061	9.870	2.527	0.256	9.18
22	341.8	0.499	0.501	2.115	2.122	6.188	6.210	1.003	11.28
23	428.4	0.600	0.400	3.188	2.122	7.443	4.954	0.666	9.00
24	505.5	0.661	0.339	4.145	2.122	8.199	4.198	0.512	7.62
25	513.0	0.333	0.667	2.115	4.244	4.123	8.274	2.007	7.51
26	599.6	0.429	0.571	3.188	4.244	5.318	7.079	1.331	6.43
27	676.7	0.494	0.506	4.145	4.244	6.125	6.272	1.024	5.70

[a]Sample calculation procedure is shown in Appendix B.

Table 9. Concentration of products[a]

Experiment #	c_{Af} (gmole/1) 10^3	c_{Bf} (gmole/1) 10^3	c_{Cf} (gmole/1) 10^3	c_{Df} (gmole/1) 10^3
1	9.602	4.503	1.263	0.316
2	10.900	3.207	1.263	0.315
3	11.693	2.571	1.135	0.284
4	7.060	7.087	1.230	0.307
5	8.664	5.573	1.157	0.289
6	9.649	4.674	1.089	0.272
7	4.612	9.777	1.035	0.259
8	6.103	8.295	1.028	0.257
9	7.249	7.433	0.802	0.200
10	6.946	2.631	3.430	0.857
11	8.193	1.655	3.212	0.803
12	9.174	1.357	2.667	0.667
13	5.096	5.118	2.920	0.730
14	6.342	3.712	3.047	0.762
15	7.309	3.050	2.836	0.709
16	3.431	7.904	2.023	0.506
17	4.597	6.488	2.223	0.556
18	5.378	5.535	2.361	0.590
19	5.014	1.304	4.863	1.216
20	6.313	0.651	4.346	1.087
21	7.176	0.403	3.854	0.964
22	3.329	3.349	4.575	1.144
23	4.462	2.204	4.585	1.146
24	5.211	1.573	4.490	1.123
25	2.044	5.898	3.564	0.891
26	2.979	4.604	3.851	0.963
27	3.608	3.743	4.037	1.009

[a]Sample calculation procedure is shown in Appendix D.

showed a slightly better correlation. They are:

Model 2 $- r_A = k_1 c_B^{1/2}$ $R^2 = 0.42$

Model 3 $- r_A = k_1 c_B$ $R^2 = 0.29$

Model 7 $- r_A = k_1 c_A^{1/2} c_B^{1/2}$ $R^2 = 0.58$

Model 8 $- r_A = k_1 c_A^{1/2} c_B$ $R^2 = 0.34$

Model 12 $- r_A = k_1 c_A c_B^{1/2}$ $R^2 = 0.77$

Model 13 $- r_A = k_1 c_A c_B$ $R^2 = 0.43$

Model 14 $- r_A = k_1 c_A c_B^{3/2}$ $R^2 = 0.27$

Correlation coefficient values at $879^\circ K$ did not vary significantly from those at $777^\circ K$.

The equilibrium constant was evaluated using Equation (70), and the values are:

$$K_e(777) = 3.8587$$

$$K_e(879) = 6.3054$$

$$K_e(983) = 9.4118$$

Based on stoichiometry, a model was developed using the reverse reaction. This model was subjected to analysis for the data at $983^\circ K$, where the value of $K_e(983)$ was used to replace the backward reaction rate constant, k_{-1}. The resulting equation when treated by the integral analysis was found to be inconsistent with the data.

It is, therefore, concluded that the rate law representing the

reverse Deacon reaction is not elementary in nature. It is a complex expression consisting of reactant concentrations, and possibly product concentrations. The integral approach is particularly helpful to determine the specific reaction rates at different temperatures when the rate law at one temperature is known. It is thus decided to use the differential approach, where an approximate rate expression can be developed. And when such an expression is known, the rate expression will be subjected to verification by the integral approach.

Differential Analysis of Reactor Data

A rate law can be synthesized from experimental data, provided the rate is known at various initial compositions. The differential rates are obtained by plotting conversion against V/v_o (reciprocal of space-velocity). Generally, the slope of this curve is equal to the differential reaction rate at conditions corresponding to the reactants. The conversion versus V/v_o curve was obtained from a series of runs in the integral reactor. The reaction temperature in this experimental work was held constant at 879°K, which corresponds to the middle level of the experimental work designed for the integral analysis. These data were obtained in three operating modes: (a) C_{Ao} varied with C_{Bo} constant, (b) C_{Bo} varied with C_{Ao} constant, and (c) at equi-molar flow rates, i.e., $\theta_B = 1$.

C_{Ao} varied with C_{Bo} constant

The partial pressure of chlorine was varied and five such values were considered: 0.2, 0.15, 0.1, 0.05, and 0.01 atm. In this case,

the partial pressure of water vapor was held constant at 0.8 atm. Helium

was used as the inert gas to maintain the desired partial pressures.

The flow rates of chlorine, water vapor and the inert gas are shown in

Table 10. The values of experimental conversions and the equilibrium

conversions at reaction conditions are calculated and are reported in

the same table. It is observed that with low chlorine concentrations

(i.e., P_{A_O} = 0.01 and P_{B_O} = 0.8 atm), the theoretical conversion

approaches 100%. For these experimental conditions, the molar flow

rates, mole fractions and initial concentrations are shown in Table 11

along with corresponding space-times. Five values of molar flow

ratios (θ_B's) were used in this experimental work, and Figure 6 repre-

sents five conversion versus space-time plots. Slopes of these curves

at various space-times were determined graphically. At corresponding

space-times the product concentrations were calculated by use of

Equations (25) through (28). The value of experimental conversion

was either read from Figure 6 or was obtained from Table 10. A sample

procedure to evaluate rate and corresponding product concentrations

is shown in Appendix D. This procedure was applicable to all five

curves and the results are shown in Table 12. All five curves were

considered for space-time equal to 4.03 seconds, 2.02 seconds, and 1.01

seconds. But only one curve (i.e., θ_B = 80) was considered for other

space-times as reported in Table 12. This represents a slower rate

than others. It is evident from this table that the value of C_B

does not change appreciably; hence, it could be considered constant.

Once the rate and product concentrations are known for one space-

time, the rate is plotted against C_A on log-log graph paper. This

Table 10. Experimental and equilibrium conversion[a]

Expt. #	Water vapor[b] flow rate (cc/min)	Chlorine[b] flow rate (cc/min)	Inert gas[b] flow rate (cc/min)	Experimental conversion (%)	Equilibrium conversion (%)
28	102.40	25.64	0.0	32.04	94.55
29	256.00	64.11	0.0	29.94	94.55
30	512.00	128.22	0.0	24.45	94.55
31	1024.00	256.44	0.0	16.75	94.55
32	102.40	19.23	19.17	27.28	96.49
33	256.00	48.08	47.93	24.43	96.49
34	512.00	96.16	95.86	20.05	96.49
35	1024.00	192.32	191.72	14.25	96.49
36	102.40	12.82	38.33	22.73	98.12
37	256.00	32.08	95.91	18.56	98.12
38	512.00	64.16	191.82	13.75	98.12
39	1024.00	128.32	383.65	9.01	98.12
40	102.40	6.41	57.49	18.02	99.35
41	256.00	16.03	143.75	12.13	99.35
42	512.00	32.06	287.50	7.15	99.35
43	1024.00	64.12	575.00	3.66	99.35
44	102.40	1.28	72.83	6.25	99.94
45	256.00	3.21	182.11	2.93	99.94
46	512.00	6.42	364.22	1.51	99.94
47	1024.00	12.84	728.44	0.63	99.94

[a]Observations are made keeping C_{Bo} constant, and varying C_{Ao} at different space-times.

[b]At 294°K and 1 atm.

Table 11. Reactant flow rates, mole fraction and concentrations with space-time[a,b]

Expt. #	v^c (cc/min)	y_{Ao}	y_{Bo}	Y_{Io}	F_{Ao} (gmole/min) 10^3	F_{Bo} (gmole/min) 10^3
28	382.82	0.2	0.8	0.0	1.06	4.25
29	957.06	0.2	0.8	0.0	2.65	10.61
30	1914.13	0.2	0.8	0.0	5.29	21.06
31	3828.27	0.2	0.8	0.0	10.58	42.33
32	382.82	0.15	0.8	0.05	0.7963	4.25
33	957.06	0.15	0.8	0.05	1.99	10.61
34	1914.13	0.15	0.8	0.05	3.97	21.16
35	3828.27	0.15	0.8	0.05	7.94	42.33
36	382.82	0.10	0.8	0.10	0.534	4.25
37	957.06	0.10	0.8	0.10	1.33	10.61
38	1914.13	0.10	0.8	0.10	2.65	21.16
39	3828.27	0.10	0.8	0.10	5.29	42.33
40	382.82	0.05	0.8	0.15	0.264	4.25
41	957.06	0.05	0.8	0.15	0.66	10.61
42	1914.13	0.05	0.8	0.15	1.32	21.16
43	3828.27	0.05	0.8	0.15	2.65	42.33
44	382.82	0.01	0.8	0.19	0.0536	4.25
45	957.06	0.01	0.8	0.19	0.13	10.61
46	1914.13	0.01	0.8	0.19	0.26	21.16
47	3828.27	0.01	0.8	0.19	0.53	42.33

[a] Sample calculation procedure is shown in Appendix D.

[b] Experiment #32 and #36 were repeated with oxygen as diluent in place of helium.

[c] At reaction temperature and 1 atm.

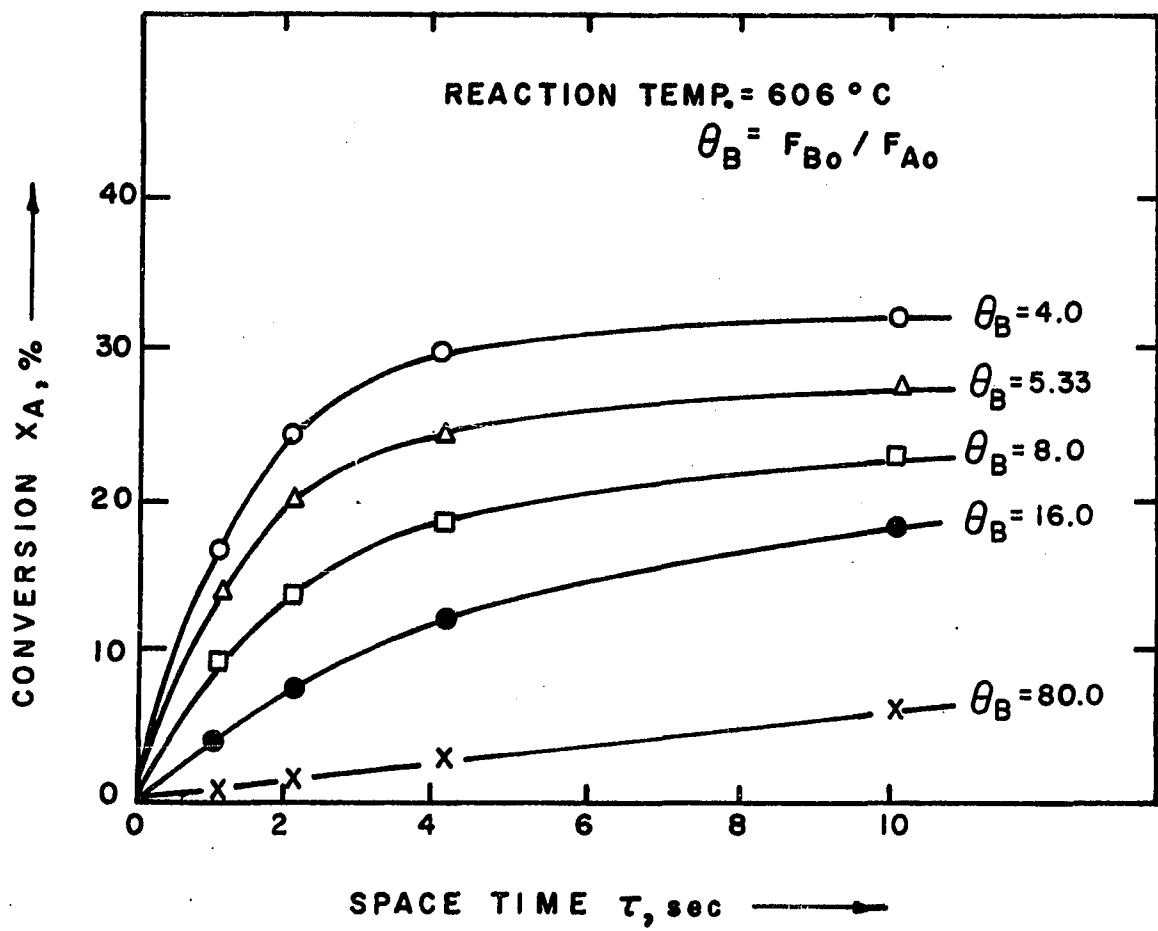| F_{Io} (gmole/min) 10^3	C_{Ao} (gmole/1) 10^3	C_{Bo} (gmole/1) 10^3	θ_B	Space-time τ (sec)
0.0	2.77	11.09	4.0	10.07
0.0	2.77	11.09	4.0	4.03
0.0	2.77	11.09	4.0	2.02
0.0	2.77	11.09	4.0	1.01
0.265	2.08	11.09	5.33	10.07
0.66	2.08	11.09	5.33	4.03
1.32	2.08	11.09	5.33	2.02
2.65	2.08	11.09	5.33	1.01
0.531	1.39	11.09	8.0	10.07
1.33	1.39	11.09	8.0	4.03
2.65	1.39	11.09	8.0	2.02
5.29	1.39	11.09	8.0	1.01
0.796	0.69	11.09	16.00	10.07
1.99	0.69	11.09	16.0	4.03
3.97	0.69	11.09	16.0	2.02
7.94	0.69	11.09	16.0	1.01
1.008	0.14	11.09	80.0	10.07
2.52	0.14	11.09	80.0	4.03
5.03	0.14	11.09	80.0	2.02
10.05	0.14	11.09	80.0	1.01

Figure 6. Space-time vs. conversion when C_{Bo} is kept constant

Table 12. Reaction rate and concentration of products[a,b]

Space-time[c] (sec)	Rate (gmole/1/sec) 10^3	C_A (gmole/1) 10^3	C_B (gmole/1) 10^3	C_C (gmole/1) 10^3	C_D (gmole/1) 10^3
4.03	0.0646	1.89	9.96	1.61	0.40
4.03	0.0420	1.54	10.39	1.00	0.25
4.03	0.0267	1.12	10.73	0.51	0.13
4.03	0.0109	0.61	10.97	0.17	0.042
4.03	0.000875	0.13	11.06	0.008	0.002
2.02	0.1346	2.04	10.16	1.32	0.33
2.02	0.0846	1.64	10.52	0.82	0.21
2.02	0.0491	1.19	10.83	0.43	0.09
2.02	0.0202	0.64	11.02	0.10	0.025
2.02	0.001085	0.13	11.07	0.005	0.001
1.01	0.3049	2.27	10.45	0.91	0.23
1.01	0.1716	1.76	10.68	0.59	0.15
1.01	0.0869	1.26	10.92	0.25	0.06
1.01	0.0246	0.67	11.06	0.05	0.0126
1.01	0.00126	0.13	11.08	0.0018	0.00044
3.0	0.00095	0.137	11.065	0.00602	0.0015
6.0	0.00087	0.134	11.029	0.0117	0.00293
8.0	0.00087	0.132	11.021	0.0144	0.0036
10.0	0.000865	0.131	11.018	0.01738	0.00435

[a]Rate of disappearance of chlorine is considered as rate.

[b]Sample calculation procedure is shown in Appendix D.

[c]At space-time 3.0, 6.0, 8.0 and 10.0 seconds, only one X-τ plot was considered corresponding to θ_B = 80.0, y_{Ao} = 0.01, C_{Ao} = 0.14 x 10^3 gmole/1.

relationship is shown in Figure 7, where a straight line gives the best fit. The slope of these lines is 1.92, or approximately 2.0. Therefore, it was concluded that the rate is second order with respect to chlorine concentration when C_{B_0} is held constant, i.e.,

$$- r_A \propto C_A^2 \tag{88}$$

From the results of Table 12, a similar plot between the rate and C_C resulted in a straight line relationship with a slope of 1. This plot is shown in Figure 8. It is to be noted that in this case the concentration of chlorine was allowed to vary while that of water was held constant. However, for further analysis and verification, we will consider that the rate of dissociation of chlorine is first order with respect to hydrogen chloride concentration:

$$- r_A \propto C_C \tag{89}$$

C_{B_0} varied with C_{A_0} constant

In this case, the partial pressure of chlorine was held constant at 0.8 atm, while that of water vapor was allowed to vary from 0.2 to 0.01 atm. Table 13 shows the detailed experimental conditions along with measured conversions. Equilibrium conversions are reported for comparison purposes. The molar flow rates, mole fractions, and inlet reactant conditions were calculated in a similar manner to that described earlier and are listed in Table 14. Figure 9 shows the results as obtained in this experimental work. Four molar flow ratios were considered in this case. In Part (a), the calculated space-times were the same for each molar flow ratio. They were changed by changing the volumetric
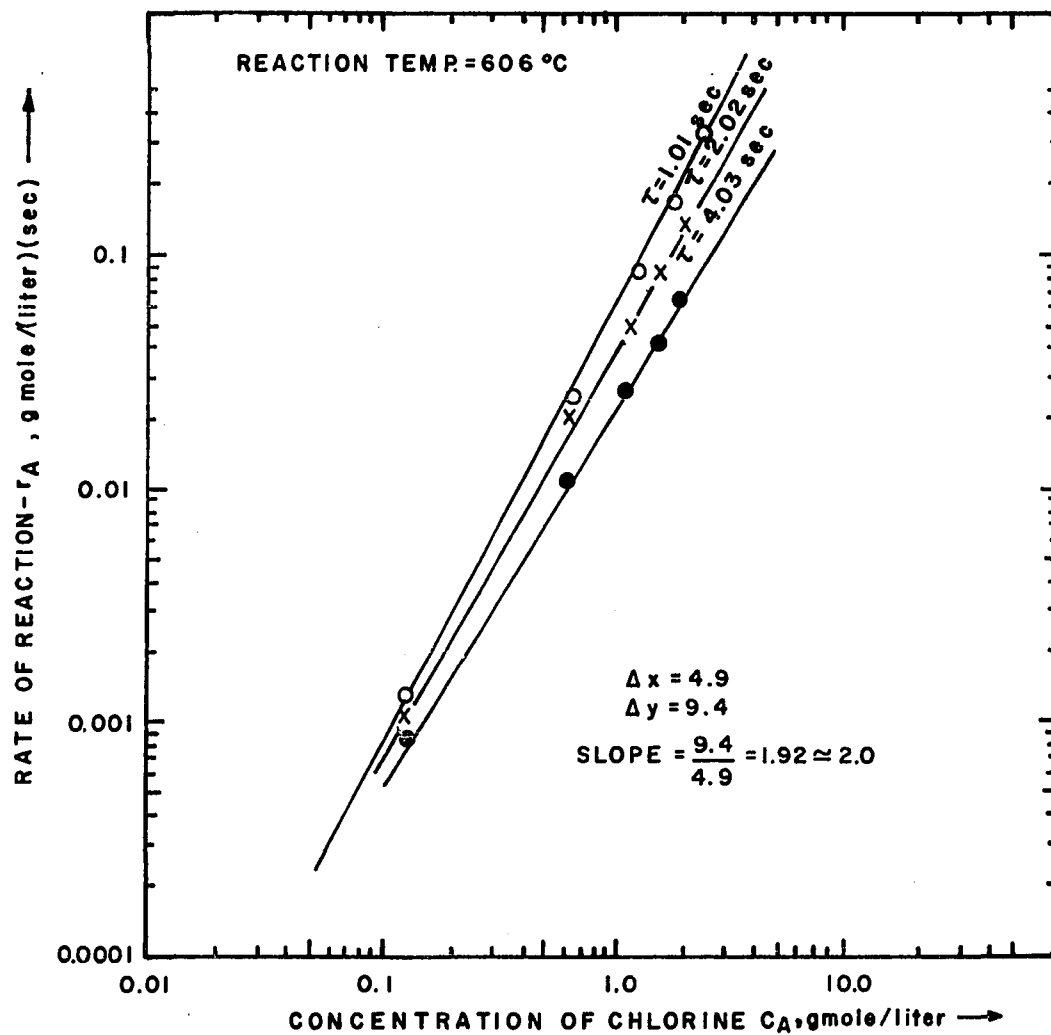
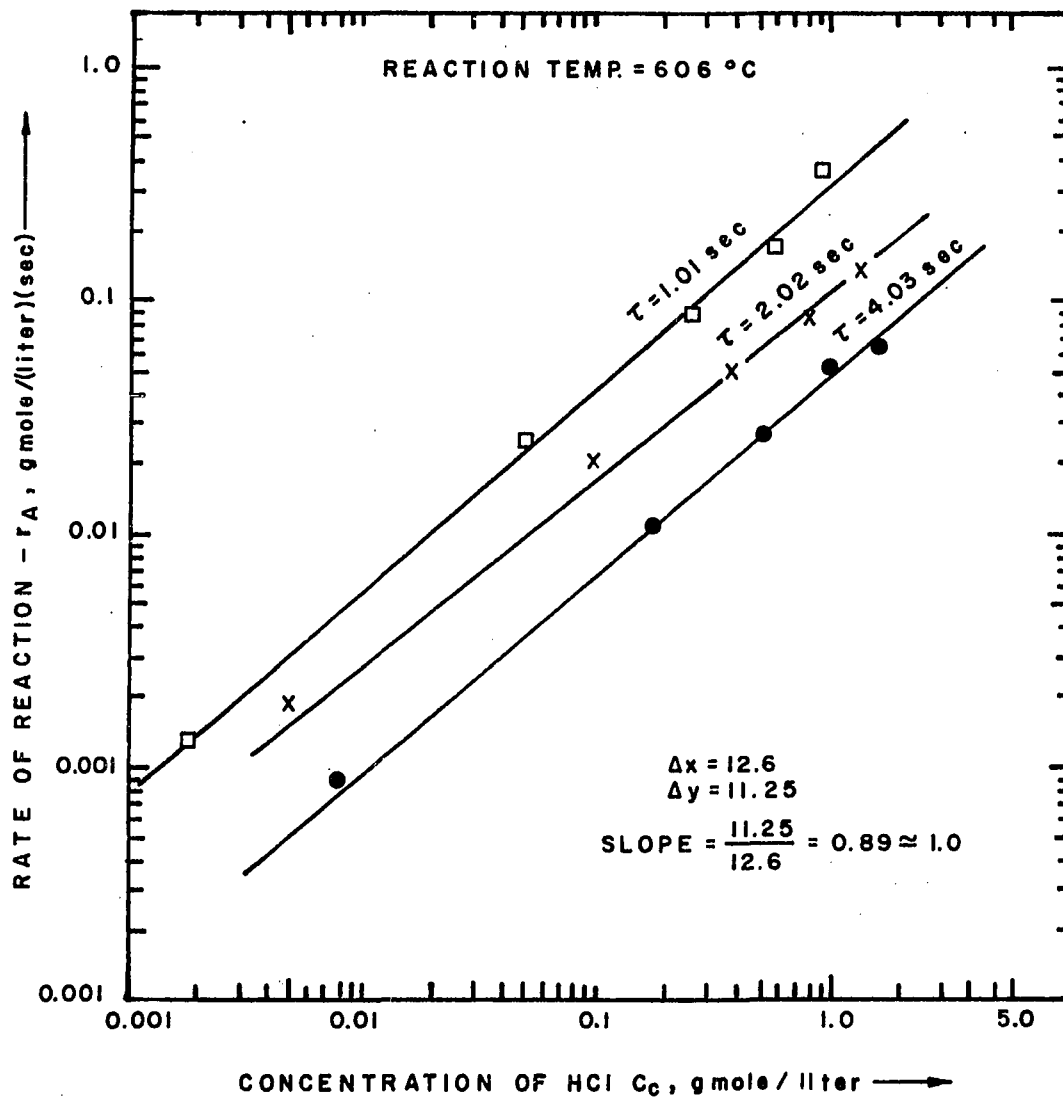Figure 7. Rate of reaction vs. concentration of chlorine when C_{Bo} is kept constant

Figure 8. Rate of reaction vs. concentration of HCl when C_{Bo} is kept constant

Table 13. Experimental and equilibrium conversions[a]

Expt. #	Water vapor[b] flow rate (cc/min)	Chlorine[b] flow rate (cc/min)	Inert gas[b] flow rate (cc/min)	Experimental conversion (%)	Equilibrium conversion (%)
48	10.24	41.04	0.0	14.751	23.64
49	25.60	102.56	0.0	10.952	23.64
50	51.20	181.34	0.0	7.801	23.64
51	10.24	54.71	3.42	10.902	18.09
52	25.60	136.77	8.55	8.403	18.09
53	51.20	241.91	15.11	4.106	18.09
54	10.24	82.07	10.24	9.202	12.27
55	25.60	205.15	25.60	6.103	12.27
56	51.20	362.67	51.20	2.850	12.27
57	10.24	164.14	30.78	5.204	7.21
58	25.60	410.30	76.93	2.903	7.21
59	51.20	725.35	136.00	1.296	7.21
60	10.24	819.20	194.56	1.170	1.81

[a]Observations are made keeping C_{Ao} constant, and varying C_{Bo} at different space-times.

[b]At 294°K and 1 atm.

Table 14. Reactant flow rates, mole fraction and concentrations with space-time[a,b]

Expt. #	v_o^c (cc/min)	y_{Ao}	y_{Bo}	y_{Io}	F_{Ao} (gmole/min) 10^3	F_{Bo} (gmole/min) 10^3
48	153.32	0.8	0.20	0.0	1.7	0.43
49	383.52	0.8	0.20	0.0	4.25	1.06
50	695.74	0.8	0.20	0.0	7.72	1.93
51	204.48	0.8	0.15	0.05	2.28	0.43
52	511.19	0.8	0.15	0.05	5.67	1.06
53	1529.52	0.8	0.15	0.05	16.96	3.18
54	306.63	0.8	0.10	0.10	3.40	0.43
55	766.28	0.8	0.10	0.10	8.50	1.06
56	1529.52	0.8	0.10	0.10	16.96	2.12
57	613.76	0.8	0.05	0.15	6.81	0.43
58	1529.52	0.8	0.05	0.15	17.02	1.06
59	7272.45	0.8	0.05	0.15	80.66	5.04
60	3061.55	0.8	0.01	0.19	33.96	0.42

[a]Sample calculation procedure is shown in Appendix D.

[b]Experiment #51 and #54 were repeated with oxygen as diluent in place of helium.

[c]At reaction temperature and 1 atm.

F_{Io} (gmole/min) 10^3	C_{Ao} (gmole/l) 10^3	C_{Bo} (gmole/l) 10^3	θ_B	Space-time τ (sec)
0.0	11.09	2.77	0.25	25.14
0.0	11.09	2.77	0.25	10.06
0.0	11.09	2.77	0.25	5.54
0.14	11.09	2.08	0.1875	18.85
0.35	11.09	2.08	0.1875	7.54
1.06	11.09	2.08	0.1875	2.52
0.43	11.09	1.39	0.125	12.57
1.06	11.09	1.39	0.125	5.03
2.12	11.09	1.39	0.125	2.52
1.28	11.09	0.69	0.0625	6.28
3.19	11.09	0.69	0.0625	2.52
15.12	11.09	0.69	0.0625	0.53
8.06	11.09	0.14	0.0125	1.26
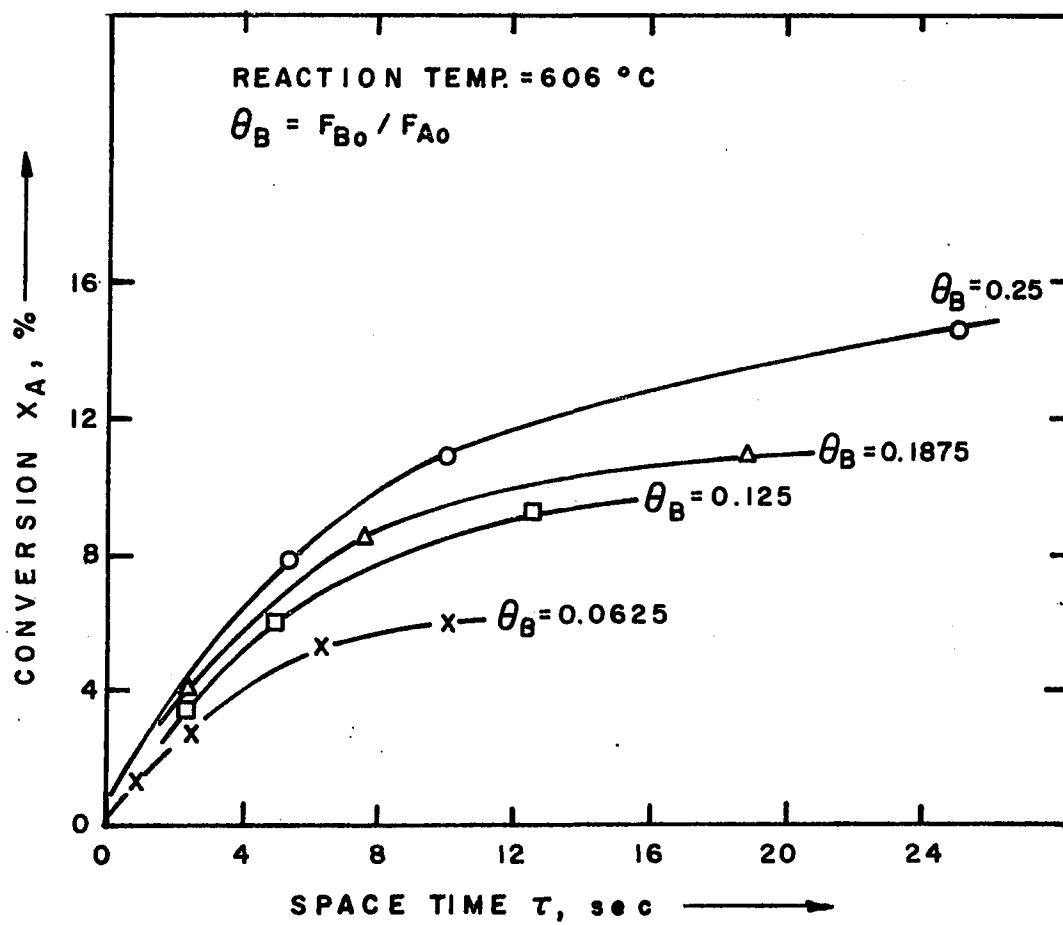
Figure 9. Space-time vs. conversion when C_{Ao} is kept constant

flow rates. But this is not the case for the present situation. The injection to the steam vaporizer was operated in a fixed gear system; therefore, it was difficult to have a flexible water flow rate to the system. Instead, chlorine flow rates were adjusted for a fixed water flow rate to maintain the desired partial pressures. This resulted in different space-times for each molar flow ratio. However, this adjustment did not affect the results, as the intermediate conditions were obtained either by interpolation or were read from the graph.

Figure 9 was used for determining slopes at observed points. The rates for various initial concentrations were calculated and the resulting values were plotted against space-time. This relationship is shown in Figure 10, and this figure was used for interpolation to find rate at desired space-time for various θ_B's. Four such space-times, such as 10.5, 8.0, 6.0, and 4.0 seconds were chosen, and the rates at these space-times were obtained from Figure 10. The values are shown in Table 15. The fractional conversions for the corresponding space-times were read from Figure 9. By use of Equations (25) through (28), the product concentrations were calculated, and they are shown in Table 15 against rate. (See Appendix D for detailed calculation procedure.)

From Table 15, it could be observed that the value of C_A did not change appreciably; but a substantial change in C_B is obtained. The calculated rate was then plotted against C_B on log-log axis as shown in Figure 11. The slope of these lines was measured. It is evident from this figure that the slope has changed its magnitude from 1 to 0.5 with respect to low to high concentration of water C_B. From the
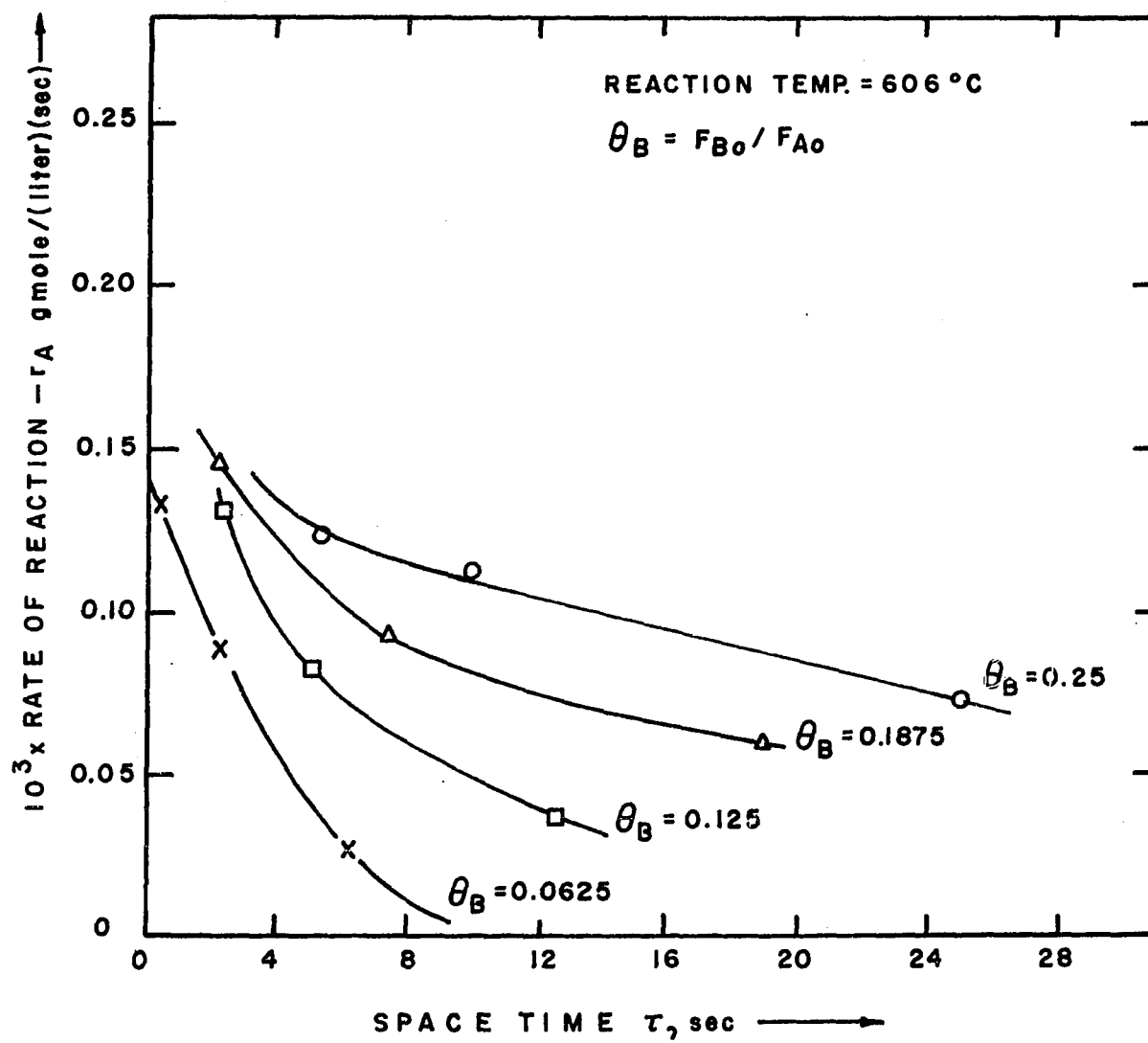
Figure 10. Space-time vs. rate of reaction when C_{Ao} is kept constant

Table 15. Reaction rate and concentration of products[a,b]

Rate (gmole/(1)(sec)) 10^3	c_A (gmole/1) 10^3	c_B (gmole/1) 10^3	c_C (gmole/1) 10^3	c_D (gmole/1) 10^3
Space-time = 10.5 sec				
0.110	9.437	1.474	2.361	0.590
0.078	9.461	0.829	2.327	0.582
0.045	9.798	0.417	1.846	0.462
0.002	10.166	0.016	1.321	0.330
0.00108	10.910	0.0088	0.258	0.065
Space-time = 8.0 sec				
0.116	9.622	1.619	2.098	0.524
0.089	9.782	1.075	1.869	0.467
0.058	9.933	0.519	1.653	0.413
0.0102	10.190	0.038	1.281	0.322
0.0055	10.920	0.0188	0.238	0.060
Space-time = 6.0 sec				
0.122	9.849	1.797	1.773	0.443
0.104	9.976	1.224	1.592	0.398
0.073	10.083	0.631	1.439	0.360
0.033	10.310	0.122	1.115	0.279
Space-time = 4.0 sec				
0.143	10.133	2.021	1.367	0.342
0.1245	10.235	1.423	1.221	0.305
0.096	10.310	0.800	1.115	0.279
0.060	10.467	0.237	0.890	0.223

[a]Rate of disappearance of chlorine is considered as rate.

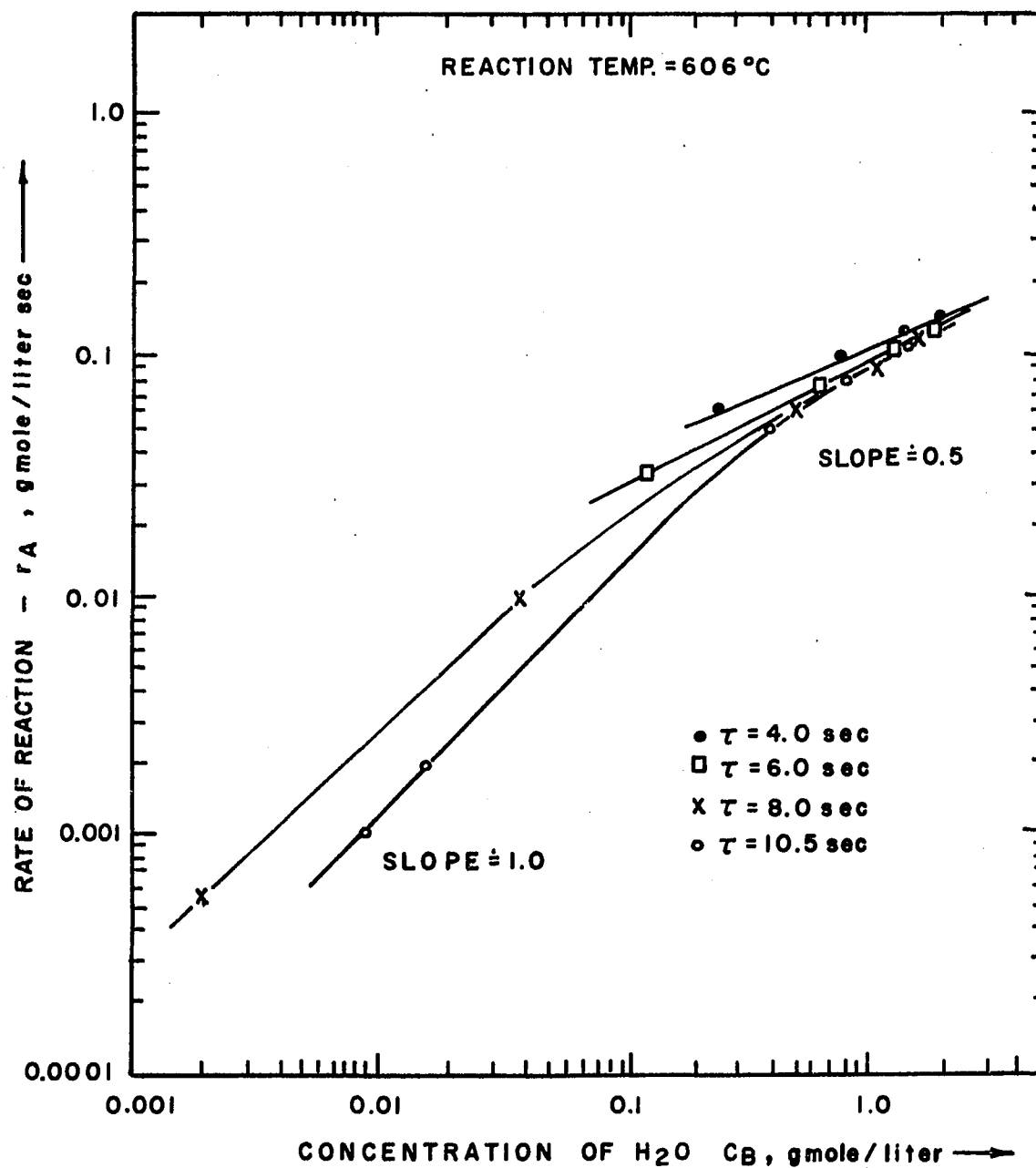[b]Sample calculation procedure is shown in Appendix D.

Figure 11. Concentration of H_2O vs. rate of reaction when C_{Ao} is kept constant

information presented in Figure 11, we find that at low concentrations of water vapor, the reaction rate is first order with respect to water vapor concentrations, i.e.,

$$- r_A \ \alpha \ C_B \tag{90}$$

and at relatively high concentrations of water vapor, the reaction rate is half order with respect to water vapor concentration, i.e.,

$$- r_A \ \alpha \ C_B^{1/2} \tag{91}$$

We would like to find a rate law that is consistent with the reaction rate data at both high and low water vapor concentrations. When the above two equations are combined into the form:

$$- r_A \ \alpha \ \frac{C_B}{1 + k_1' C_B^{1/2}} \tag{92}$$

for condition 1: at low C_B, $k_1' C_B^{1/2} \ll 1$ Equation (92) reduces to

$$- r_A \ \alpha \ C_B \tag{90}$$

for condition 2: at high C_B, $k_1' C_B^{1/2} \gg 1$ Equation (92) reduces to

$$- r_A \ \alpha \ C_B^{1/2} \tag{91}$$

A similar plot on log-lot scale between the rate and C_C is shown in Figure 12. There is no definite conclusion from this figure. The slopes were measured to be 2.0 for space-times 4 and 6 seconds. At the same time they were found to be nonlinear for the remaining two space-times.
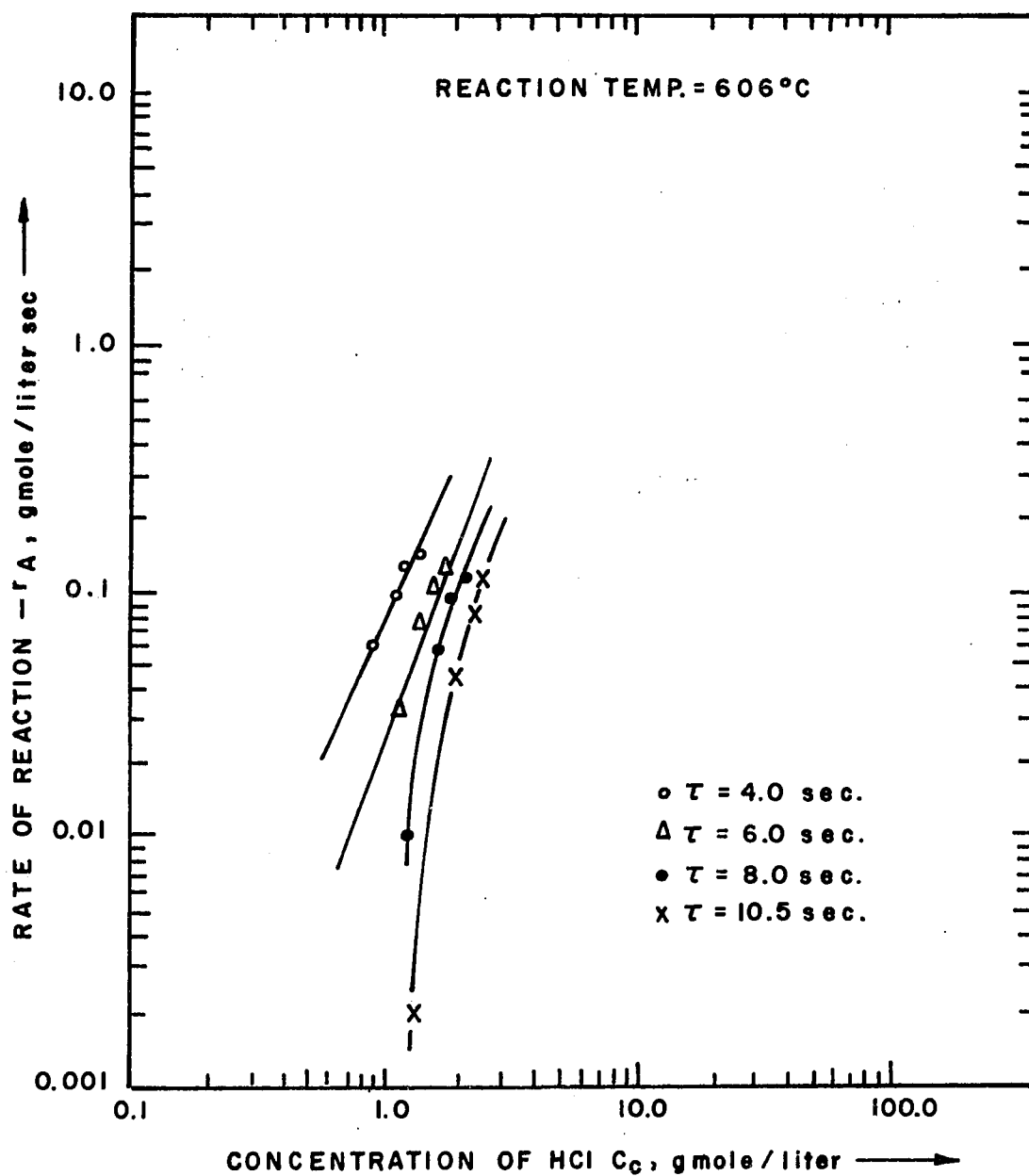
Figure 12. Concentration of HCl vs. rate of reaction when C_{Ao} is kept constant

Equi-molar flow rates

The concentrations of the reactants were held constant with

$\theta_B = 1$ for this experimental work. The partial pressure for each

reactant was at 0.5 atm. No inert gas was used in the system. Eight

experiments (Experiment #63 through #70) are presented in Table 16 with

their reaction conditions. The observed conversion values along with the

equilibrium conversions are also shown in this table. The detailed

flow conditions along with their space-times are reported in Table 17.

Figure 13 shows the relationship between space-time and conversion for

equi-molar flow conditions; and this curve was used for determination

of rate and corresponding product concentrations. The computed values

are listed in Table 18. In this experimental work C_{A_O} and C_{B_O} were

held constant for each run, as required to determine the effects of the

product concentrations on rate. A plot of rate versus C_C is shown in

Figure 14. From this log-log plot, it is observed that the rate of

conversion of chlorine decreases with increasing HCl concentration in a

nonlinear manner. It is believed that when no HCl is present in the

system, the rate is independent of hydrogen chloride concentration;

therefore, it has been represented by the dotted line in Figure 14.

One rate expression in which the concentration dependence of HCl is

consistent with the experimental observation is:

$$- r_A \propto \frac{1}{[C_C] + [\ ]} \tag{93}$$

In the above discussions, the effect of oxygen concentration on rate

was not considered. This is because it was found a small amount of

oxygen was present in the products with little or no variation in its

Table 16. Experimental and equilibrium conversions[a]

Expt. #	Water vapor[b] flow rate (cc/min)	Chlorine[b] flow rate (cc/min)	Experimental conversion (%)	Equilibrium conversion (%)
63	9.05	9.05	31.02	67.10
64	10.24	10.24	30.50	67.10
65	22.87	22.87	28.12	67.10
66	51.12	51.12	20.98	67.10
67	56.00	56.00	20.01	67.10
68	90.79	90.79	17.85	67.10
69	102.32	102.32	15.92	67.10
70	226.17	226.17	10.62	67.10

[a]Observations are made at equi-molar flow rates.

[b]At 294°K and 1 atm.

Table 17. Reactant flow rates, mole fraction, and concentrations with space-time[a]

Expt. #	v_o[b] (cc/min)	y_{Ao}	F_{Ao} (gmole/min) 10^3	C_{Ao} (gmole/1) 10^3	Space-time τ (sec)
63	54.12	0.5	0.38	6.93	71.22
64	61.23	0.5	0.42	6.93	62.95
65	136.78	0.5	0.94	6.93	28.52
66	306.15	0.5	2.12	6.93	12.59
67	334.87	0.5	2.32	6.93	11.51
68	542.87	0.5	3.76	6.93	7.10
69	611.81	0.5	4.24	6.93	6.30
70	1352.42	0.5	9.37	6.93	2.85

[a]Sample calculation procedure is shown in Appendix D.

[b]At reaction temperature and 1 atm.
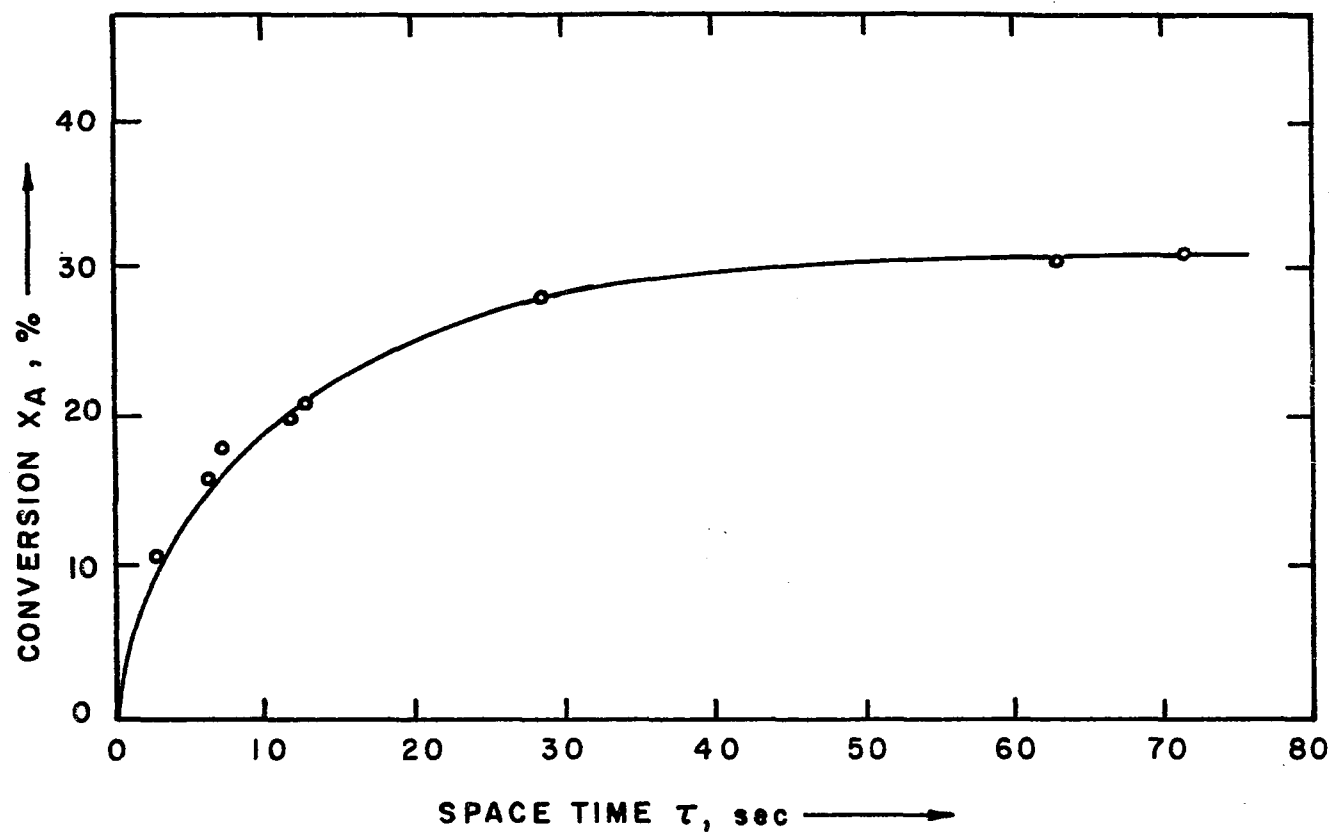
Figure 13. Space-time vs. conversion at equi-molar flow rate

Table 18. Reaction rate and concentration of products[a,b]

Expt. #	Rate (gmole/(1)(sec)) 10^3	c_A (gmole/1) 10^3	c_B (gmole/1) 10^3	c_C[c] (gmole/1) 10^3	c_D (gmole/1) 10^3
63	0.00447	4.44	4.44	3.99	1.00
64	0.0055	4.48	4.48	3.93	0.98
65	0.0144	4.66	4.66	3.64	0.91
66	0.0465	5.20	5.20	2.76	0.69
67	0.0522	5.28	5.28	2.64	0.66
68	0.0618	5.45	5.45	2.37	0.59
69	0.075	5.61	5.61	2.12	0.53
70	0.17464	6.03	6.03	1.44	0.36

[a]Rate of disappearance of chlorine is considered as rate.

[b]Sample calculation procedure is shown in Appendix D.

[c]Equilibrium hydrogen chloride concentration is 7.98×10^{-3} gmole/liter.
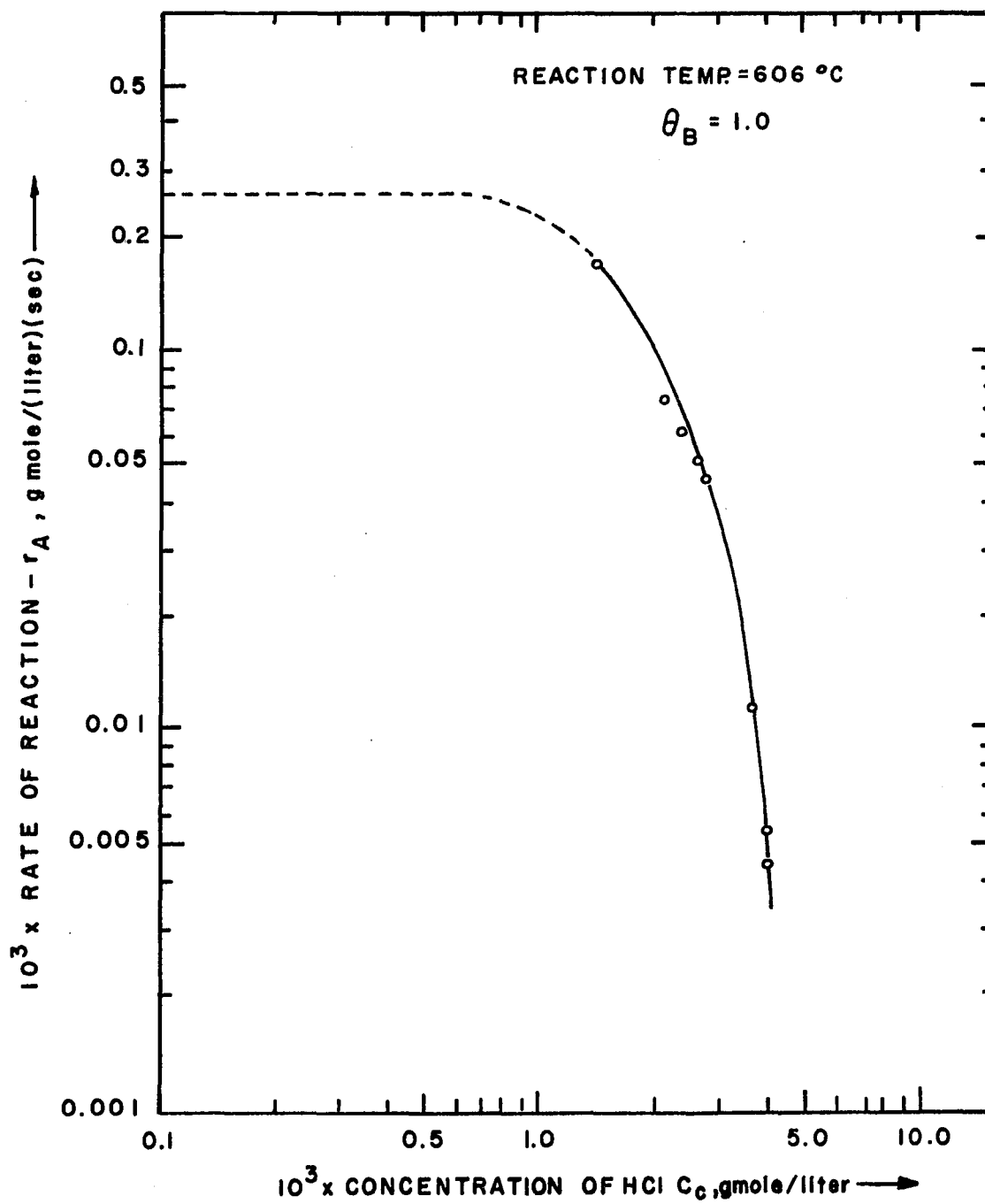
Figure 14. Concentration of HCl vs. rate at equi-molar flow rates

concentration. In addition to this, Experiments #51, 54, 32 and 36 were conducted with oxygen as a diluent instead of helium. These experiments were done independently in addition to original experiments with inert gas helium. The conversion data were unchanged when oxygen replaced helium; hence, the results were not reported independently. From these observations, we conclude that the forward rate is independent of oxygen concentration.

Synthesis of Rate Law

The concentration dependence of species A, B and C in the rate expressions are, respectively:

(1) $\quad - r_A \propto C_A^2$ $\qquad$ (from Figure 7) $\qquad$ (88)

(2) $\quad - r_A \propto \dfrac{k_1 C_B}{[\ ] + k_1' C_B^{1/2}}$ $\qquad$ (from Figure 11) $\qquad$ (92)

(3) $\quad - r_A \quad \dfrac{1}{C_C + [\ ]}$ $\qquad$ (from Figure 14) $\qquad$ (93)

Equations (88), (92), and (93) are combined to give

$$- r_A = \frac{k_1 C_A^2 C_B}{C_C + k_1' C_B^{1/2}} \qquad (94)$$

Also, we arrive at the following conclusions from Figures 8 and 12, respectively:

$$- r_A \propto C_C \qquad (89)$$

$$- r_A \propto C_C^2 \quad \text{or} \quad - r_A \neq f(C_C) \qquad (95)$$

Considering the above relationship, we approximate the following

rate expressions:

$$\text{Model } 102 - r_A = \frac{k_1 c_A^2 c_B}{1 + k_1' c_B^{1/2}/c_C} \tag{96}$$

$$\text{Model } 103 - r_A = \frac{k_1 c_A^2 c_B}{1 + k_1' c_B^{1/2}/c_C^2} \tag{97}$$

$$\text{Model } 104 - r_A = \frac{k_1 c_A^2 c_B}{1 + k_1' c_B^{1/2} c_C} \tag{98}$$

$$\text{Model } 105 - r_A = \frac{k_1 c_A^2 c_B}{1 + k_1 c_B^{1/2}} \tag{99}$$

$$\text{Model } 106 - r_A = k_1 c_A^2 c_B / c_C \tag{100}$$

$$\text{Model } 107 - r_A = k_1 c_A^2 c_B^{1/2} \tag{101}$$

Model 105 was included arbitrarily where no effect of C_C was assumed on the rate. Data obtained do not cover this assumption. Model 106 and 107 are the limiting conditions of Model 101 (Equation (94)), as discussed earlier. The rate laws are qualitatively consistent with the experimental observations. A rearrangement can be made for these expressions in the form

$$y = mx + c \tag{102}$$

Equation (94) can be rewritten as:

$$\frac{c_A^2 c_B}{- r_A c_C} = \frac{1}{k_1} + \frac{k_1'}{k_1} \frac{c_B^{1/2}}{c_C} \tag{103}$$

which represents an equation of a straight line with slope of (k_1'/k_1), and intercept of $(1/k_1)$, when $c_A^2 c_B - r_A c_C$ (call it X101) is plotted as

a function of $c_B^{1/2}/c_C$ (call it X101). A similar rearrangement can be done for Equations (96) through (99). The values of Y's and X's were computed and the following results were obtained when a regression analysis was made to determine the correlation between Y and X:

Model 101 $R^2 = 0.972$

Model 102 $R^2 = 0.025$

Model 103 $R^2 = 0.016$

Model 104 $R^2 = 0.534$

Model 105 $R^2 = 0.002$

This analysis suggests that Model 101 is consistent with the experimental observations. Computed values of Y101 and X101 are plotted in Figure 15. From regression analysis, the parameters were determined as:

Intercept = 0.987 ± 0.24 Slope = 0.00184 ± 0.00005

which resulted in:

reaction rate constant, $k_1 = 1.0132$ liter/gmole/sec, and

$$k_1' = 0.00186 \text{ (gmole/liter)}^{1/2}$$

From the above analysis, we conclude that the reverse Deacon reaction is approximately represented by

$$- r_A = \frac{1.0132 \ c_A^2 c_B}{c_C + 0.00186 \ c_B^{1/2}} \tag{104}$$

Equation (104) is consistent with the observed data obtained at 606°C, and there is no effect of the reverse reaction.
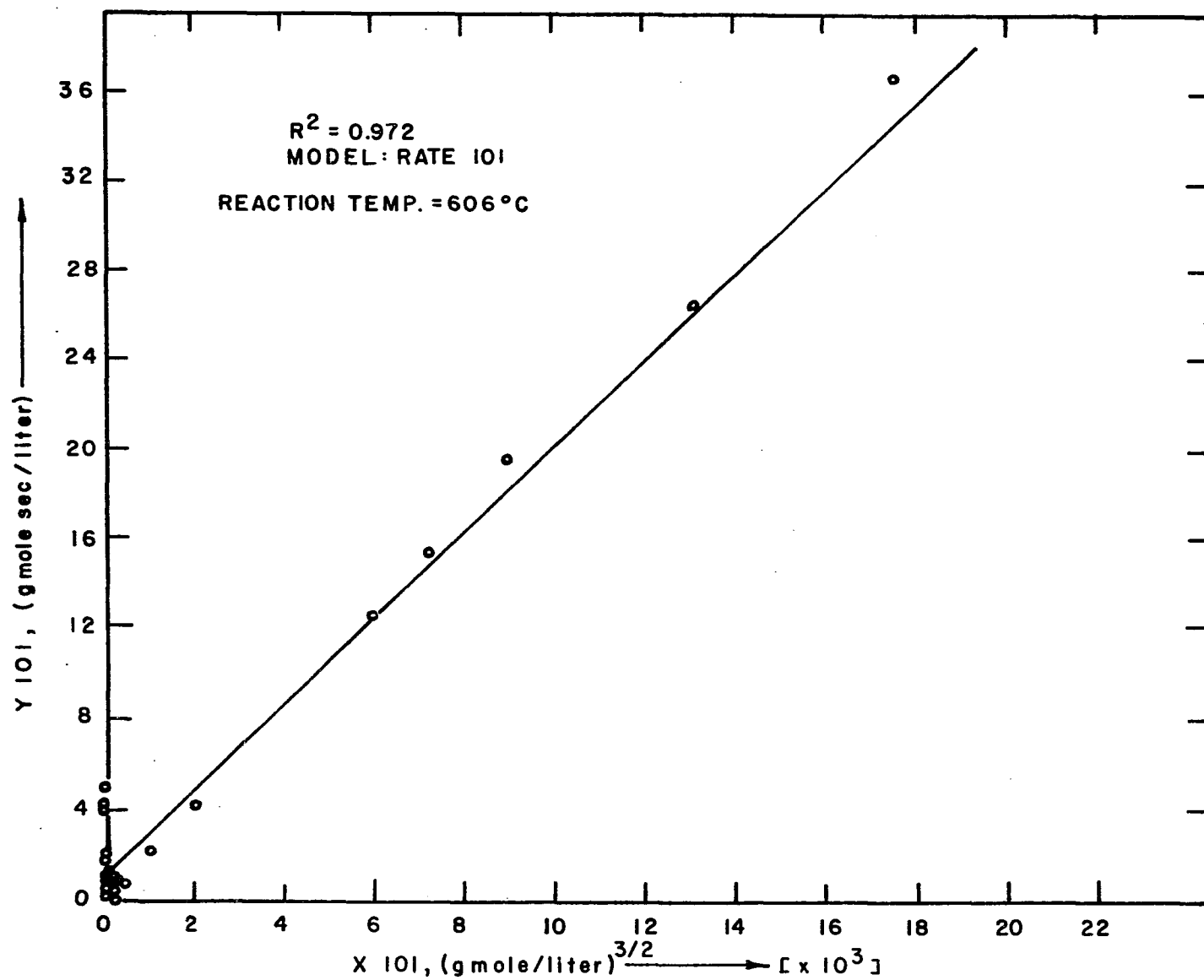
Figure 15. Correlation between X101 and Y101 at 606°C

Verification of Rate Law by Integral Method

Equation (94) was used for verification of consistency with the

observed data obtained for integral analysis at 606°C (Experiments

#10 through #18). In this equation, the product concentrations C_A,

C_B, and C_C were replaced by Equations (25), (26), and (27),

respectively. The value of the constant k_1' was taken as 0.00186 (gmole/

liter)$^{1/2}$ in the rate expression. The resulting integral form of the

design equation is:

$$\tau = \frac{1}{k_1} \int_0^{X_{Af}} \frac{C_{Ao}\left\{\dfrac{2C_{Ao}X_A}{1 + \epsilon_A X_A}\right\} + 0.00186 \left\{\dfrac{C_{Ao}(\theta_B - X_A)^{1/2}}{1 + \epsilon_A X_A}\right\}^{1/2}}{\left\{\dfrac{C_{Ao}(1 - X_A)}{1 + \epsilon_A X_A}\right\}^2 \left\{\dfrac{C_{Ao}(\theta_B - X_A)}{1 + \epsilon_A X_A}\right\}} dX_A$$

(105)

Let I606 represent the integral in the above equation, then we write

$$I606 = k_1 \tau \tag{106}$$

which indicates a linear relationship between I606 and τ. Simpson's

rule was used to evaluate the integrals. They are shown against

their corresponding space-time in Table 19. A regression analysis

gave the following results:

$$R^2 = 0.88$$

$$k_1 = 1.111 \pm 0.029$$

Figure 16 represents the relationship between space-time and the value

of the integral. The slope of the curve, which is equal to the reaction

Table 19.   Value of integrals and corresponding space-times[a]

Temperature 504°C			Temperature 606°C		
Space-time (sec)	I504	Average I504	Space-time (sec)	I606	Average I606
19.034	1.242		16.825	19.403	
19.034	1.171	1.059	16.825	18.220	18.245
19.034	0.801		16.825	17.145	
14.226	1.094		12.575	19.425	
14.226	1.111	1.112	12.575	18.792	17.425
14.226	1.132		12.575	14.434	
11.612	1.105		10.264	10.922	
11.612	0.729	0.974	10.264	11.524	11.967
11.612	1.115		10.264	13.556	
14.267	1.303		12.612	14.708	
14.267	1.264	1.236	12.612	14.086	13.830
14.267	1.146		12.612	12.765	
11.383	0.851		10.062	11.074	
11.383	0.842	0.922	10.062	13.979	13.149
11.383	1.084		10.062	13.433	
9.646	0.646		8.551	10.747	
9.646	1.063	0.783	8.551	10.832	10.530
9.646	0.675		8.551	10.025	
9.506	1.714		8.403	11.885	
9.506	1.698	1.592	8.403	12.758	10.368
9.506	1.378		8.403	7.156	
8.133	1.073		7.189	7.269	
8.133	1.076	1.055	7.189	8.721	8.460
8.133	1.017		7.189	9.490	
7.206	0.481		6.369	8.346	
7.206	0.514	0.546	6.369	7.401	8.075
7.206	0.625		6.369	8.522	

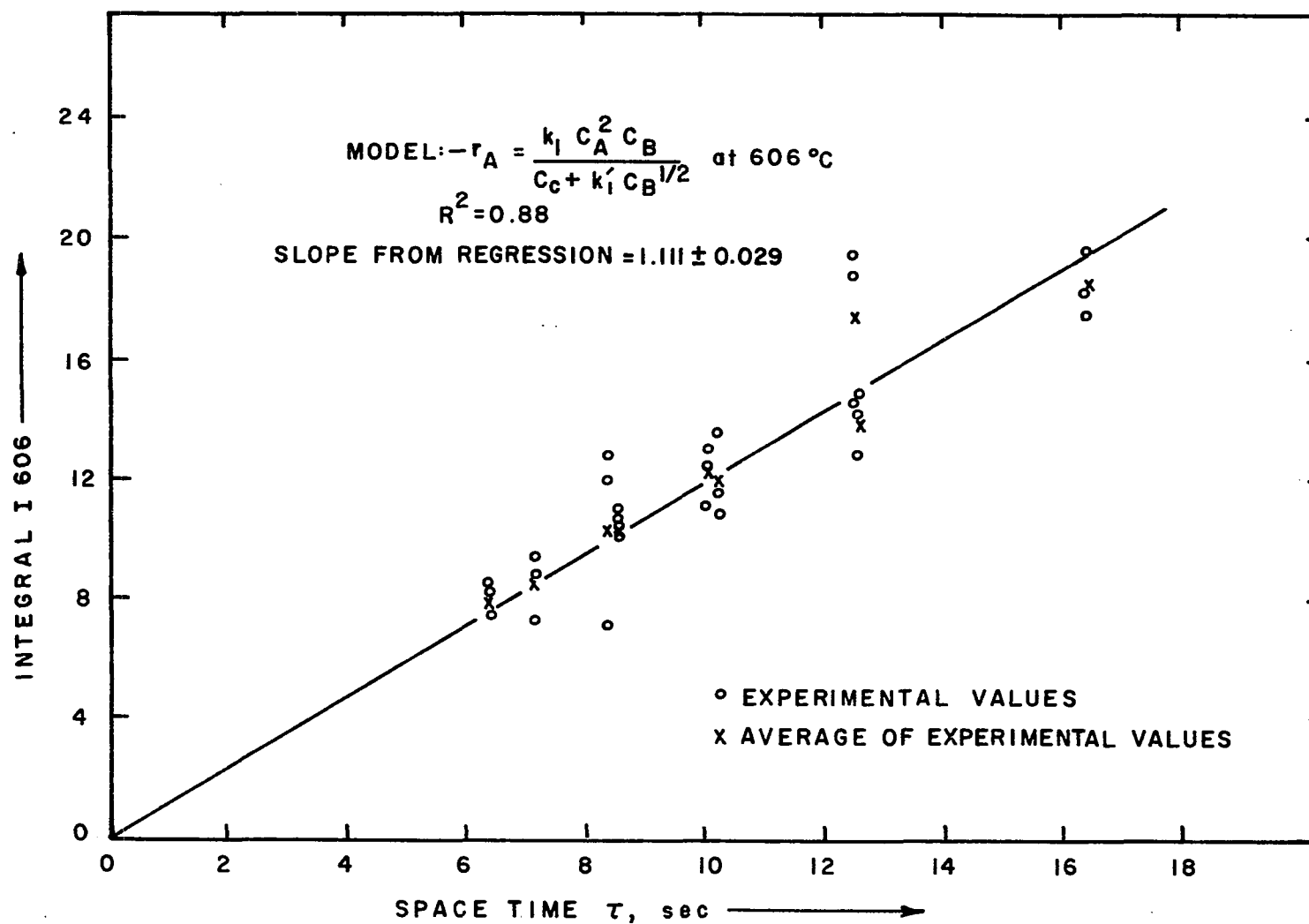[a]Values of I504 and I606 were obtained numerically.

Figure 16.   Space-time vs. value of integral I606

rate constant at 606°C was found to agree with the results as obtained in the differential method.

Therefore, the rate law as obtained by the differential method fits the data reasonably by the integral method. Equation (105) was used in a similar manner for the data obtained at 504°C and at 710°C. The integrals were evaluated numerically, and the values are reported in Table 19 (for data at 504°C, i.e., I504), and in Table 20 (for data at 710°C, i.e., I710). Figures 17 and 18 show their dependency on space-time, respectively. The results obtained from regression are summarized as:

$$\text{at } 504°C \quad R^2 = 0.92 \qquad \text{slope, } k_1 = 0.0754 \pm 0.0033$$
$$\text{at } 710°C \quad R^2 = 0.73 \qquad \text{slope, } k_1 = 7.866 \pm 0.40$$

Effects of reverse reaction

In order to determine the effect of the reverse reaction at 710°C, the following rate expression based on stoichiometry was used to represent the reverse reaction:

$$- r_A(\text{reverse}) = - k_{-1} C_C C_D^{1/2} \tag{107}$$

Equation (107) was used along with the forward reaction for the integral analysis. The resulting overall expression was integrated, and the values are shown in Table 20. These values indicate that there is no effect of this reverse reaction on overall rate. The following models representing the reverse reaction were also chosen:

Table 20. Value of integrals and corresponding space-times

With forward reaction at 710°C[a]			With reverse reaction at 710°C[a]		
Space-time (sec)	I710	Average I710	Space-time (sec)	I710	Average I710
15.045	90.382		15.045	90.382	
15.045	94.370	103.383	15.045	94.369	103.382
15.045	131.267		15.045	131.267	
11.245	142.169		11.245	142.168	
11.245	66.670	91.389	11.245	66.670	91.388
11.245	82.899		11.245	82.899	
9.178	88.567		9.178	88.569	
9.178	50.411	80.058	9.178	50.411	80.057
9.178	122.001		9.178	122.000	
11.277	94.259		11.277	94.256	
11.277	90.401	91.488	11.277	90.400	91.487
11.277	89.861		11.277	89.860	
8.998	80.740		8.998	80.739	
8.998	75.938	77.508	8.998	75.937	77.508
8.998	75.938		8.998	75.937	
7.624	86.435		7.624	86.435	
7.624	57.851	73.740	7.624	57.850	73.739
7.624	79.842		7.624	79.841	
7.514	87.306		7.514	87.305	
7.514	93.519	85.364	7.514	93.518	85.363
7.514	74.964		7.514	74.963	
6.429	64.410		6.429	64.410	
6.429	77.821	63.577	6.429	77.820	63.576
6.429	51.004		6.429	51.003	
5.696	42.503		5.696	42.502	
5.696	68.899	58.933	5.696	68.898	58.933
5.696	69.260		5.696	69.259	

[a]Values of I710 were obtained numerically.
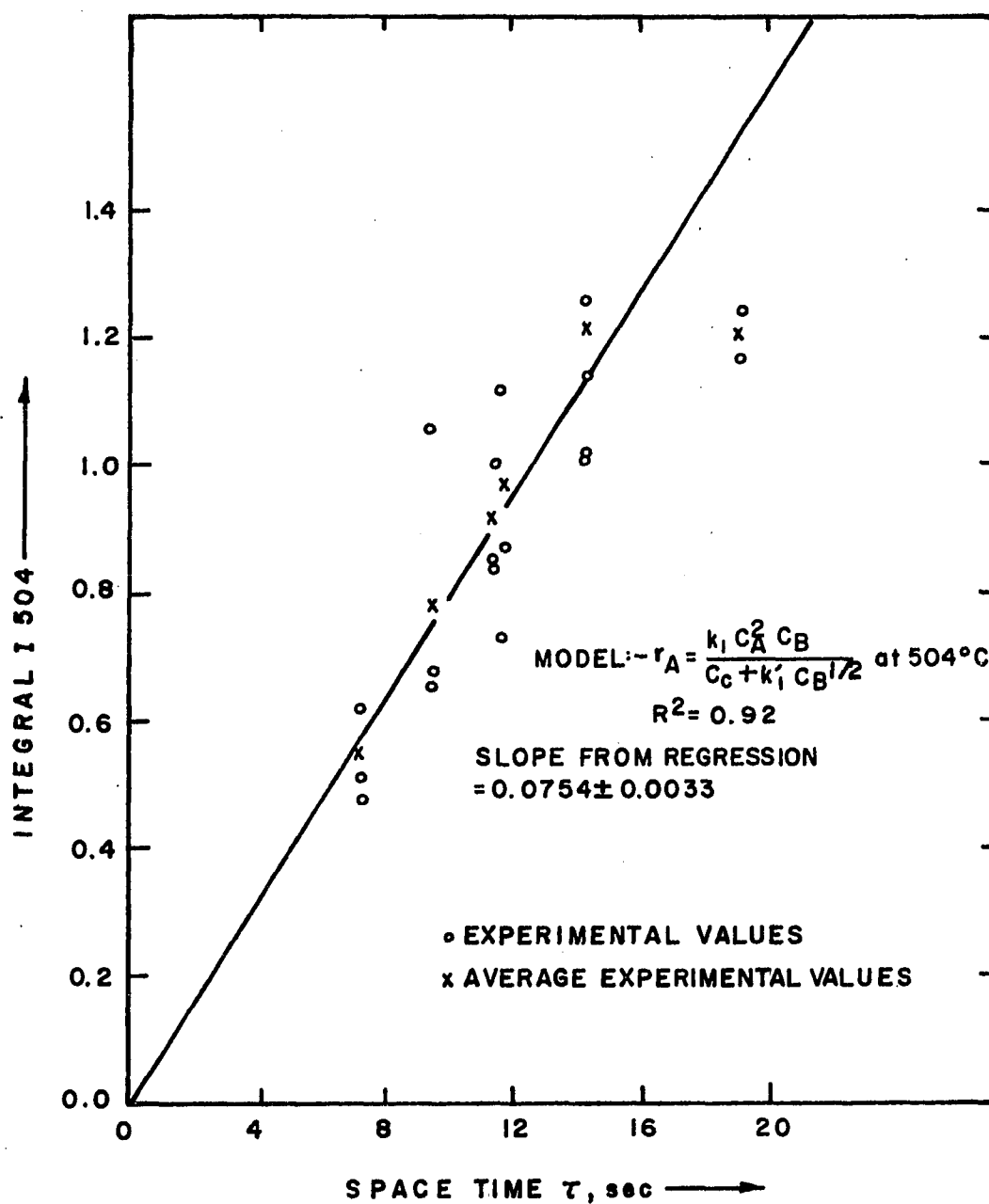
Figure 17. Space-time vs. value of integral I504

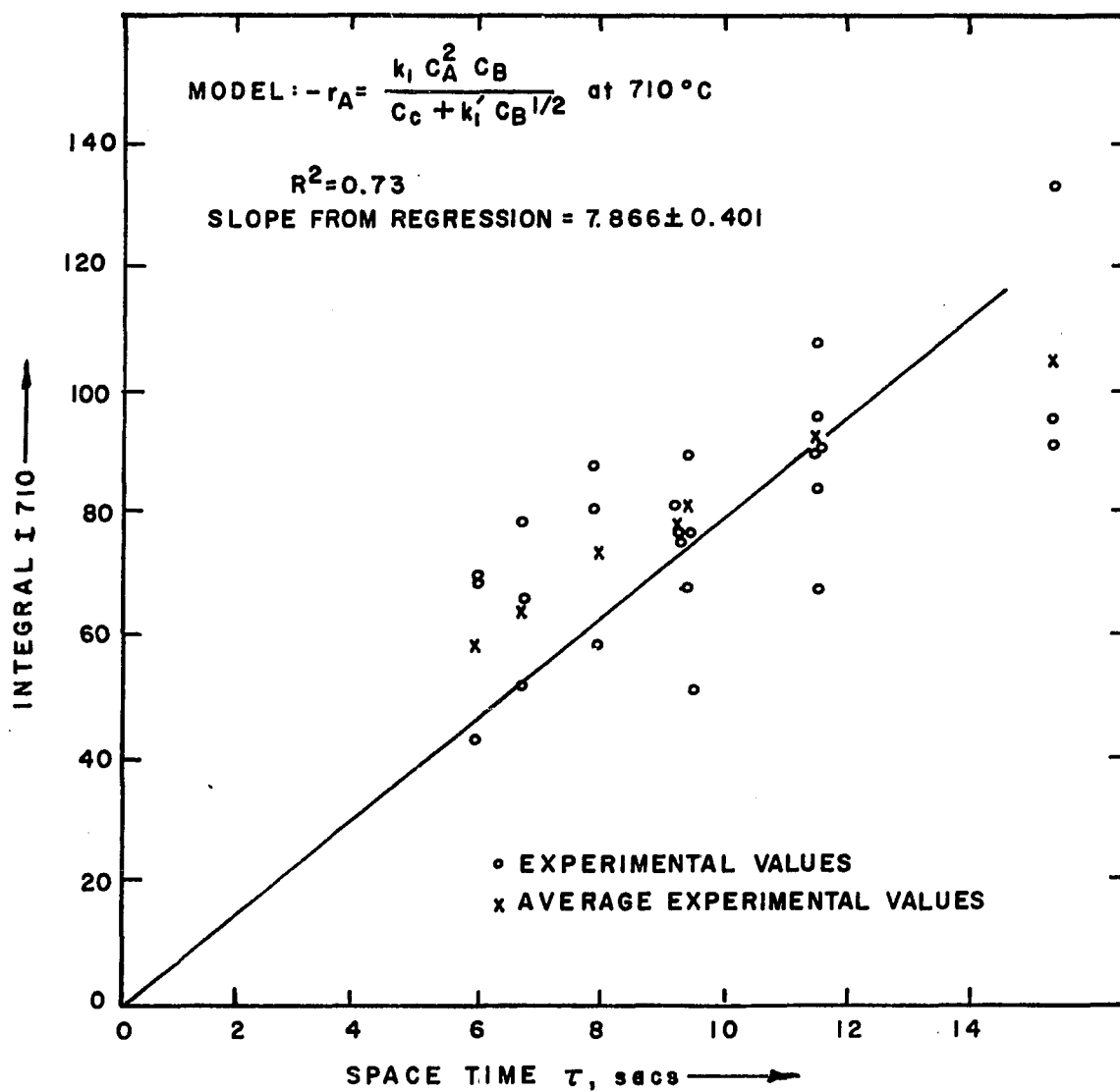Figure 18. Space-time vs. value of integral I710

$$- r_A(\text{reverse}) = - k_{-1} C_D^{1/2}$$

$$- r_A(\text{reverse}) = - k_{-1} C_C^2$$

$$- r_A(\text{reverse}) = - k_{-1} C_C \tag{108}$$

$$- r_A(\text{reverse}) = - k_{-1} C_C^{1/2}$$

Integration results were identical in each of these cases with that obtained without any reverse reaction. Therefore, these expressions do not have any impact on rate at this temperature. Considering these analyses, we conclude that the reverse reaction is negligible at the operating conditions of this experimental work.

Arrhenius Plot

The specific reaction rate is usually a function of the temperature of the reaction mixture. The temperature dependence of the reaction rate constants is usually correlated by the Arrhenius equation (79):

$$k_1(T) = A_o \exp(- E_a/RT) \tag{109}$$

where, A_o = frequency factor

E_a = Activation Energy = $RT^2(\dfrac{\partial \ln k_1}{\partial T})$

R = gas constant

T = absolute temperature.

Equation (109) can be written in logarithmic form as:

$$\ln k_1 = \ln A_o - (E_a/R)(1/T) \tag{110}$$

which is the equation of a straight line with a slope of $- E_a/R$, and

an intercept of ln A_o. In Figure 19 the reciprocal of the absolute

temperature is plotted against ln k_1 on semilogarithmic coordinates.

The parameters obtained from this plot are:

slope = - 17264.9 ± 536.15

intercept = 19.6723 ± 0.618

These results are reported on the basis of a least-mean-square fit,

and the values of the reaction rate constants as obtained earlier

were used in this analysis. The values of energy of activation and

the frequency factor were calculated from these results and they

are:

Energy of activation E_a = 34.3 ± 1.06 K-cal/gmole

Frequency factor A_o = 3.5 x 10^8 liter/gmole/second

Equation (109) correlates well the specific rate constant with

the temperature (50). It is usually believed that the activation

energy must be greater than the enthalpy of change ΔH, for the reac-

tion. This is particularly true for the endothermic reactions (79).

In Appendix E, the values of ΔH for the reverse Deacon reaction at the

reaction temperature have been reported. These computed results con-

firm that the overall heat of reaction is less than the activation

energy, obtained from experimental observations.

In the collision theory, the frequency factor is treated as a

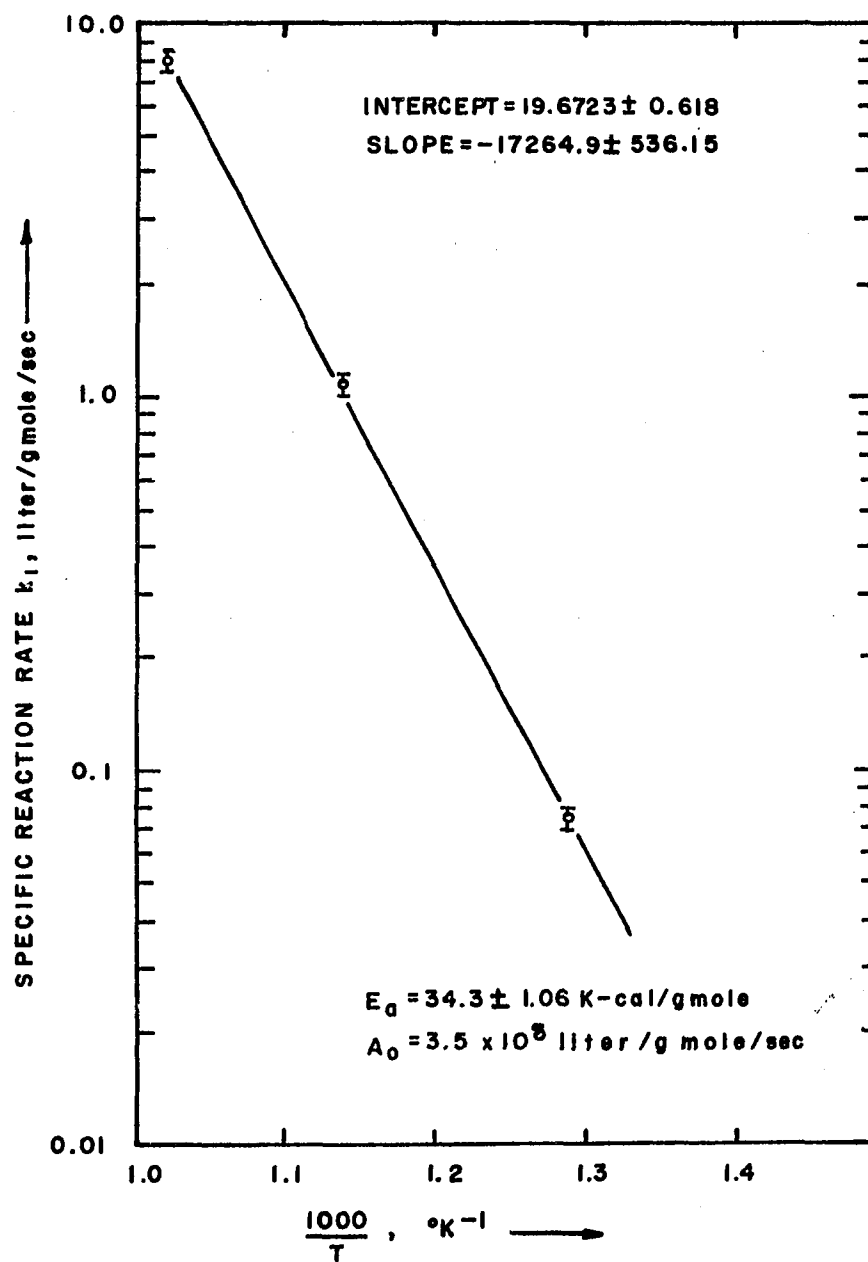collision rate, and is defined as (from kinetic theory of gaseous

molecules):

Figure 19. Plot of Arrhenius equation

$$A_o = \sigma_{AB}^2 (8\pi RT \frac{M_A + M_B}{M_A M_B})^{1/2}$$
(111)

where, σ_{AB} = effective diameter of A plus B upon collision, cm

M = molecular weight

R = gas constant = $k_B N_o$, product of Boltzman's constant

and Avogadro's number, erg/°K/gmole

= 8.3 x 10^7 ergs/°K/gmole.

Upon substitution of the above values in Equation (111) at 879°K,
we obtain:

$$A_o = 0.0683 \times 10^{-8} \text{ cm}^3/\text{molecule/second}$$

To convert this result to the usual units of liter/gmole/sec, it should
be multiplied by Avogadro's number, 6.02 x 10^{23} molecule/mole, and
divided by 1000 cm^3/liter:

Thus, $A_o = 4.112 \times 10^{11}$ liter/gmole/second

The collision theory has been found to give results in good agree-
ment with many other experimental data for simple reactions, but for
reactions involving more complex intermediates, the experimental
values are usually much less than the theory predicts (79). On comparison
with the experimental value of A_o, it is evident that the measured value
is several orders of magnitude less, thus indicating a complexity of
the reactant molecules for the reverse Deacon reaction. Also, this
suggests that only a small fraction of all collisions result in
reaction, and only those collisions that involve energies in excess
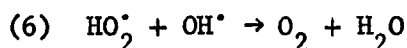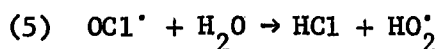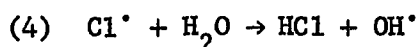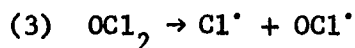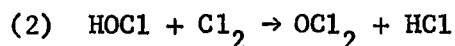of a given minimum E_a lead to reaction. The collision theory results

may be used to estimate the upper bound to the expected rate of reaction.

In activated complex theory, the essential postulate is that an activated complex (or transition state) is formed from the reactants, and the complex subsequently decomposes to the products. This theory suggests that E_a is the enthalpy change for formation of the activated complex from the reactants. In order to determine the magnitude of this value, we need to know its structure. Since it is not possible to determine the structure of the activated complex from this experimental work, we cannot make use of activated theory complex.

Mechanism of the Reverse Deacon Reaction

The kinetics of nonelementary reactions can be explained by postulating a series of elementary reactions that would occur in the process. But the intermediates formed cannot be measured or identified. To test the postulated series of reactions, it is necessary to check that the predicted kinetic expression corresponds to the experimental data. From the rate law, i.e., Equation (94), it is evident that two chlorine molecules combine with water vapor. They are believed to form the activated complex, and this may be postulated to happen with the mechanism: chlorine combines with water vapor to form HOCl, which is unstable in nature, and is susceptible to react with another chlorine molecule to form the complex. The activated complex decomposes to give radicals which carry the chain in the following way:

(1) $Cl_2 + H_2O \rightleftharpoons HOCl + HCl$

(2) $HOCl + Cl_2 \rightarrow OCl_2 + HCl$

(3) $OCl_2 \rightarrow Cl^{\cdot} + OCl^{\cdot}$

(4) $Cl^{\cdot} + H_2O \rightarrow HCl + OH^{\cdot}$

(5) $OCl^{\cdot} + H_2O \rightarrow HCl + HO_2^{\cdot}$

(6) $HO_2^{\cdot} + OH^{\cdot} \rightarrow O_2 + H_2O$
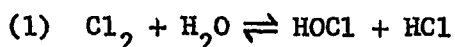
It is also believed that the first reaction is in pseudo-equilibrium state, and the rate controlling step is reaction (2). This suggests that the spontaneous decomposition of the activated complex is slow with reference to other reactions. Considering these assumptions, the following rate law can be formulated:

$$- r_{Cl_2} = \frac{k_1 k_2}{k_{-1}} \frac{c_{Cl_2}^2 \, c_{H_2O}}{c_{HCl}} \tag{112}$$

Equation (112) represents one of the two limiting conditions where concentration of water vapor is negligible compared to that of hydrogen chloride, and therefore, the mechanism involved correspond to reactions (1) through (6) as stated above. In the second limiting case, when the concentration of water vapor is high, or little or no hydrogen chloride is present in the process, the rate controlling step is different than the one discussed here, and possibly a change in mechanism is evident. Further study is needed to establish this.

RECOMMENDATIONS

(1) The rate expression was developed from the experimental
data in this investigation, and was subjected to verification by both
integral and differential approach. An attempt was made to verify the
parameters with the results from theory. Since the structure of the
activated complex cannot be verified, the entropy of activation $\Delta S\#$,
or the energy of activation $\Delta H\#$ cannot be determined from theory. Only
a knowledge of the energies of all possible intermediates will allow
prediction of the dominant path and its corresponding rate expression.
The theoretical predictions will help find the form and give us a
better understanding of chemical structure. However, the theoretical
predictions rarely match experiment by a factor of two, and there-
fore, for engineering design, this kind of information should not
be relied on; and experimentally found rates should be used in all
cases.

(2) The mechanism of the reaction as stated in this work does not
cover the total range of the experimental work. Hence, further effort
to postulate the mechanism should be made which will be consistent
with the experimentally obtained expression.

(3) Three reaction temperatures and one pressure were used in
this investigation. In order to make the derived rate expression ap-
plicable to a wider range of conditions, it is required to verify the
expression at different pressures selecting a few other temperatures.

(4) The endothermic reverse Deacon reaction needs a very high

temperature. A large amount of separation work is also required in the process. These difficulties have generated interest in finding alternate reactions, such as the hydrolysis of $MgCl_2$:

$$MgCl_2 + H_2O \rightleftharpoons MgO + 2HCl,$$

and $\qquad MgO + Cl_2 \rightleftharpoons MgCl_2 + \frac{1}{2} O_2$
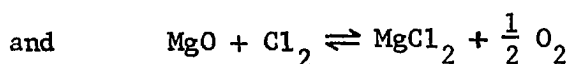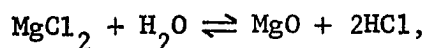
to substitute for the reverse Deacon reaction in the thermochemical cycles for production of hydrogen. The sum of the above two reactions is the reverse Deacon reaction, which can each be operated at a relatively low temperature. Hence, efforts must be made to evaluate these reactions and other similar reactions along with the reverse Deacon reaction on the basis of economics.

(5) A catalyst is required in order to secure a practical reaction rate at a temperature corresponding to favorable equilibrium conditions. It should be possible to use a catalyst in the reverse Deacon process to permit operation at a lower reaction temperature. Attempts have been made by Jones (53) to assess two types of commercial Girdler catalysts consisting of chromic oxide on activated alumina for the Deacon process at 325, 340, and 355°C. References (71) and (72) discuss some aspect of use of catalysts in the reverse Deacon process. Also, reference (24) suggests cupric chloride $CuCl_2$, which is deposited on inert porous carrier (such as broken firebrick, or the like, forming an active contact mass) for manufacturing chlorine by oxidation of hydrogen chloride. An extensive literature search for a particular catalyst which will withstand the necessary reaction

temperature would be needed. For this purpose, the prospects of using

a vertical reactor should also be investigated.

REFERENCES

1. Abraham, B. M.; and F. Schreiner. 1973. A Low Temperature Thermal Process for Decomposition of Water. Science 180 (4089): 959-60.

2. Abraham, B. M.; and F. Schreiner. 1974. General Principles Underlying Chemical Cycles Which Thermally Decompose Water into Elements. Ind. Eng. Chem. Fundam. 13 (4): 305-310.

3. Arnold, C. W.; and K. A. Kobe. 1952. Thermodynamics of the Deacon Process. Chem. Eng. Prog. 48 (6): 293-296.

4. Bamberger, C. E.; and D. M. Richardson. 1976. Hydrogen Production from Water by Thermochemical Cycles. Cryogenics 16 (4): 197-208.

5. Barnet, H.; and R. Schulten. 1974. Nuclear Watersplitting and High Temperature Reactors. Conference Proceedings. The Hydrogen Economy Miami Energy Conference (THEME), Miami, Florida, March 18-20.

6. Barstow, E. O.; and S. B. Heath. 1932. U.S. Patent 1,874,225 (to Dow Chemical Company). August 30.

7. Batzhiser, R. E.; M. R. Samuels; and J. D. Eliassen. 1972. Chemical Engineering Thermodynamics. Prentice-Hall, Inc., Englewood Cliffs, New Jersey.

8. Bethea, R. M.; B. S. Duran; and T. L. Boullion. 1975. Statistical Methods for Engineers and Scientists. Marcel Dekker, Inc., New York, NY.

9. Bird, R. B.; W. E. Stewart; and E. N. Lightfoot. 1960. Transport Phenomena. John Wiley and Sons, Inc., New York, NY.

10. Bockris, J. O'M. 1974. On Methods for the Large-Scale Production of Hydrogen from Water. Conference Proceedings. The Hydrogen Economy Miami Energy Conference (THEME), Miami, Florida, March 18-20.

11. Bowmann, M. G. 1974. Fundamental Aspects of Systems for the Thermochemical Production of Hydrogen from Water. Los Alamos Scientific Laboratory Report, LA-UR-74-1459. Los Alamos, New Mexico.

12. Bowmann, M. G. 1976. Chemistry of Thermochemical Cycles from U.S.A. Programs. A Paper Submitted to A.I.M. International Congress on Hydrogen and Its Properties, Liege, Belgium, November 15-18.

13. Brokris, J. O. 1972. The Electrochemistry of Cleaner Environments. Plenum Press, New York, NY.

14. Burke, D. P. 1975. Chemical Week Report: Methanol. Chemical Week 117 (13): 33-42.

15. Burger, J. M.; P. A. Lewis, R. J. Isler; F. J. Salzano; and J. M. King. 1974. Energy Storage for Utilities Via Hydrogen Systems. BNL-19266. A Paper Presented at 9th Intersociety Energy Conversion Engineering Conference, San Francisco, California, August 26-30.

16. Carnaham, B.; H. A. Luther; and J. O. Wilkes. 1969. Applied Numerical Methods. John Wiley and Sons, Inc., New York, NY.

17. Chao, R. E. 1974. Thermochemical Water Decomposition Process. Ind. Eng. Chem. Prod. Res. Develop. 13 (2): 94-101.

18. Chao, R. E. 1975. Thermochemical Hydrogen Production: An Assessment of Non-Ideal Cycles. Ind. Eng. Chem. Prod. Res. Develop. 14 (3): 276-279.

19. Chao, R. E.; and K. E. Cox. 1974. An Analysis of Hydrogen Production Via Closed Cycle Schemes. Conference Proceedings. The Hydrogen Economy Miami Energy Conference (THEME), Miami, Florida, March 18-20.

20. Chemical Abstracts. 1916. Hydrochloric Acid. Soc. Italiana Elettrochmiica Swed. 40: 354.

21. Chopey, N. P. 1972. Hydrogen: Tomorrow's Fuel. Chem. Eng. 79 (Dec. 25): 24-26.

22. Cox, K. E. 1974. Hydrogen Economy. 1st ed. University of New Mexico Press, Albuquerque, NM.

23. Deacon, H. W. 1870. On a New Method of Obtaining Chlorine. The Chemical News 22 (566): 157-161.

24. Deacon Reaction Patents:

    Balcar, F. R. 1942. U.S. Patent 2,271,056 (to Air Reduction Company). Jan. 27.

    Davis, C. W.; F. A. E. Antioch; and R. G. Ellis. 1951. U.S. Patent 2,547,928 (to Dow Chemical Company). April 10.

    Diamond Alkali Company. 1952. Brit. Patent 676,667. July 30.

    Institut of Francais du Petrole des Carburants et Lubrificants. 1960. Duetsches Patentamt 1,076,635. March 3.

    Johnson, A. J.; and A. J. Cherniavsky. 1953. U.S. Patent 2,644,846 (to Shell Development Company). July 7.

Johnson, A. J.; and A. J. Cherniavsky. 1956. U.S. Patent
2,746,844 (to Shell Development Company). May 22.

Krekeler, H.; and H. Schlechet. 1952. Deutsches Patentamt
857,796 (to Badische Anilin- & Soda-Fabrik). Dec. 1.

VEB Farbenfabric Wolfen. 1960. Deutsches Patentamt 1,078,100.
March 24.

VEB Farbenfabric Wolfen. 1960. Deutsches Patentamt 1,086,677.
Aug. 11.

VEB Farbenfabric Wolfen. 1960. Deutsches Patentamt 1,088,933.
Sept. 15.

25. De Beni, G.; and C. Marchetti. 1973. Mark-1: A Chemical Process
    to Decompose Water Using Nuclear Heat. A Paper Submitted at the
    Symposium on Non-Fossil Chemical Fuels, 166th National American
    Chemical Society Meeting, Chicago, Ill., Aug., 1973.

26. De Beni, G. 1970. Hydrogen Production Cyclic Process. French
    Patent 2,035,558. Feb. 17.

27. Denbigh, K. 1965. Chemical Reactor Theory. Cambridge University
    Press, London, England.

28. Dovner, S. 1971. Contribution to Hydrogen Production with Nuclear
    Heat. Kernsforschung Zentrum Karlsrule Report No. INR-4/71-35.

29. Engel, W. F.; M. J. Wade; and S. Muller. 1962. Recent Develop-
    ments in the Oxidative Recovery of Chlorine from Hydrochloric
    Acid. Chemistry and Industry 13: 76-83.

30. Euratom. 1973. Hydrogen Production from Water Using Nuclear Heat.
    Progress Report No. 3: EUR/C-IS/35/73e.

31. Falckenstein, K. V. 1907. Equilibrium of Deacon Process. Z.
    Physik. Chem. 59: 313-335.

32. Fein, E.; and F. J. Salzano. 1974. The Hydrogen Economy: A Utility
    Prospective. C74 099-8. A Paper recommended by the IEEE Power
    Generation Committee of the IEEE Power Engineering Society for
    Presentation at the IEEE PES Winter Meeting, New York, NY, Jan. 27-
    Feb. 1.

33. Funk, J. E. 1972. Thermodynamics of Multistep Water Decomposition
    Process. A Paper Presented at the Symposium of Non-Fossil Fuels
    at the 163rd National American Chemical Society Meeting, Boston,
    Mass., April, 1972.

34. Funk, J. E. 1974. The Generation of Hydrogen by Thermal Decomposition of Water. Conference Proceedings. 9th Intersociety Energy Conversion Engineering Conference, San Francisco, Calif., Aug. 26-30.

35. Funk, J. E.; and R. M. Reinstrom. 1966. Energy Requirements in the Production of Hydrogen from Water. Ind. Eng. Chem. Proc. Des. Develop. 5 (3): 336-342.

36. Funk, J. E.; W. L. Couger; and R. H. Carty. 1974. Evaluation of Multistep Thermochemical Processes for the Production of Hydrogen from Water. Conference Proceedings. The Hydrogen Economy Miami Energy Conference, Miami, Florida, March 18-20.

37. Froment, G. F.; and K. B. Bischoff. 1979. Chemical Reactor Analysis and Design. John Wiley and Sons, Inc., New York, NY.

38. Fogler, H. Scott. 1974. The Elements of Chemical Kinetics and Reactor Calculations. Prentice-Hall, Inc., Englewood Cliffs, New Jersey.

39. Giauque, W. F.; and R. Overstreet. 1932. The Hydrogen, Chlorine and Hydrogen Chloride Equilibrium at High Temperatures. J. Am. Chem. Soc. 54 (5): 1731-1744.

40. Gibbs, H. D. 1920. The Production of Hydrochloric Acid from Chlorine and Water. J. Ind. Eng. Chem. 12: 538-541.

41. Gordon, A. R.; and C. Barnes. 1933. Thermodynamic Quantities from Spectroscopic Data. J. Chem. Physics 1 (1933): 297-307.

42. Gregory, D. P. 1972. Hydrogen: Transportable Storable Energy Medium. Am. Chem. Soc., Div. Fuel Chem. Prep. 16 (4): 88-94.

43. Gregory, D. P.; D. Y. C. Ng; and G. M. Long. 1972. The Electrochemistry of Cleaner Environments. Plenum Press, New York, NY.

44. Gregory, D. P. 1973. A Hydrogen Economy System. American Gas Association, New York, NY.

45. Griffith, E. J. 1974. Hydrogen Fuel. Nature 248 (March 29): 458.

46. Hardy, C. 1973. Thermal Decomposition of Water Using Cycles of the $FeCl_2$ Family. Report EUR 4958f.

47. Hickman, R. G.; O. H. Krikorian; and W. J. Ramsey. 1974. Thermochemical Hydrogen Production Research at Lawrence Livermore Laboratory. Conference Proceedings. The Hydrogen Economy Miami Energy Conference (THEME), Miami, Florida, March 18-20.

48. Hinselwood, C. N. 1940. Kinetics of Chemical Change. The
    Clarendon Press, Oxford, London.

49. Hirschkind, W. 1925. Manufacture of Hydrochloric Acid from
    Chlorine. Ind. Eng. Chem. 17: 1071-1073.

50. Hougen, O. A.; and K. M. Watson. 1947. Chemical Process Principles.
    John Wiley and Sons, Inc., New York, NY.

51. Hougen, O. A.; K. M. Watson; and R. A. Ragatz. 1960. Chemical
    Process Principle Charts. 2nd ed. John Wiley and Sons, Inc., New
    York, NY.

52. Johnstone, H. F. 1948. Chlorine Production: Nonelectrolytic
    Processes. Chem. Eng. Prog. 44 (9): 657-668.

53. Jones, Alva. 1965. Kinetics of the Oxidation of Hydrogen Chloride.
    Ph.D. Dissertation. Yale University, New Haven.

54. Keilly, J. J.; R. R. Wiswall; and K. C. Hoffman. 1963. Metal
    Hydrides as a Source of Hydrogen Fuel. Brookhaven National Labora-
    tory Report, Upton, NY.

55. Kerns, G. P. 1972. Hydrogen Production for Eco-energy. GE Tempo
    Report, 72-TMP 53, Santa Barbara, California.

56. Knoche, K. F.; H. Cremer; G. Steinborn; and W. Schneider. 1974.
    Feasibility Studies of Chemical Reactions for Thermochemical Water-
    Splitting Cycles of the Iron-Chloride, Iron-Sulfer-, and Manganese-
    Sulfer- Families. Conference Proceedings. The Hydrogen Economy
    Miami Energy Conference (THEME), Miami, Florida, March 18-20.

57. Knoche, K. F.; H. Cremer; and G. Steinborn. 1975. A Thermochemical
    Process for Hydrogen Production. Conference Proceedings. The
    Hydrogen Economy Miami Energy Conference (THEME), Miami, Florida,
    March 3-5.

58. Knoche, K. F. 1969. Euratom Report EUR/C1S/1062. Euratom, Ispra,
    Italy, Dec. 1969.

59. Knoche, K. F.; and J. Schubert. 1973. Euratom Study Agreement Re-
    port 045-727-ECID(f), Euratom, Ispra, Italy, May 1973.

60. Kobrin, C. L. 1967. New Life for the HyL Process. The Iron Age
    199 (11): 74-76.

61. Koricinski, P. F. 1974. Hydrogen for Subsonic Transport.
    Conference Proceedings. The Hydrogen Miami Energy Conference
    (THEME), Miami, Florida, March 18-20.

62. Lessing, L. 1972. The Coming Hydrogen Economy. Fortune 86 (5): 138-144.

63. Levenspiel, O. 1972. Chemical Reaction Engineering. 2nd ed. John Wiley and Sons, Inc., New York, NY.

64. Maugh, T. H. 1972. Hydrogen: Synthetic Fuel of the Future. Science 178 (4063): 849-852.

65. McAlvery, R. F.; and R. B. Cole. 1974. Hydrogen as a Fuel. Stevens Institute of Technology Report ME-RT-74011.

66. Michel, J. W. 1973. Hydrogen and Exotic Fuel. Oakridge National Laboratory Report ORNL-TM-4461.

67. Nerst, Von W. 1918. Zur Anwendung des Einsteinschen photochemischen Aquivalentgesetzes, I. Z. Elektrochem. 24 (May): 335-36.

68. Ohkawa, T. 1949. Japan Patent 180,186. Sept. 8.

69. Pangborn, J. B.; and J. C. Sharer. 1974. Analysis of Thermochemical Water-Splitting Cycles. Conference Proceedings. The Hydrogen Economy Miami Energy Conference (THEME), Miami, Florida, March 18-20.

70. Parthasarathy, P. 1960. Utilization of Hydrogen Chloride and Air for Chlorination of Ethane. Ph.D. Dissertation, University of Florida.

71. Paulus, H. W. 1922. U.S. Patent 1,420,209 (to Royal Baking Company). June 20.

72. Peter, A. H. 1917. U.S. Patent 1,229,509 (to Royal Baking Company). June 12.

73. Quade, R. M.; and A. T. McMillan. 1974. Hydrogen Production with a High Temperature Gas Cooled Reactor (HTGR). General Atomic Report. GA-A12876, HY-1208 (1974).

74. Reaction of Cl_2 and H_2O (Patents):

Behrman, A. S. 1932. U.S. Patent 1,843,196. Feb. 2.

Doma, G.; and G. Andreani. 1922. Brit. Patent 189,723. May 19.

Hirschkind, W.; and C. W. Schedlar. 1928. U.S. Patent 1,695,552. Dec. 18.

Kenkyujo, R. 1935. Japan Patent 111,410. July 2.

Krebs et Cie. Soc. 1951. French Patent 992,928. Oct. 24.

Randaccio, C. 1954. Ital. Patent 507,052. Dec. 28.

Rosenstein, L. 1924. U.S. Patent 1,485,816 (to Great Western Electro Chemical Company). March 4.

75. Russel, J. L. 1974. Nuclear Water Splitting and the Hydrogen Economy. Power Engineering 78 (4): 48-51.

76. Safrany, D. R. 1974. Nitrogen Fixation. Scientific American 231 (4): 64-70.

77. Sconee, J. S. 1972. Chlorine: Its Manufacture, Properties and Uses. Reinhold Publishing Corp., New York, NY.

78. Shelud'ko, M. K. 1934. Catalytic Preparation of Hydrochloric Acid from Chlorine and Water. Ukrain, Khem. Zhur. 9: 410-416.

79. Smith, J. M. 1974. Chemical Engineering Kinetics. 2nd ed. McGraw-Hill Book Company, New York, NY.

80. Strickland, G.; J. Reilly; and R. H. Wiswall. 1974. An Engineering Scale Energy Storage Reservoir of Iron-Titaneum Hydride. Conference Proceedings. The Hydrogen Economy Miami Energy Conference (THEME), Miami, Florida, March 18-20.

81. Stull, D. R.; and H. J. Prophet. 1971. Thermochemical Tables. 2nd ed. NSRDS-NBS 37, U.S. Dept. of Commerce, Washington, D.C.

82. Synthetic Fuel Panel. Hydrogen and Other Synthetic Fuels: A Summary of the Work of the Synthetic Fuel Panel. Report No. TID-26136. U.S. Govt. Printing Office, Washington, D.C.

83. Tantram, A. D. S. 1974. Fuel Cells: Past, Present and Future. Energy Policy 2 (March, 1974): 55.

84. U.S. Bureau of Mines, U.S. Department of Interior. 1970. Mineral Facts and Problems. U.S. Bureau of Mines USDI Bulletin No. 650.

85. van Dijk, C. P.; and W. C. Schreiner. 1973. Hydrogen Chloride to Chlorine Via the Kel-Chlor Process. Chem. Eng. Prog. 69 (4): 57-63.

86. Wentorf, R. H.; and R. E. Hannman. 1974. Thermochemical Hydrogen Generation. Science 185 (4148): 311-319.

87. William, L. O. 1974. Electrolysis of Sea Water. Conference Proceedings. The Hydrogen Economy Miami Energy Conference (THEME), Miami, Florida, March 18-20.

88. Winsche, W. E.; K. C. Hoffman; and F. J. Salzano. 1973. Hydrogen: Its Future Role in the Nation's Energy Economy. Science 180 (4093): 1325.

89. Yeh, Yu sung. 1976. Preliminary Kinetics of High-Temperature Reaction of Chlorine and Steam. M.S. Thesis, Iowa State University, Ames.

ACKNOWLEDGMENTS

The author wishes to express gratitude to Dr. Dean L. Ulrichson for his supervision and valuable guidance throughout this research work and in preparation of this manuscript.

The help extended by Dr. A. H. Pulsifer for executing the stimulus response experiment and by Dr. D. S. Martin for developing the reaction mechanism is sincerely appreciated. I am obliged to Drs. M. A. Larson and G. W. Smith for serving on my committee and advising for major and minor courses.

I sincerely acknowledge the help given by my good friend Douglas Adelman and by my younger brother-like Rudra Kar. Indebtedness is expressed to Mrs. Letha DeMoss for so patiently, yet so quickly, typing this dissertation.

Sincerely appreciation is expressed to the Chemical Engineering Department and to the Ames Laboratory for providing the graduate assistantships under which this work was done.

APPENDIX A.

PARTIAL LIST OF THERMOCHEMICAL CYCLES WHICH

USE THE REVERSE DEACON REACTION

(1) DeBeni, Mark 3 (26)

Elements	Temperature	Cycle
V, Cl	1073°K	$Cl_2 + H_2O \rightarrow 2HCl + \frac{1}{2} O_2$
	443°K	$2VOCl_2 + 2HCl \rightarrow 2VOCl_2 + H_2$
	873°K	$4VOCl_2 \rightarrow 2VOCl_2 + 2VOCl_3$
	473°K	$2VOCl_3 \rightarrow 2VOCl_2 + Cl_2$

(2) Dovner (28)

Elements	Temperature	Cycle
V, Cl	973°K	$Cl_2 + H_2O \rightarrow 2HCl + \frac{1}{2} O_2$
	298°K	$2VCl_2 + 2HCl \rightarrow 2VCl_3 + H_2$
	973°K	$4VCl_3 \rightarrow 2VCl_4 + 2VCl_2$
	298°K	$2VCl_4 \rightarrow 2VCl_3 + Cl_2$

(3) Hickman (47)

Elements	Temperature	Cycle
Ta, Cl	1300°K	$Cl_2 + H_2O \rightarrow 2HCl + \frac{1}{2} O_2$
		$2TaCl_2 + 2HCl \rightarrow 2TaCl_3 + H_2$
		$2TaCl_3 \rightarrow 2TaCl_2 + Cl_2$

(4) Hardy, Mark 4 (46)

Elements	Temperature	Cycle
S, Cl	1073°K	$H_2O + Cl_2 \rightarrow 2HCl + \frac{1}{2} O_2$
	1073°K	$H_2S \rightarrow S + H_2$
	373°K	$S + HCl + 2FeCl_2 \rightarrow H_2S + 2FeCl_3$
	693°K	$2FeCl_3 \rightarrow 2FeCl_2 + Cl_2$

(5) Dovner (28)

Elements	Temperature	Cycle
Hg, Cl	—	$H_2O + Cl_2 \rightarrow 2HCl + \frac{1}{2} O_2$
		$2HgCl + 2HCl \rightarrow 2HgCl_2 + H_2$
		$2HgCl_2 \rightarrow 2HgCl + Cl_2$

(6) Dovner (28)

Elements	Temperature	Cycle
Fe, Cl	1000°K	$H_2O + Cl_2 \rightarrow 2HCl + \frac{1}{2} O_2$
		$2FeCl_2 + 2HCl \rightarrow 2FeCl_3 + H_2$
		$2FeCl_3 \rightarrow 2FeCl_2 + Cl_2$

(7) Hickman (47)

Elements	Temperature	Cycle
Fe, Cl	1100°K	$H_2O + Cl_2 \rightarrow 2HCl + \frac{1}{2} O_2$
		$3FeCl_2 + 4H_2O \rightarrow Fe_3O_4 + 6HCl + H_2$
		$Fe_3O_4 + 8HCl \rightarrow FeCl_2 + 2FeCl_3 + 4H_2O$
		$2FeCl_3 \rightarrow 2FeCl_2 + Cl_2$

(8) De Beni (26)

Elements	Temperature	Cycle
Fe, Cl	$1073^{O}K$	$3/2Cl_2 + 3/2H_2O \rightarrow 3HCl + 3/4O_2$
	$923^{O}K$	$3FeCl_2 + 4H_2O \rightarrow Fe_3O_4 + 6HCl + H_2$
	$623^{O}K$	$Fe_3O_4 + 1/4O_2 \rightarrow 3/2Fe_2O_3$
	$423^{O}K$	$3/2Fe_2O_3 + 9HCl \rightarrow 3FeCl_3 + 9/2H_2O$
	$693^{O}K$	$3FeCl_3 \rightarrow 3FeCl_2 + 3/2Cl_2$

(9) Hickman (47)

Elements	Temperature	Cycle
Cu, Cl	$973^{O}K$	$Cl_2 + H_2O \rightarrow 2HCl + 1/2O_2$
	$473^{O}K$	$2CuCl_2 + 2HCl \rightarrow 2CuCl_2 + H_2$
	$873^{O}K$	$2CuCl_2 \rightarrow 2CuCl + Cl_2$

(10) De Beni (26)

Elements	Temperature	Cycle
Cr, Cl	$1073^{O}K$	$Cl_2 + H_2O \rightarrow 2HCl + 1/2O_2$
(Cu, Fe)	$443^{O}K$	$2CrCl_2 + 2HCl \rightarrow 2CrCl_3 + H_2$
	$973^{O}K$	$2CrCl_3 + 2FeCl_2 \rightarrow 2CrCl_2 + 2FeCl_3$
	$423^{O}K$	$2FeCl_3 + 2CuCl \rightarrow 2FeCl_2 + 2CuCl_2$
	$773^{O}K$	$2CuCl_2 \rightarrow 2CuCl + Cl_2$

(11) Hickman (47)

Elements	Temperature	Cycle
Bi, Cl	—	$Cl_2 + H_2O \rightarrow 2HCl + 1/2O_2$
		$2BiCl_2 + 2HCl \rightarrow 2BiCl_3 + H_2$
		$2BiCl_3 \rightarrow 2BiCl_2 + Cl_2$

(12) Dovner (28)

Elements	Temperature	Cycle
Cr, Cl	1100°K	$Cl_2 + H_2O \rightarrow 2HCl + 1/2O_2$
(Fe)		$2CrCl_2 + 2HCl \rightarrow 2CrCl_3 + H_2$
		$2CrCl_3 + 2FeCl_2 \rightarrow 2CrCl_2 + 2FeCl_3$
		$2FeCl_3 \rightarrow 2FeCl_2 + Cl_2$

(13) Knoche (57)

Elements	Temperature	Cycle
Cr, Cl	973°K	$Cl_2 + H_2O \rightarrow 2HCl + 1/2O_2$
		$2HCl + 2CrCl_2 \rightarrow 2CrCl_3 + H_2$
		$2CrCl_3 \rightarrow 2CrCl_2 + Cl_2$

(14) Knoche (57)

Elements	Temperature	Cycle
Fe, Cl	1300°K	$3FeCl_2 + 3H_2 \rightarrow 6HCl + 3Fe$
	600°K	$3Fe + 4H_2O \rightarrow Fe_3O_4 + 4H_2$
	700°K	$H_2O + Cl_2 \rightarrow 2HCl + 1/2O_2$
	1300°K	$1/2Cl_2 + Fe_3O_4 + 8HCl \rightarrow 3/2Fe_2Cl_6 + 4H_2O$
	600°K	$3/2Fe_2O_6 \rightarrow 3FeCl_2 + 3/2Cl_2$

(15) Chao (18)

Elements	Temperature	Cycle
Cl	973°K	$H_2O + Cl_2 \rightarrow 2HCl + 1/2O_2$
	1073°K	$2HCl \rightarrow H_2 + Cl_2$

APPENDIX B.

SAMPLE CALCULATION PROCEDURE FOR INTEGRAL REACTOR DATA

Flow Rate of Reactants at Reaction Temperature for Experiment #3

Reaction temperature = $777^{\circ}K$

Operating pressure = 1 atm

Gas constant = 0.08206 atm-liter/gmole/$^{\circ}K$

MW of water vapor = 18 gm/gmole

MW of chlorine = 71 gm/gmole

Room temperature = $294^{\circ}K$

Flow rate of water
at RT and 1 atm   = 0.0191 cc/min

= 0.0191 gm/min

Flow rate of water
vapor at $777^{\circ}K$ and 1 atm = v_{Bo} = nRT/P

$$= (0.08206) \frac{atm\ liter}{gmole\ ^{\circ}K} (777^{\circ}K)(\frac{0.0191}{18}) \frac{gmole}{min} \frac{1}{atm}$$

= 0.06766 liter/min = 67.66 cc/min

Flow rate of chlorine
at $777^{\circ}K$ and 1 atm   = v_{Ao} = $(Pv_A/T)(T_{rxn}/P_{rxn})$

= (100)(777/294) = 264.29 cc/min

Total flow rate of the reactants = v_o = v_{Ao} + v_{Bo}

= 264.29 + 67.66 = 331.95 cc/min

Hence, $y_{Ao} = \dfrac{264.29}{264.29 + 67.66} = 0.796$

$y_{Bo} = \dfrac{67.66}{264.29 + 67.66} = 0.204$

$P_{Ao} = y_{Ao}$ (total pressure) = 0.796 atm

$$P_{Bo} = y_{Bo} \text{ (total pressure)} = 0.204 \text{ atm}$$

$$C_{Ao} = P_{Ao}/RT = 0.796/777/0.08206$$

$$= 0.0124842 \text{ gmole/liter}$$

$$C_{Bo} = P_{Bo}/RT = 0.204/777/0.08206$$

$$= 0.0031967 \text{ gmole/liter}$$

$$F_{Ao} = C_{Ao}v_o = 0.004145 \text{ gmole/min}$$

$$F_{Bo} = C_{Bo}v_o = 0.001061 \text{ gmole/min}$$

$$\theta_B = F_{Bo}/F_{Ao} = 0.256$$

$$\tau = V/v_o = 64.25/331.95 \text{ min} = 11.61 \text{ secs.}$$

Calculation of Experimental Conversion of Chlorine for Experiment #3A

Average weight of pure chlorine
peaks as found by calibration   = 0.1180958 gm

Average weight of pure oxygen peaks
as found by calibration   = 0.0159292 gm

Average weight of chlorine peaks
as found by experiment   = 0.117434 gm

Average weight of oxygen peaks
as found by experiment   = 0.000409 gm

$$\% \text{ chlorine} = \frac{\text{wt of chlorine peaks as found by experiments}}{\text{wt of pure chlorine peaks at same conditions}}$$

$$= 99.44$$

$$\% \text{ oxygen} = \frac{\text{wt of oxygen peaks as found by experiments}}{\text{wt of pure oxygen peaks at same conditions}}$$

$$= 2.57$$

Each time a sample of 0.25 ml of chlorine was injected into the chromatograph, hence the amount of chlorine in the effluent stream:

$$= (0.25)(0.9944) = 0.2486 \text{ ml}$$

and amount of pure oxygen in the effluent stream:

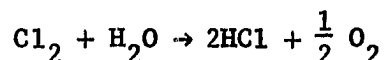$$= (0.25)(0.0257) = 0.006425 \text{ ml}$$

Total amount of effluent gas $= 0.2486 + 0.006425 = 0.2550$ ml.

Hence, in the effluent stream,

% chlorine $= 0.2486/0.2550 = 97.48$

% oxygen $= 0.006425/0.2550 = 2.52$

The reverse Deacon reaction proceeding in the forward direction is:

$$Cl_2 + H_2O \rightarrow 2HCl + \frac{1}{2} O_2$$

Let the flow rate of chlorine be F_{Ao} gmole/min, and let x gmole of chlorine be converted in the course of reaction during steady state. For each gmole of chlorine 1/2 gmole of oxygen will be produced. Therefore, for x gmole of chlorine x/2 gmole of oxygen will be produced. Then, in the effluent gas $(F_{Ao} - x)$ gmole of chlorine will go to the vent per minute along with other products. The water scrubber in the set up will absorb water vapor and hydrogen chloride. The remaining gas will consist of unreacted chlorine and oxygen. The total effluent will be $(x/2 + F_{Ao} - x)$ gmole per minute. In the effluent stream,

$$\% \text{ of oxygen} = \frac{x/2}{x/2 + F_{Ao} - x} = \frac{x/2}{F_{Ao} - x/2} \text{ (100) \%}$$

and $\quad$ $$\% \text{ of chlorine} = \frac{F_{Ao} - x}{x/2 + F_{Ao} - x} = \frac{F_{Ao} - x}{F_{Ao} - x/2} \text{ (100) \%}$$

For Experiment #3A,

$$0.0252 = \frac{x/2}{F_{Ao} - x/2} \text{ and } 0.9748 = \frac{F_{Ao} - x}{F_{Ao} - x/2}$$

Given that $F_{Ao} = 0.004145$ gmole/min

Solving for x from either of these equations, we find,

$$x = 0.000203934$$

Then, the fractional conversion is given by,

$$X_A = x/F_{Ao} = 4.92\%,$$

which has been reported in Table 4.

Calculation of Equilibrium Conversion

Using Equation (70), the value of equilibrium constant at 777°K was found to be:

$$K_e(777) = 3.858713238$$

for Experiment #3,

$$y_{Ao} = 0.796 \text{ and } \theta_B = 0.256.$$

Equation (69) with these values can be solved either numerically or by trial-and-error for equilibrium conversion X_e,

$$X_e = 0.23505 \text{ or } 23.50\%$$

but, $X_A = 4.92\%$

Conversion as % of equilibrium conversion $= (X_A/X_e)(100)$

$$= 19.65\%$$

Calculation of Reynold's Number

$y_{Ao} = 0.796$, $y_{Bo} = 0.204$, MW(chlorine) = 71, MW(water) = 18

Average MW of gas mixture $= MW_{avg}$

$$= (0.796)(71) + (0.204)(18) = 60.188$$

Density of gas mixture, $\rho_m = \dfrac{MW_{avg} P}{RT} = \dfrac{(60.188)(1)}{(0.08206)(777)}$

$$= 0.94379 \text{ gm/liter}$$

The critical properties of chlorine and water vapor are (50):

T_c(steam) $= 647^{\circ}$K T_c(chlorine) $= 417^{\circ}$K

P_c(steam) $= 217.7$ atm P_c(chlorine) $= 76.1$ atm

μ_c(steam) $= 495$ μpoise μ_c(chlorine) $= 420$ μpoise

T_c(average) $= (0.796)(417) + (0.204)(647) = 463.92^{\circ}$K

P_c(average) $= (0.796)(76.1) + (0.204)(217.7) = 104.99$ atm

μ_c(average) $= (0.796)(420) + (0.204)(495) = 435.3$ μpoise

$T_r = T/T_c = 506/463.92 = 1.6749$

$P_r = P/P_c = 1/104.99 = 0.009525$

The value of μ_r corresponding to the values of T_r and P_r are read from the chart (51) and they are found to be:

$\mu_r = 0.74$

Hence, $\mu = \mu_r \mu_c = (0.74)(435.3) = 322.122$ μpoise

diameter of the reactor tube $D_t = 0.4$ cm

flow rate of reactants $v_o = 331.95$ cc/min

$$u = 44.0486 \text{ cm/min}$$

Reynold's number $= D_t u \rho_m / \mu = \dfrac{(0.4)(44.0486)(0.94397)}{(322.122)(10^{-6})(1000)}$

$$= 51.633$$

APPENDIX C.

CALCULATION OF DISPERSION NUMBER

Helium gas at the rate of 1000 ml/minute flowed through the reactor in one of the experiments. One-hundred ml of air was injected in the helium flow as a pulse input. The response was recorded as sharp peaks by the recorder. The response peaks are shown in Figure 20. The height of the peaks was considered to vary directly with the concentrations. The measured heights were tabulated against time for each observation, and the mean value was calculated for determining the variance and dispersion number as shown in Table 21.

Table 21. Time and concentration data from stimulus response experiment

θ (sec)	Concentration $C'(\theta)$ (cm)	Mean value of concentration, $C'(\theta)$ (cm)
0.0	0.0	0.00
4.6875	4.0 4.2 4.1	4.10
9.375	10.7 10.8 10.9	10.8
14.0675	3.45 3.50 3.55	3.5
0.0	0.0	0.0

$V = 1000$ CC/min

$u = 132.7$ cm/sec

10.7 cm   10.8 cm   10.9 cm
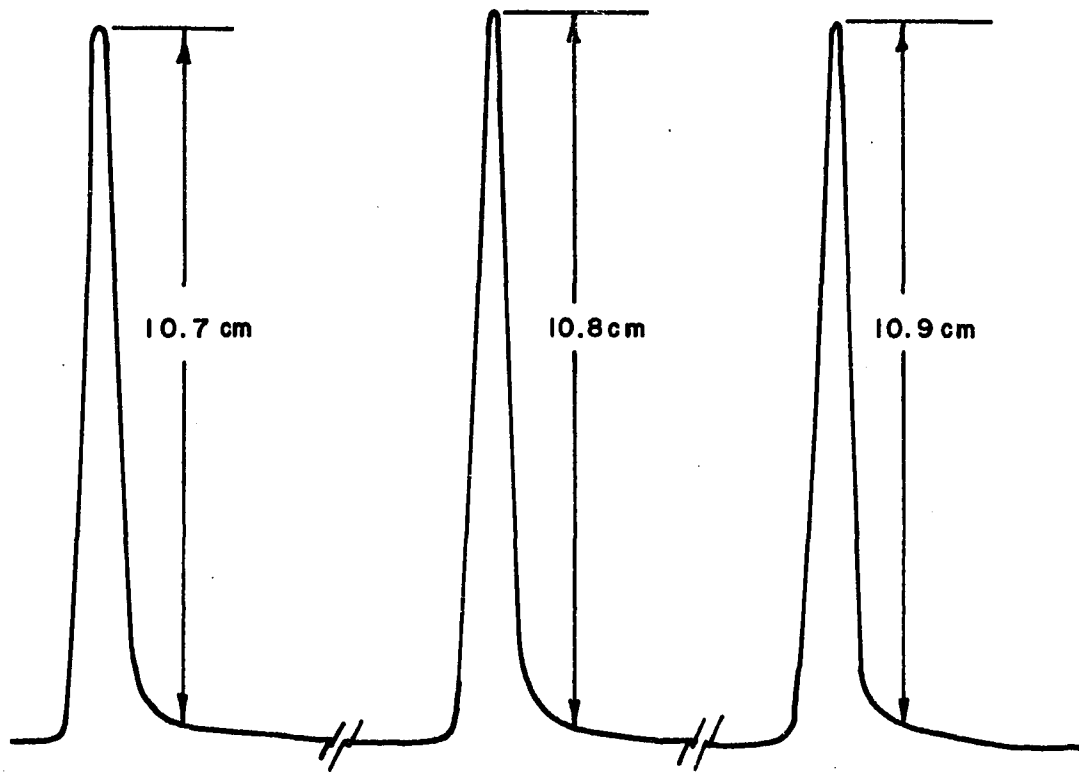
Figure 20.   Response peaks as obtained in stimulus response experiment

volumetric flow rate of helium, v_o = 1000.0 ml/min

linear velocity of helium, u = 1000.0 (cm^3/min) $\dfrac{1}{(\pi/4)(0.4)^2 cm^2}$

$$= 7961.8 \text{ cm/min}$$

$$= 132.7 \text{ cm/sec}$$

Earlier in the theory section, the mean holding time and RTD are defined as:

$$\theta' = \theta/\overline{\tau}, \qquad E(\theta) = C'(\theta)/ \int_0^\infty C'(\theta)d\theta$$

The values of the integrals were calculated by use of Simpson's rule, and they are:

$$\int_0^\infty C'(\theta)d\theta = 81.25,$$

$$\int_0^\infty \theta^2 E(\theta)d\theta = 84.0583$$

$$\overline{\tau} = \int_0^\infty \theta E(\theta)d\theta = 9.16 \text{ seconds}$$

Table 22. Concentration and residence time distribution

θ (sec)	$C'(\theta)$ (cm)	$E(\theta)$	θ'	$E(\theta')$
0.0	0.0	0.0	0.0	0.0
4.6875	4.10	0.0505	0.5117	0.4623
9.375	10.80	0.1329	1.0235	1.2177
14.0675	3.5	0.0431	1.5357	0.3946
18.75	0.0	0.0	2.0469	0.0

In Table 22, the residence time distribution with the corresponding concentration is shown in dimensionless form. From this table, the values of the variance and dispersion number are calculated as follows:

$$\sigma^2 = \int_0^\infty \theta^2 E(\theta) d\theta - \bar{\tau}^2 = 0.1527$$

$$\sigma_\theta^2 = \sigma^2/\bar{\tau}^2 = 0.1527/(9.16)^2 = 0.0018199$$

$$D_1/uL = \sigma_\theta^2/2 = 0.0009097 \doteq 0.00091$$

APPENDIX D.

SAMPLE CALCULATION PROCEDURE FOR DIFFERENTIAL REACTOR DATA

Flow Rate of Reactants at Reaction Temperature for Experiment #55

Reaction temperature = 879°K

Operating pressure = 1 atm

Gas constant = 0.08206 atm-liter/gmole/°K

Room temperature = 294 K

Flow rate of water
at RT and 1 atm   = 0.0191 cc/min

                   = 0.0191 gm/min

Flow rate of chlorine
at RT and 1 atm   = 205.15 cc/min

Flow rate of inert
at RT and 1 atm   = 25.60 cc/min

v_{Bo} = nRT/P = (0.08206)(879)(0.0191/18) liter/min

          = 76.54 cc/min

v_{Ao} = (205.15)(879/294) = 613.36 cc/min

v_{Io} = (25.6)(879/294) = 76.54 cc/min

Total flow rate of the reactants = v_o = v_{Ao} + v_{Bo} + v_{Io}

      = 76.54 + 613.36 + 76.54 = 766.44 cc/min

Hence, mole fractions are:

y_{Ao} = 613.36/766.44 = 0.8 and P_{Ao} = 0.8

y_{Bo} = 76.54/766.44 = 0.1 and P_{Ao} = 0.1

y_{Io} = 76.54/766.44 = 0.1 and P_{Io} = 0.1

and the corresponding concentrations are:

C_{Ao} = P_{Ao}/RT = 0.8/(0.08206)(879) = 11.09 x 10^{-3} gmole/1

$$C_{Bo} = P_{Bo}/RT = 0.1/(0.08206)(879) = 1.39 \times 10^{-3} \text{ gmole/l}$$

$$C_{Io} = P_{Io}/RT = 0.1/(0.08206)(879) = 1.39 \times 10^{-3} \text{ gmole/l}$$

Therefore, the molar flow rates can be calculated as:

$$F_{Ao} = C_{Ao}v_o = 11.09 \times 10^{-3} \times 0.76644 = 8.5 \times 10^{-3} \text{ gmole/min}$$

$$F_{Bo} = C_{Bo}v_o = 1.39 \times 10^{-3} \times 0.76644 = 1.06 \times 10^{-3} \text{ gmole/min}$$

$$F_{Io} = C_{Io}v_o = 1.39 \times 10^{-3} \times 0.76644 = 1.06 \times 10^{-3} \text{ gmole/min}$$

and the molar flow ratio,

$$\theta_B = F_{Bo}/F_{Ao} = 1.06 \times 10^{-3}/8.5 \times 10^{-3} = 0.125$$

Space-time $\tau = V/v_o = 64.25 \times 60/766.644 = 5.03$ seconds

These values are reported in Table 14 against Experiment #55.

Calculation of Experimental Conversion for Experiment #55

Average weight of pure chlorine
peaks as found by calibration   = 0.1965 gm

Average weight of pure oxygen
peaks as found by calibration   = 0.02602 gm

Average weight of pure nitrogen
peaks as found by calibration   = 0.02186 gm

In this experiment, the partial pressures of the reactants were calculated to be $P_{Ao} = 0.8$ atm, $P_{Bo} = 0.1$ atm and $P_{Io} = 0.1$ atm. Hydrogen chloride and water vapor were absorbed in the scrubber before entering the gas chromatograph. Chlorine was diluted by introduction of the inert gas in the feed stream. It was necessary to consider this dilution effect on peaks obtained for the chlorine gas. Suppose chlorine was introduced with inert to the reactor and there was no chemical reaction. Then, the partial pressures of the gases

entering the chromatograph would be as follows:

$$\text{partial pressure of oxygen} = \frac{0.8}{0.8 + 0.1} \text{ atm} = 0.8889 \text{ atm}$$

and $\qquad$ $$\text{partial pressure of inert} = \frac{0.1}{0.1 + 0.8} \text{ atm} = 0.1111 \text{ atm}$$

The chlorine peaks (with inerts) would result in 88.89% of the pure peaks (witho t inerts). Considering this effect on resultant peaks, average weight of pure chlorine peaks (with inerts) would be taken as:

$$0.1965 \times 0.8889 = 0.17467 \text{ gm}$$

However, there was no effect on oxygen peaks, since oxygen was produced during the course of the reaction.

Average weight of chlorine peaks
as obtained by experimentation $\quad = 0.16982 \text{ gm}$

Average weight of oxygen peaks
as obtained by experimentation $\quad = 0.000823 \text{ gm}$

$$\% \text{ chlorine} = \frac{\text{wt. of chlorine peaks as obtained by experimentation}}{\text{wt. of pure chlorine peaks at same conditions}}$$

$$= 97.223\%$$

$$\% \text{ oxygen} = \frac{\text{wt. of oxygen peaks as obtained by experimentation}}{\text{wt. of pure oxygen peaks at same conditions}}$$

$$= 3.163\%$$

When reaction occurs, the total mole of the effluent gas per minute is $(x/2 + F_{Ao} - x)$ gmole; where x is the amount of chlorine converted. And for each x mole of chlorine conversion, x/2 mole of oxygen is produced. Thus:

$$\% \text{ of oxygen} = \frac{x/2}{x/2 + F_{Ao} - x}$$

and $$\% \text{ of chlorine} = \frac{F_{Ao} - x}{x/2 + F_{Ao} - x}$$

The composition of the effluent gas was determined earlier, and when substituted in the above equations, we obtain per minute:

$$x = 0.00051875 \text{ gmole for } F_{Ao} = 0.0085 \text{ gmole}$$

Therefore, the fractional conversion as percent of chlorine flow rate is:

$$X_A = x/F_{Ao} = 6.103\%$$

Determinations of Rate of Reaction and Product Concentrations

In this sample calculation procedure, Experiment #'s 54, 55 and 56 are considered for which,

$$y_{Ao} = 0.8, \ y_{Bo} = 0.1 \text{ and } y_{Io} = 0.1$$

$$\theta_B = 0.125$$

$$C_{Ao} = 11.09 \times 10^{-3} \text{ gmole/l and } C_{Bo} = 1.39 \times 10^{-3} \text{ gmole/l}$$

But the space-times and the molar flow rates are different in each case. The fractional conversion and space-times for each experiment were calculated by the methods as described earlier. The computed values are shown in Tables 13 and 14, respectively. In Figure 9, their relationship is shown along with the results for other molar flow ratios. The plot of space-time versus conversion for $\theta_B = 0.125$ is redrawn in Figure 21. Experimental results of Experiment #55 correspond
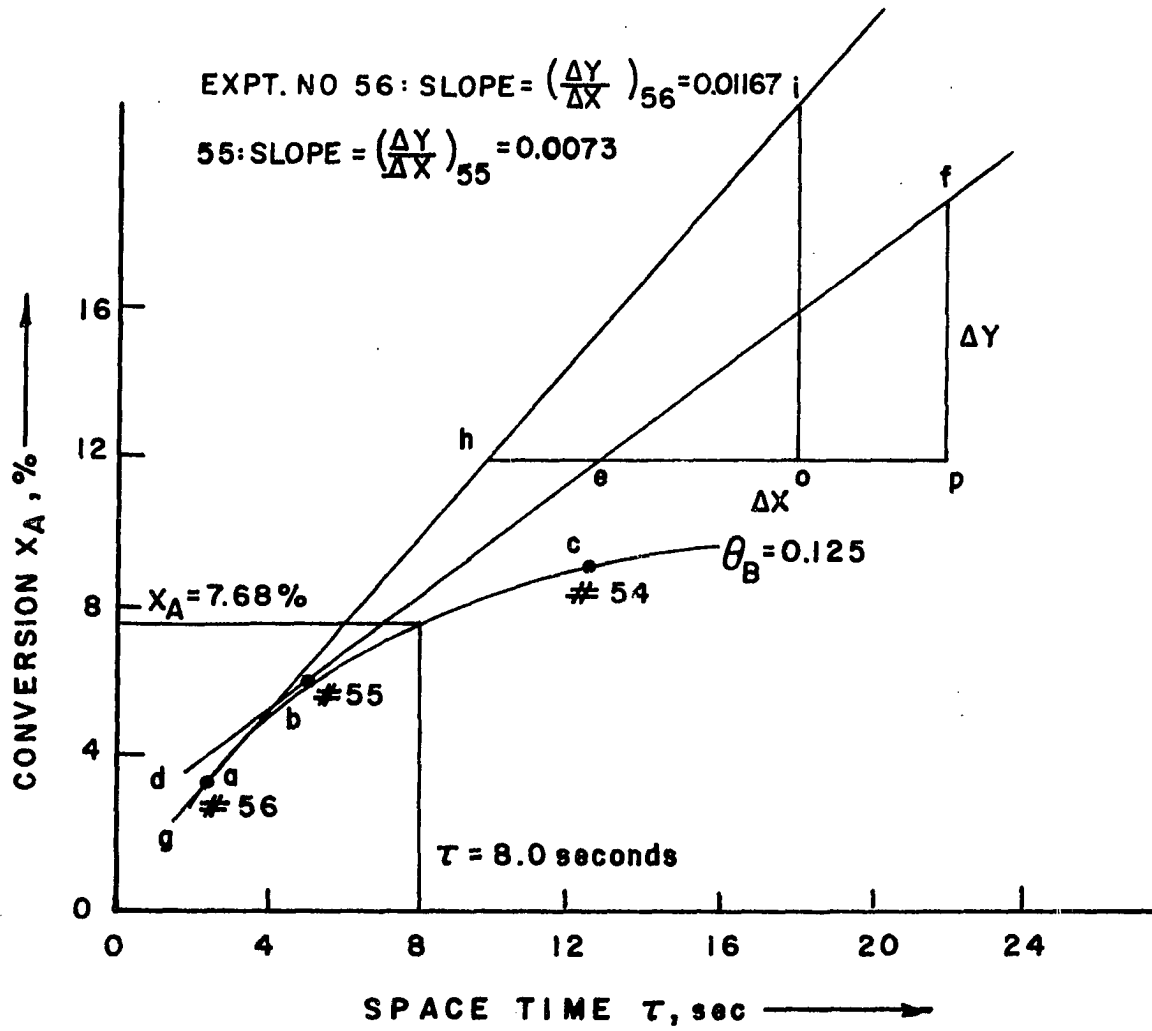
Figure 21. Determination of slopes when C_{A_o} is kept constant

to point b in this figure (i.e., for τ = 5.03 seconds and X_A = 6.103%).

A tangent dbef passing through point b is drawn, the slope of which

corresponds to the rate. The slope is calculated as follows:

$$fp = \Delta y = 0.132$$

$$pe = \Delta x = 18.2 \text{ sec}$$

$$slope = (\Delta y / \Delta x)_{55} = 0.0072527 \text{ per second}$$

Therefore,

$$\frac{dX}{d\tau} = 0.0072527 \text{ sec}^{-1}$$

Hence, $- r_A = C_{Ao} \frac{dX}{d\tau} = 11.09 \times 10^{-3} \times 0.00072527$

$$= 0.0804 \text{ gmole/liter/second}$$

Similarly, the rate of reaction at point a and c could be determined,

and the procedure can be extended to other τ versus X_A curves for

θ_B = 0.0675, θ_B = 0.1875, and θ_B = 0.25. The results obtained by this

graphical procedure have been summarized in Table 23.

Table 23. Space-time and rate of reaction

θ_B = 0.25		θ_B = 0.1875		θ_B = 0.125		θ_B = 0.0675	
Space-time τ (sec)	Rate 10^3	Space-time τ (sec)	Rate 10^3	Space-time τ (sec)	Rate 10^3	Space-time τ (sec)	Rate 10^3
25.14	0.073	18.85	0.060	12.57	0.0387	6.28	0.026
10.06	0.112	7.54	0.085	5.03	0.0804	2.52	0.0895
5.54	0.123	2.52	0.1468	2.52	0.2294	0.53	0.1327

These results are used in plotting the rate of reaction versus space-

time as shown in Figure 10. Figure 10 was used for interpolation.

At space-time τ = 10.5, 8.0, 6.0 and 4.0 seconds, the rate of

reaction for each θ_B was read from this figure, and the corresponding

conversion values were read from Figure 9; these values are shown in

Table 24.

Table 24. Interpolated value of rate of reaction with corresponding space-time

τ (sec)	$\theta_B = 0.25$		$\theta_B = 0.1875$		$\theta_B = 0.125$		$\theta_B = 0.0675$	
	Rate 10^3	X_A (%)	Rate 10^3	X_A (%)	Rate 10^3	X_A (%)	Rate 10^3	X_A (%)
10.5	0.110	11.12	0.078	9.83	0.045	8.26	0.002	6.32
8.0	0.116	10.95	0.089	8.72	0.058	7.39	0.0102	5.63
6.0	0.112	8.61	0.104	7.68	0.073	6.66	0.033	5.132
4.0	0.143	6.10	0.1245	5.91	0.096	5.13	0.060	4.08

Let us consider space-time = 6.0 seconds, and $\theta_B = 0.1875$ for which

the rate of reaction is 0.058 gmole/liter/second, and conversion

X_A is 7.68%. Using Equations (25), (26), (27), and (28), we obtain

the following product concentrations:

$$C_A = \frac{11.09 \times 10^{-3}(1 - 0.0768)}{1 + (0.5)(0.8)(0.0768)} = 9.933 \; 10^{-3} \text{ gmole/liter}$$

$$C_B = \frac{11.09 \times 10^{-3}(0.125 - 0.0768)}{1 + (0.5)(0.8)(0.0768)} = 0.519 \; 10^{-3} \text{ gmole/liter}$$

$$C_C = \frac{11.09 \times 10^{-3} \times 2 \times 0.0768}{1 + (0.5)(0.8)(0.0768)} = 1.653 \; 10^{-3} \text{ gmole/liter}$$
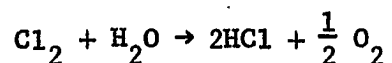
$$C_D = \frac{11.09 \times 10^{-3} \times 0.5 \times 0.0768}{1 + (0.5)(0.8)(0.0768)} = 0.413 \; 10^{-3} \text{ gmole/liter}$$

The procedure was repeated for all space-times and all θ_B

values. The computed product concentrations at various space-times

along with corresponding rates of reaction are shown in Table 15.

APPENDIX E.

THERMODYNAMIC PROPERTIES

The thermodynamic values for the reaction,

$$Cl_2 + H_2O \rightarrow 2HCl + \frac{1}{2} O_2$$

are reported in Table 25. The values of ΔG, ΔH, and ΔS for each product and reactant were obtained from reference (52). By use of Newton's interpolation formula, specific heat, free energy, enthalpy and entropy at each reaction temperature were determined, and the final values for the reverse Deacon reaction were computed for the stoichiometry as written.

Table 25. Thermodynamic data for the reverse Deacon reaction

Reaction temperature T (°K)	Specific heat C_p (cal/gmole/°K)	Free energy ΔG (K-cal/gmole)	Enthalpy ΔH (K-cal/gmole)	Entropy ΔS (cal/gmole/°K)
777	0.484	- 1.556	14.164	16.03
879	0.460	- 0.006	14.215	16.10
983	0.443	+ 2.072	14.259	16.23